ASSESSMENT OF LAND SUBSIDENCE IN NEW ORLEANS

FINAL VERSION
MAY 2023

Deltares

Authors:

Henk Kooi (Deltares)
Jacqueline Salzer (SkyGeo, processing and analyzing satelite data)
Begoña Arellano Jaimerena (Deltares, report editing and urban planning)
Roelof Stuurman (Deltares, groundwater and project organization)

Supporting team:

Gilles Erkens (Deltares)
Geoff Zimmel (Deltares)
Otto Levelt (Deltares, geographical data analysis)
Roel Melman (Deltares, groundwater model)
Daan Rooze (Deltares)

Utrecht, The Netherlands
March, 2023 (submitted in 2019)

ASSESSMENT OF LAND SUBSIDENCE IN NEW ORLEANS

FINAL VERSION
MARCH 2023

CITY OF NEW ORLEANS
MAYOR LATOYA CANTRELL

Deltares

CONTENT

EXECUTIVE SUMMARY

Founded over 300 years ago, New Orleans has undergone a radical transformation as anthropogenic and natural forces have worked in tandem to shape the modern-day landscape along the edge of the Mississippi.

Similar to many other deltas in the world, the land surface subsidence in the Mississippi Delta and in the Greater New Orleans area at present, and over the last decades, is the compound expression of various processes that occur over a very large depth range, from the top few decimeters to more than one hundred kilometres below the land surface. In the shallower subsurface, subsidence originating within the Holocene sediments and unsaturated zone is the sum of the effects of loading compaction, drainage compaction, drainage oxidation, natural compaction and shrink/swell. Deep subsurface activities and processes include regional oil and gas extraction, industrial and domestic water production, isostasy and plate tectonics. The combination of shallow and deep inputs, over time, produce a complex dynamic scenario whose surface expressions affect the stability of local infrastructure and the livelihoods of the residents. To identify and study historic and ongoing subsidence, monitoring techniques were identified, a groundwater - subsidence study was applied, and a review of relevant literature was completed. These data were acquired from previously completed work and compared and reviewed.

Geodetic levelling information was collected from the National Geodetic Survey archives and allowed for the comparison of height changes against benchmark locations since the beginning of the program in 1955. Levelling data indicates up to 0.8 meters of subsidence between 1955 – 1995 at the Michoud plant location that remains enigmatic. GPS measurement points throughout the state of Louisiana that were installed in the mid 1990's provide state wide, point source ground deformation information. This network revealed minor motion in central and northern Louisiana, but significant subsidence and southward motion of the stations south of the Tepatate-Baton Rouge fault. Extensometers and tidal gauge information is also discussed, adding to the regional subsidence knowledge of Mississippi Delta. InSAR (Interferometric Synthetic Aperture Radar) information over the city was newly acquired and includes all available Sentinel 1 data between 2016 and 2019 as well as Envi-

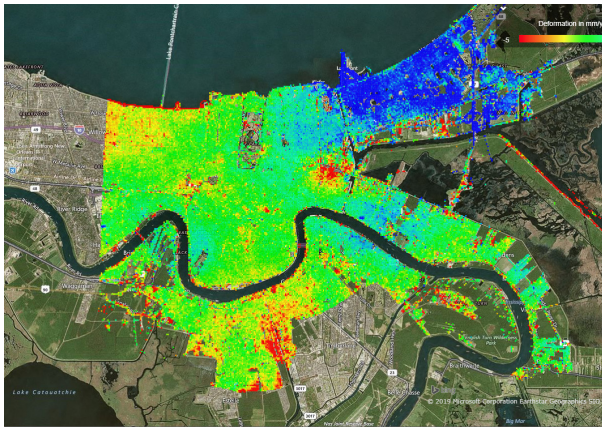

Figure S1. InSAR results: green is stable, blue equals uplift (2016-2019).

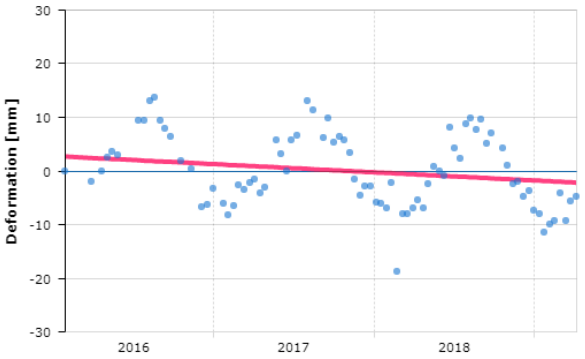

Figure S2. Example time series of the amplitude of seasonal variation of the vertical movement (Sentinel-1) for the location indicated with the white circle in Figure 3.35. This variation follows the seasonal rainfall fluctuation.

SAT data from 2004 – 2009. Previous InSAR studies (see Figure S1) were completed and published in 2006 and 2016, the results of which are discussed and compared with the results of the updated study. Localized areas of subsidence can be seen most prominently along the Lake Pontchartrain seawall, in north east New Orleans as well as within the Florida area (St. Roch). Most parts of the city appear relatively stable during the measurement period with the exception on the area east of Gentilly which exhibits an uplifting pattern caused by the cessation of industrial groundwater abstraction at the Michoud plant. This is confirmed by a local GPS station and a parallel InSAR study by Tulane University (Fiaschi et al., 2020). Amplitude data also received from the InSAR study provides an approximation of the seasonality relating to the shrink / swell nature of the soil. The yearly low elevations occur in January-March and the highs in July-August (see Figure S2).

Within this report, data was collected and analysed to provide a synthesis of subsidence information for both New Orleans as well as the regional Mississippi Delta area over varying depths and times. Overall, present subsidence rates in the greater New Orleans area are lower than several studies have indicated over the last decades. Locally, high rates of ten to several tens of mm/year occur and these rates are largely of anthropogenic origin, mostly by shallow groundwater drainage. This implies that high rates can be influenced positively, or prevented, through integrated urban (ground) water management. Figure S3 and S4 summarize subsidence processses and evolution in New Orleans.

Subsidence vulnerability varies greatly across New Orleans. After more than 100 years of rapid subsidence due to land reclamation and urbanization, in most areas the subsidence rate has reduced significantly. Remarkably, due to the cessation of groundwater pumping at the Michoud plant in 2016, subsidence shifted into uplift in New Orleans North-East. This uplift was still active in 2020, but additional research is needed to understand the possible continuation. Still, more intense local subsidence areas also exist or can develop because of the presence of shallow peat or muck deposits (also in the uplift area). These areas are vulnerable for groundwater drainage by leaking pipes and pumping during construction works.

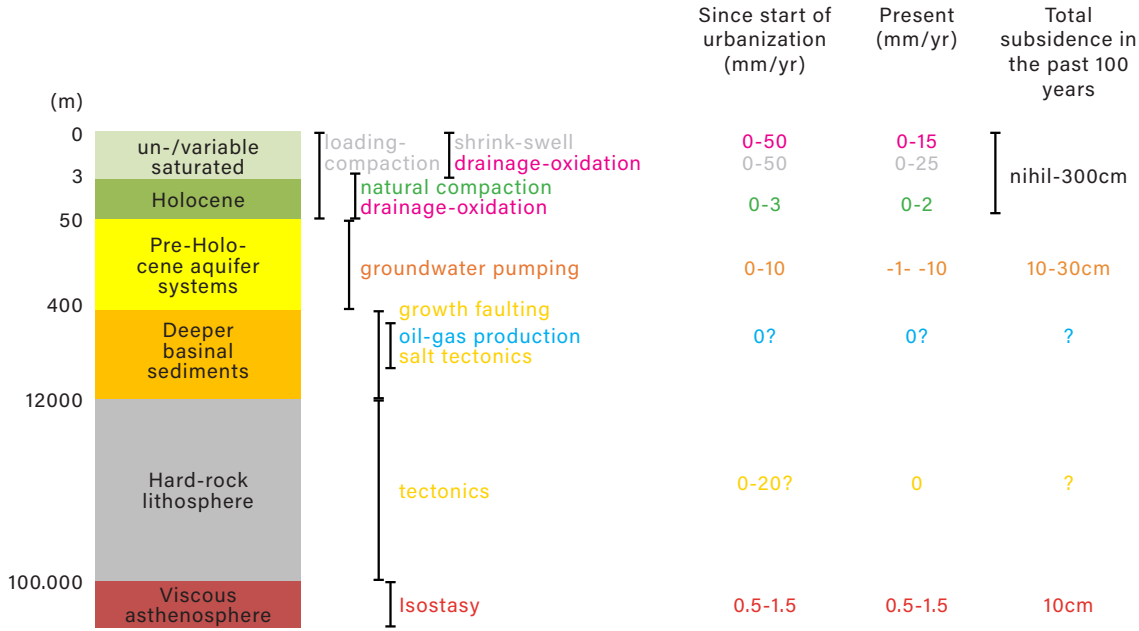

Figure S3. Summary of estimated subsidence in New Orleans (study area), both in historic times (since start urbanization) and at present. Negative values indicate uplift. Ranges are shown to indicate uncertainty and/or expected variance in space and in time.

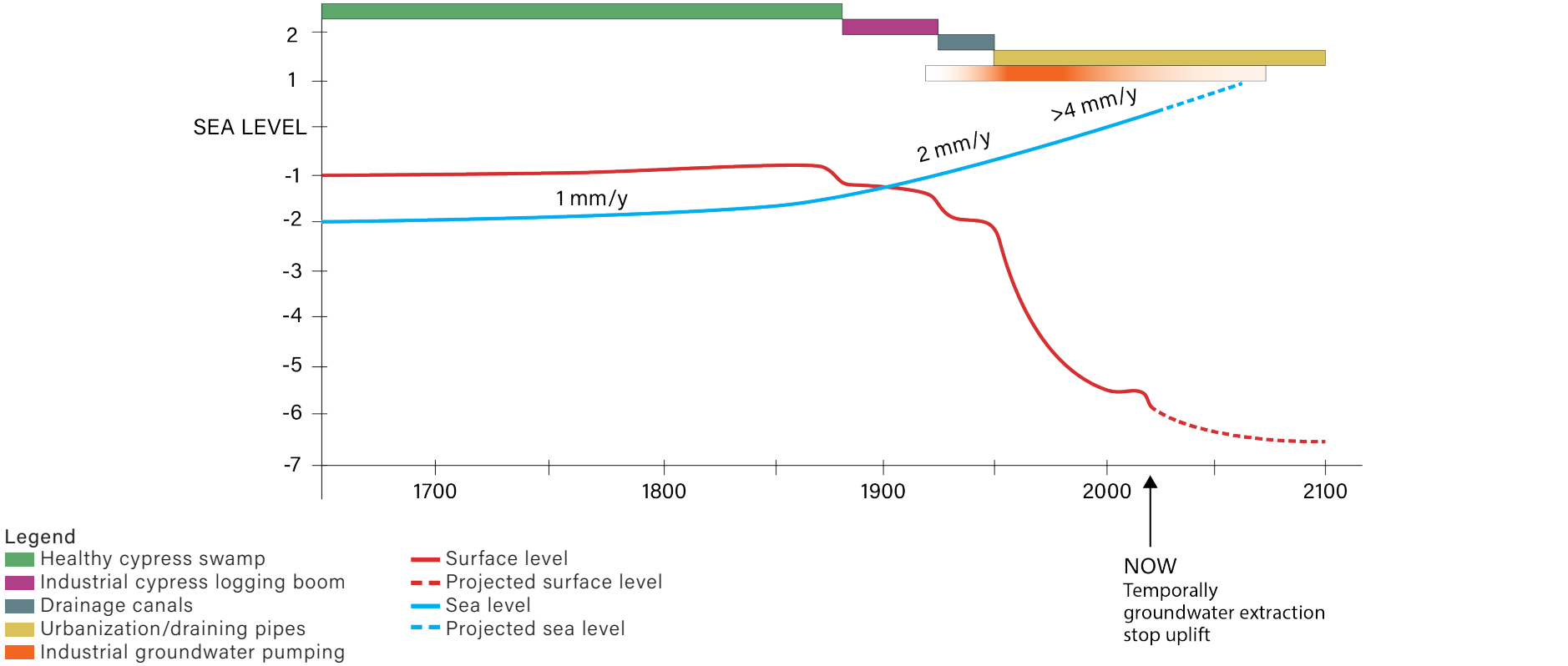

Figure S4. New Orleans subsidence process in time. Until the end of the 19th century, the northern part of New Orleans was covered with fresh water cypress swamps. These swamps raised gradually in equilibrium with sea level rise. After the start of the industrial cypress logging boom and the creation of the cypress wood transport canals, serious subsidence started (dewatering). A next subsidence phase started after the construction of the (urban) drainage canals at the begining of the 20th century. But real acceleration in subsidence started during urbanization of this area. The main factor was groundwater drainage by underground storm drainage and sewerage pipes. Groundwater pumping starting at the beginning of 20th century with the highest extraction ratesbetween 1950-1980, also added to subsidence, but to a much smaller amount. The stop of the Michoud extraction created a temporarily uplift.

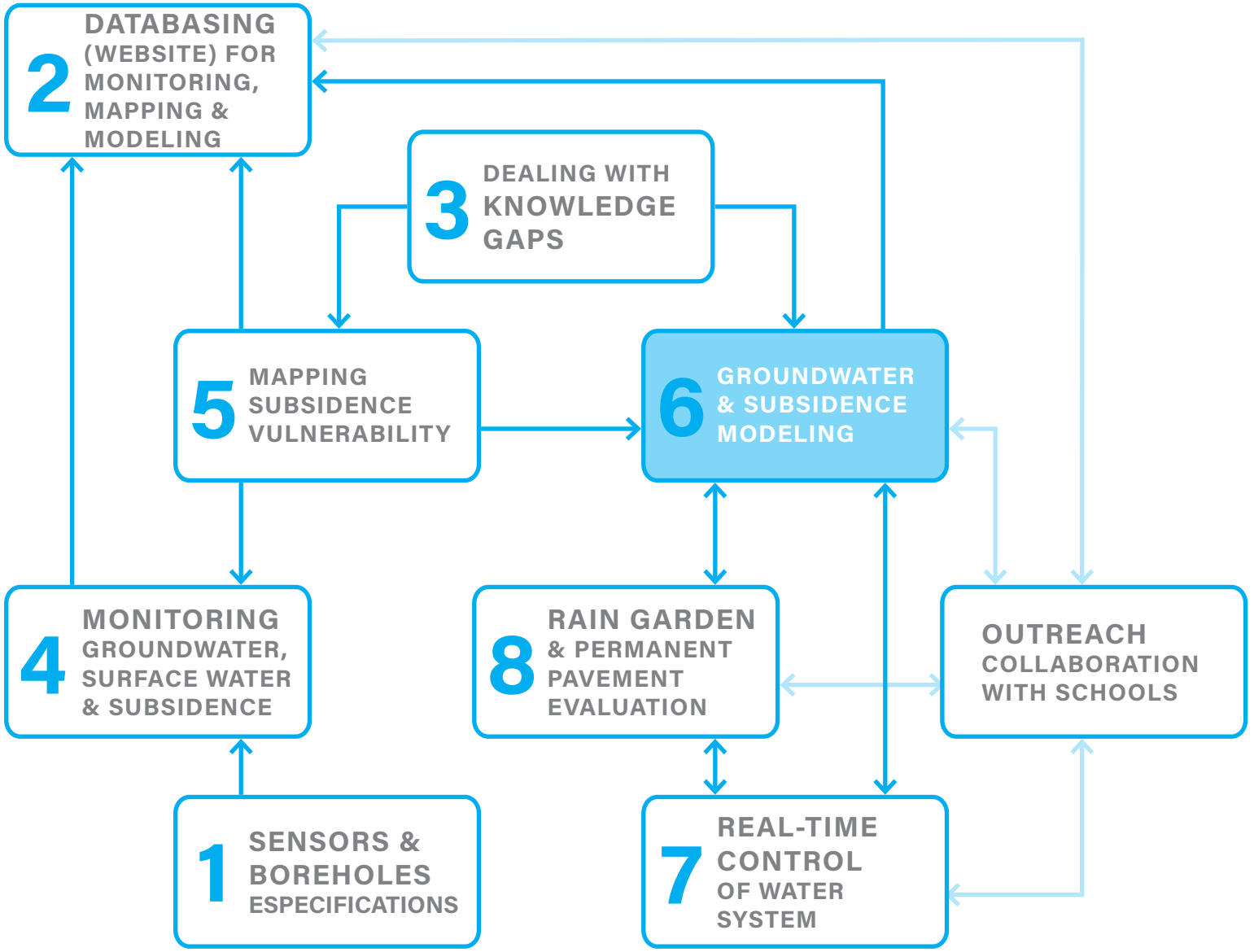

Figure 1.1. Phases of the project

1.INTRODUCTION

The project 'Reshaping the Urban Delta', funded by the National Disaster Resilience Competition (NDRC), aims to deliver groundwater and subsurface insights and data which will help in the planning of initiatives that increase flood resilience and can be used in the design of the same initiatives. The project consists of eight subprojects (see Figure 1.1).

Subproject 6 "Groundwater and subsidence modeling" focuses on the construction of a 3D deep groundwater-subsidence model through the use of existing and new cross sections and borehole information. The model will elucidate the effects of groundwater extraction at greater depth on land subsidence. This subproject adds to the findings from subproject 5 about mapping shallow subsidence vulnerability, allowing for a comprehensive understanding of land subsidence. A major difference with regards to the shallow component is the scale on which this happens and the impact it has on all kinds of infrastructure.

Chapter 2 of this report covers the methods used to conduct the subsidence analysis, including the review of literature, modeling subsidence due to groundwater abstraction, and acquisition and analysis of InSAR satellite data.

Chapter 3 addresses the various components of subsidence in and around New Orleans, the findings from literature review, the results from the modelling assessment of the role of groundwater extraction, and a synopsis of the integrated results.

Finally, findings and recommendations for the assessment of land subsidence are provided in Chapter 4 and 5 respectively.

Objectives

The main objective of this work is to create a comprehensive, integrated understanding of surficial land subsidence.

Similar to many other deltas in the world, the land surface subsidence in the greater New Orleans (GNO) area is the compound expression of various natural and human-induced processes that occur over a very large depth range, from the top few decimeters to more than one hundred kilometers below the land surface. Therefore, understanding of the total system is important. Some subsidence components, in particular the oxidation of organic matter and compaction and shrinkage processes that occur at relatively shallow depth (within the Holocene cover layer), are directly tied to and influenced by urban design and water management. Other, mostly deeper-based subsidence components are largely independent from the near-surface interventions, but are nevertheless important, since they will also modify the land surface elevation over the next decades and centuries.

A resilient design needs to consider both shallow and deep subsidence contributions. Therefore, in this study we distinguish so-called "shallow subsidence" caused by oxidation and compaction of the shallow sediments (meters below surface) and human-induced "deep subsidence" mainly caused by consolidation of deeper aquifers due to pumping.

2.METHODOLOGY

2.1 Subsidence analysis

The subsidence analysis consisted of the following three steps:

- Review of literature
- Modeling subsidence due to groundwater abstraction
- Acquisition and analysis of InSAR satellite data

Subsequently, an assessment was made of the results of these steps in the form of a synthesis/synopsis.

2.2 Literature review

A literature review was conducted to provide a comprehensive picture of what is currently known about subsidence in the greater New Orleans area. Literature was obtained from scientific literature databases, general internet searchs, and through colleagues and experts at various institutes in the state of Louisiana.

2.3 Modeling subsidence due to groundwater abstraction

Regional subsidence modeling was conducted to shed more light on the role of groundwater extraction from aquifer systems underlying Greater New Orleans (GNO), and its potential contribution at present. Modeling was done with iMOD (groundwater flow modeling) in combination with the SUB-CR package (land subsidence). An extensive report regarding model design, parameterization and results have been laid out in a MSc-thesis (Melman, 2019). Some essential aspects are summarized here, focusing on abstraction history in the study area and head data of the most important aquifers that were used in calibration of the groundwater model. The model domain extends significantly beyond the area of interest around GNO (Figure 2.1) and consists of 268*413 grid cells of 1*1 km. The subsurface was schematized by eight model layers representing the alternation of the main confining layers and aquifers (Figure 2.2)

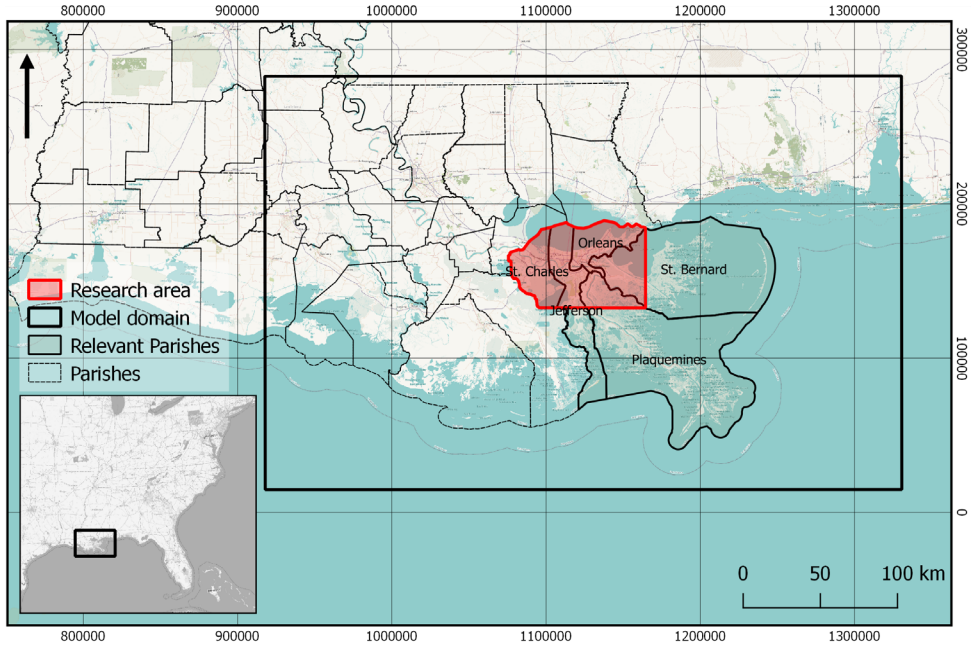

Figure 2.1. Delineation of the model domain in map view (large box).

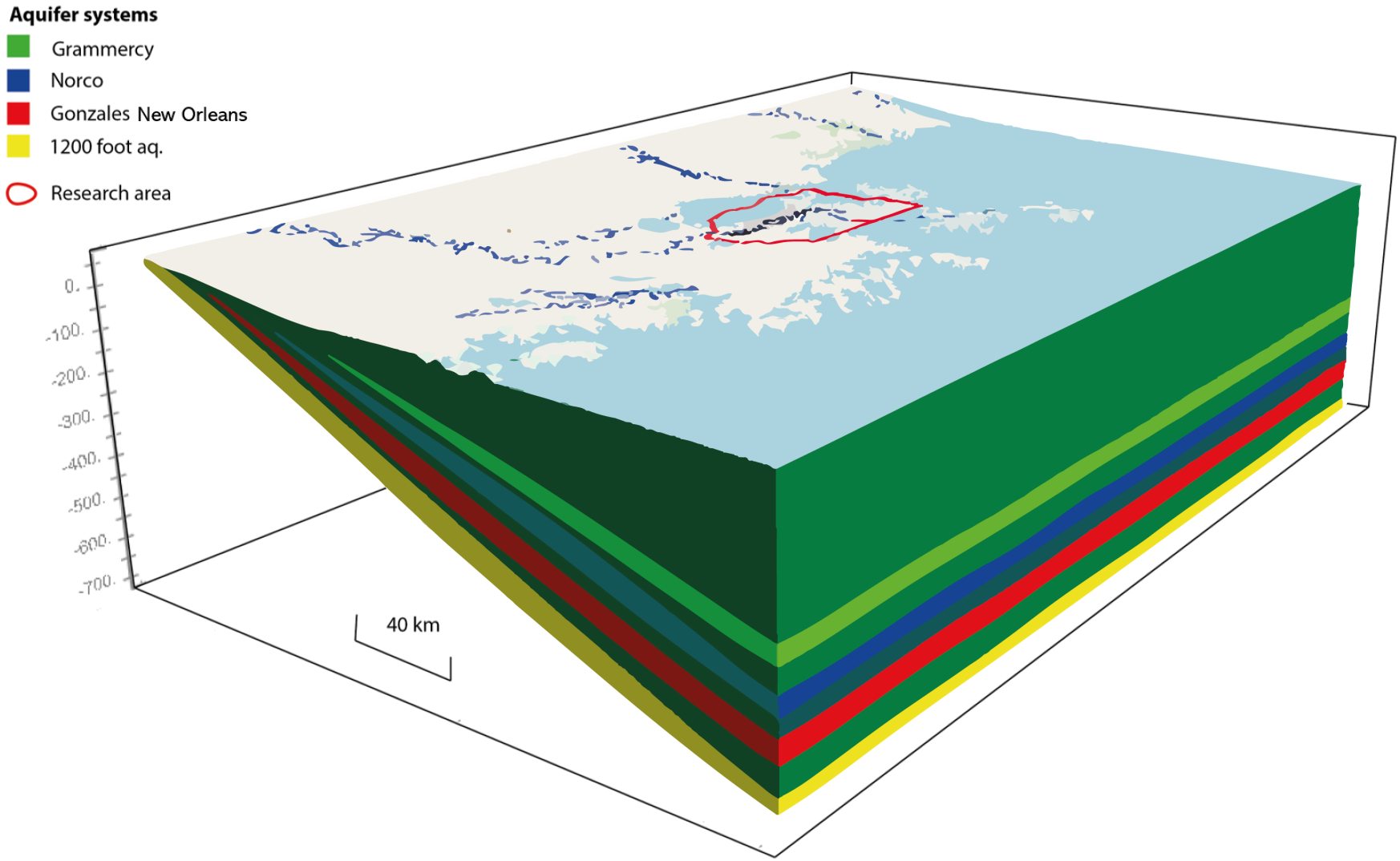

Figure 2.2. 3-Block diagram of the geological schematization, showing the depth of aquifers dipping into southern direction. Largely based on the schematization of Dial and Sumner (1989). Names of the key aquifers are given in the legend. Dark-green layers represent confining units.

Groundwater wells and their time-varying extraction in different aquifers in the model were defined/constructed based on information in the SONRIS database (www.SONRIS.com) and 5-yearly reports about total groundwater use per parish. Several assumptions were made to fill in data gaps, and to define complete time series for each individual (known) well (Melman 2019). 118 Wells were implemented in the Gonzales aquifer and 57 wells in the Norco aquifer (Figure 2.3, left; Figure 2.4). The right panel of Figure 2.3 shows yearly cumulative extracted groundwater for both aquifers in the model. Around 1955 the total yearly extraction in Jefferson and New Orleans was approximately 50 million (Eddards et al., 1956). Note the significant reduction in groundwater use from these aquifers since about 1970.

The groundwater model was calibrated/validated against hydraulic head data for the Gonzales-NO aquifer for 1963 (Figure 2.5) and 2008 (Figure 2.6), and time series of hydraulic head retrieved from the USGS waterdata website (waterdata.ugsg.gov). Information about the wells with monitoring data is given in Table 2.1.

The groundwater model was developed in a step-wise fashion. Following initial parameterization described in detail by Melman (2019), the hydraulic parameters were optimized in steady-state models for 1963 and 2008. For each parameter set, uncertainties

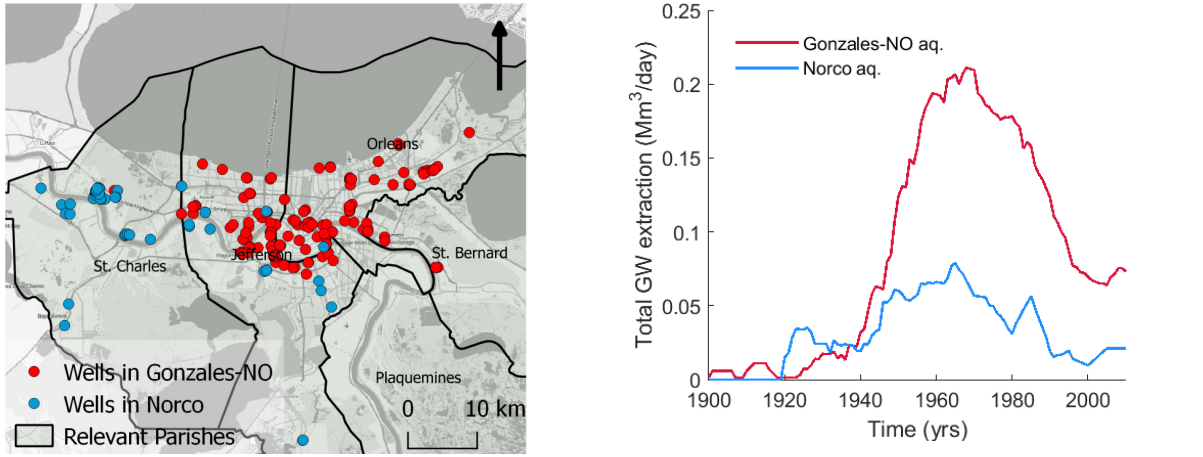

Figure 2.3 Left: Groundwater extraction wells in the Norco (blue) and Gonzales-NO aquifer (red). Right: Total groundwater extraction from both aquifers in the model (only data until 2010 available).

Table 2.1 Information about the wells for which hydraulic head monitoring data were used.

Observation well	Aquifer	Location (x;y)	Period
Or-42	Gonzales NO	1125504.2;161287.2	1942-2010
Or-47 & Or-128	Gonzales NO	1121966.0;170534.7	1943-1986
Or-175	Gonzales NO	1150132.8;176754.1	1963-2010
Or-206	Gonzales NO	1126110.2;167929.4	1970-2010
Jf-178	Gonzales NO	1104740.5;170938.6	1984-2010
Jf-156	Gonzales NO	1112995.6;162419.2	1974-2010
Sc-6	Norco	1089441.4; 166976.0	1943-1953
Sc-24	Norco	1097192.2;160067.4	1921-1985
Sc-82	Norco	1082764.3;165748.4	1957-1989

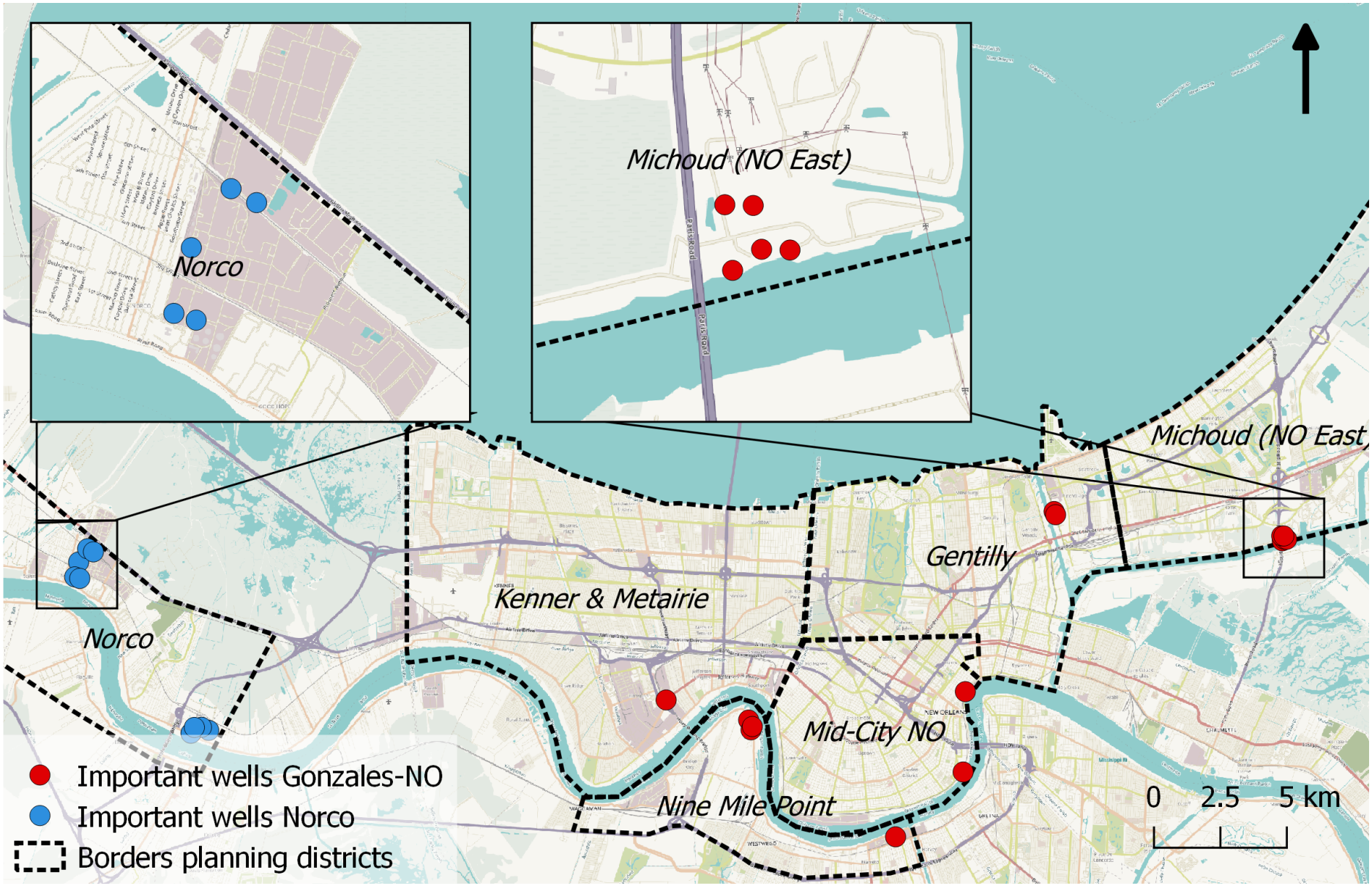

Figure 2.4 Upper left: Groundwater extraction wells in the Norco (blue) and Gonzales-NO aquifer (red). Bottom: zoom in showing 15 wells with largest cumulative extraction amounts in the Gonzales aquifer and 10 wells with largest cumulative extraction amounts in the Norco aquifer. Upper right: Total groundwater extraction from both aquifers in the model.

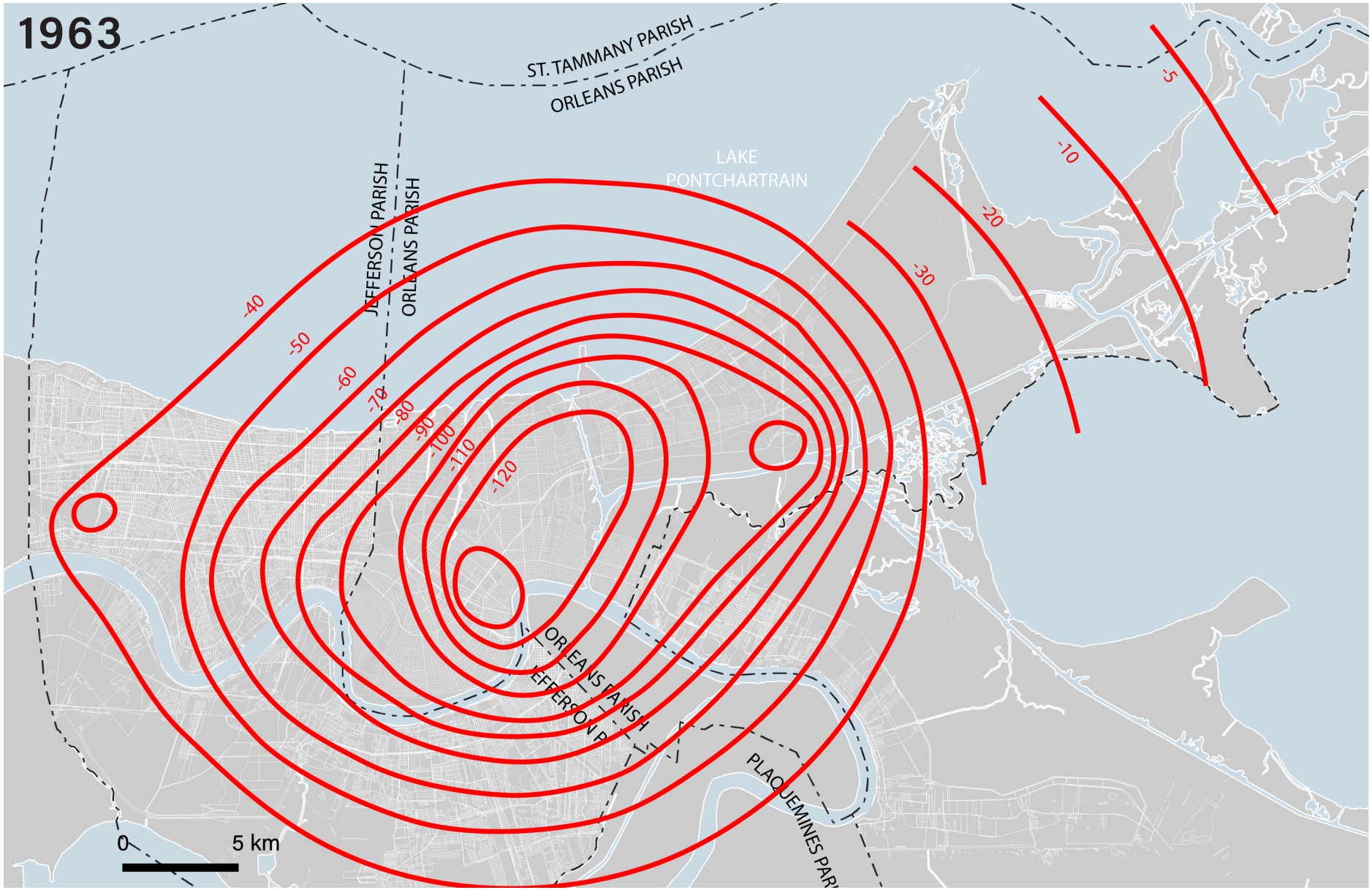

Figure 2.5 Hydraulic head of the Gonzales-NO aquifer in 1963 (feet below sea level). The contours are based on interpolation of observation well data. Adapted from Rollo (1966).

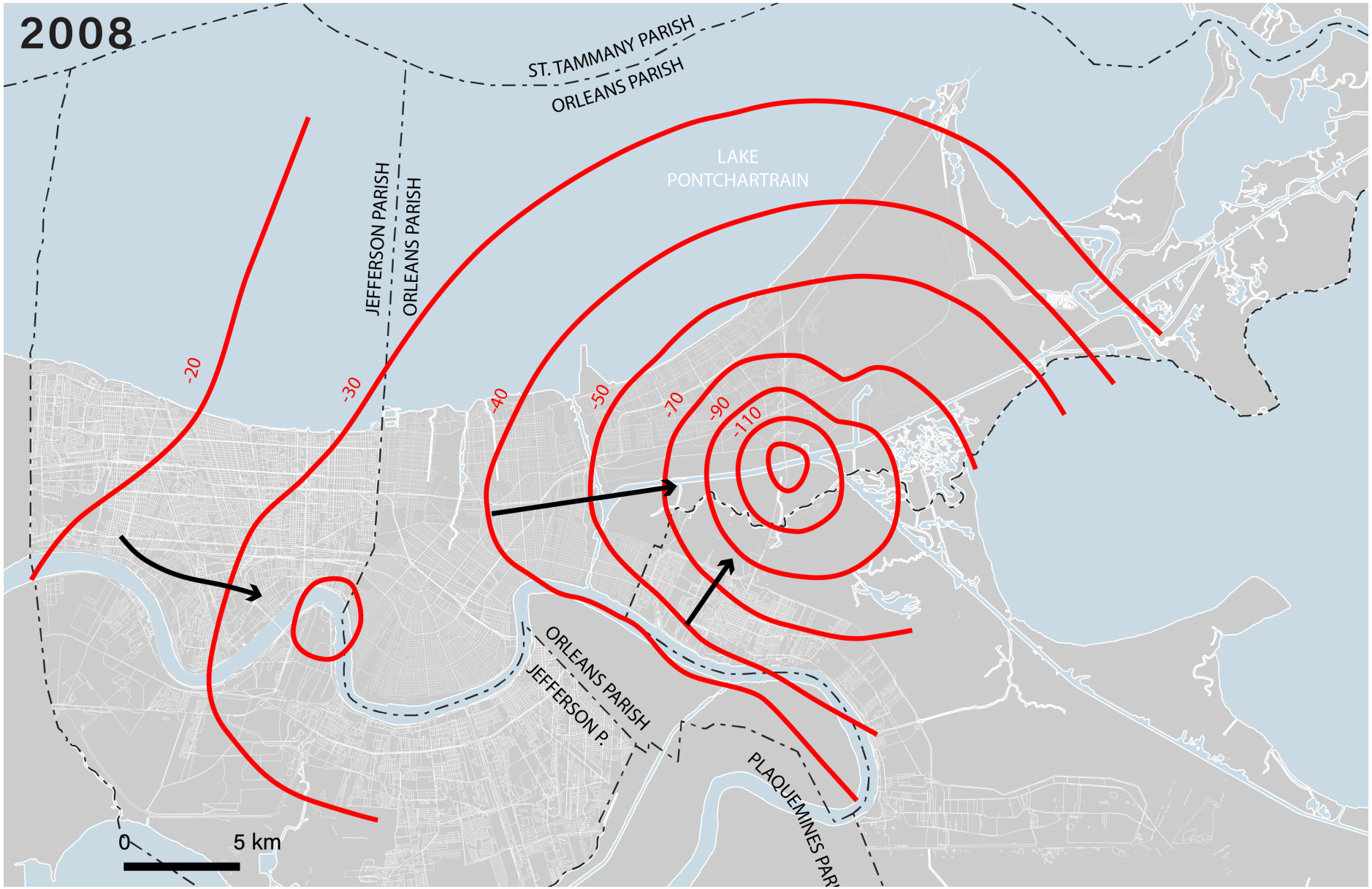

Figure 2.6 Hydraulic head of the Gonzales-NO aquifer in 2008 (feet below sea level). The contours are based on interpolation of observation well data. Adapted from Prakken (2009).

were obtained from sensitivity analysis on individual model layers. From the two parameter sets and their uncertainties, a very large set of parameter combinations for the model layers (2*3125) was constructed and tested for performance relative to the head data for both 1963 and 2008. The best 1% performing parameter sets was selected (31) and subsequently used in transient modeling for the period 1900-2010. The transient models were also combined with SUB-CR to come up with simulated subsidence for the period 1900-2010. In the latter runs, also a range of geotechnical parameter values were used to obtain a large suite of results that provide an impression of expected uncertainty in the predicted land subsidence history.

2.4 Acquisition and analysis of InSAR data

InSAR data were acquired for two satellites by SkyGeo, Delft, The Netherlands. The data were made available through a web-based portal for online study. Information is summarized in Table 2.2.

Interferometric measurements are relative, and determination of vertical movement requires calibration with an independent reference. For the calibration three different references were tested/used: (i) network referencing using multiple points in a radius of 50 km; (ii) a single tall building (Mercedes Benz, Superdome); (iii) multiple tall buildings in New Orleans. All references yielded virtually the same rates. Several checks against independent subsidence data were done and are reported in the results. Subsidence rate per scatterer (PS/DS) is based on a best-fit model that includes a quadratic term and sinusoidal component with a period of one year. The amplitude of the latter component provides a measure of seasonality in the vertical movement.

General patterns of subsidence were studied for the two periods and compared to InSAR results reported by Dixon et al. (2006) for the period 2002-2005. Special attention was paid to seasonal motion.

Table 2.2 Metrics and information about the two satellite data sets

Satellite	Period	SAR acquisitions	Tracks	Type & resolution
Envisat	2004-05-04 2009-03-24	33	Decending	PS/DS 3.9*19.2m
Sentinel-1	2016-01-28 2019-04-06	82	Ascending	PS 13.3*3.5m

3. SUBSIDENCE IN & AROUND NEW ORLEANS

Section 3.1 starts with a general description the various component processes that likely or potentially contribute to land surface movement in the Mississippi Delta (MD) and the greater New Orleans (GNO) area. Section 3.2 summarizes the findings of the literature review to elucidate the existing observational data, and to evaluate what is currently known, both about the rates of land surface subsidence, and about the contributions therein by the various component processes. Section 3.3 presents results of the modelling assessment of the role of groundwater extraction. Finally, section 3.4 provides a synopsis of the integrated results.

3.1 General overview of component processes

Similar to many other deltas in the world, the land surface subsidence in the MD and in the GNO area at present, and over the last decades, is the compound expression of various natural and man-induced processes that occur over a very large depth range, from the top few decimeters to more than one hundred kilometer below the land surface. Figure 3.1 schematically shows the component contributions that are expected to play a role in GNO and indicates the typical source-depth range of the underlying process. All component processes involve deformation of subsurface materials, except for oxidation of organic matter, which involves mass loss to the atmosphere and hydrosphere.

Isostasy refers to the bending/flexing of the lithosphere (continental crust and part of the underlying mantle) due to changes in 'surficial' loads on geological timescales. In the Mississippi delta (MD), two main components have been considered: glacio-isostatic adjustment (GIA) and sediment-isostatic adjustment (SIA). GIA is caused by load changes due to the progression and retreet of the continental ice sheets in the northern hemisphere over the last glacial cycle, and the associated changes in water mass in the Gulf of Mexico (sometimes referred to as hydro-isostasy). SIA is caused by the massive sediment deposition and southward expansion of the MD after the last ice age. The rate at which the viscous rock in the asthenosphere can flow away from subsiding areas, and toward rising areas, largely dictates the rates of adjustment. Present-day isostatic land movement, therefore, is influenced by load changes that occurred up to about thousands of years ago. Isostasy is characterized by very long wavelength variation (several hundreds of kilometers) and rather stable rates of land movement over timescales of hundreds of years.

Tectonics refers to intra-lithosphere deformation caused by intra-lithospheric extensional or compressional stresses that are of plate-tectonic origin. The prime expression is the movement on geological faults, which is characterized by localized displacements. However, faulting generally is associated with warping and bending of large volumes of crustal rock. Tectonic movement can, therefore, cause vertical land movement over extensive areas of tens of kilometers or more. On more local scales, in particular in the vicinity of faults, land movement can be irregular or intermittent on timescales varying from months to tens of years. In the MD, a special class of faults that are referred to as growth faults, are known. Growth faults in deltas are not the expression of deep plate-tectonic stresses, but develop in response to a lack of lateral support (or a backstop) due to the presence of a deep ocean water body next to the delta. Growth faults, which generally sole-out in a sub-horizontal low-friction shear zone, accommodate the lateral movement of the stack of sedimentary strata towards the ocean on geological time scales when sediments ac-

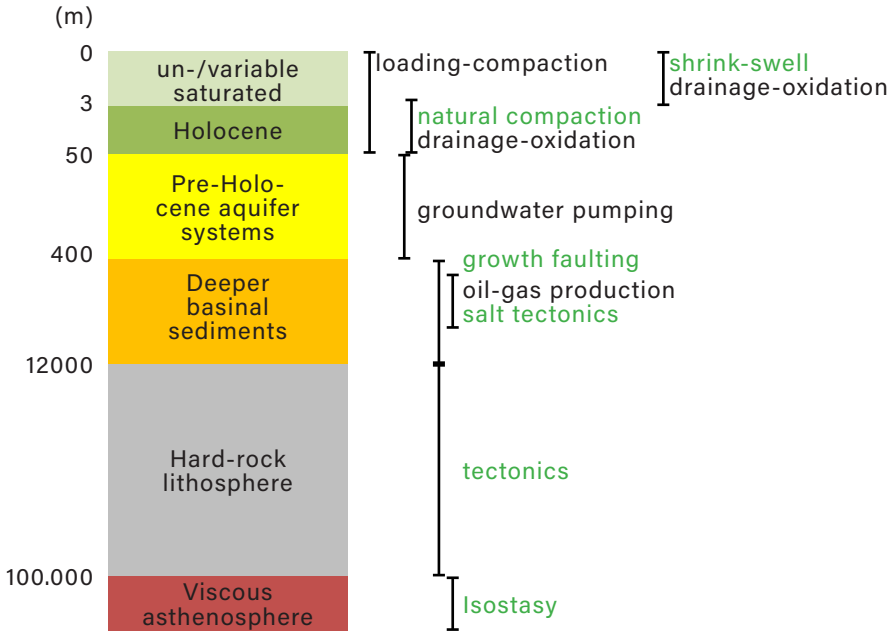

Figure 3.1 Schematic representation of the source-depth of various component processes that are expected to or potentially contribute to land subsidence in GNO. Green and black denote natural and anthropogenic components/causes. Depths (in m) are indicative. Note the depth-scale is highly non-linear for reasons of legibility.

cumulate in the delta. In the MD this shear zone coincides with extensive salt layers which extend underneath the continental shelf. During delta growth, the downward displacement on the downthrown side of the fault generally balances sediment accumulation to maintain a fairly constant topographic profile (hence the term 'growth'). Due to these characteristics, growth faults are generally considered "weak" and in a fairly critical state that readily allows further displacement. In addition to, and often associated with, faulting, salt tectonics (or: halokinesis) can further cause deformation and vertical land movement. Both subsidence and uplift can occur in particular above and in the surroundings of salt walls or salt diapirs.

Apart from oxidation of organic matter, all other processes components involve in Figure 3.1 involves vertical compression of porous sediments or sedimentary rock that may be referred to as compaction. Compaction is intimately coupled reduction of porosity and expulsion or evacuation of pore fluids (including gas) and (generally) an increase of intergranular stress (also: **effective stress**).

Oil/gas production from a reservoir causes compaction of the reservoir (and sometimes compaction of adjacent of overlying strata as groundwater moves into the pumped reservoir). Overlying strata sag in response to the reducing thickness of the reservoir. Gen-

erally, a bowl-shaped subsidence of the land surface develops that can extend several kilometers beyond the edge of the reservoir due to the strength of the strata that overlie the reservoir.

Groundwater abstraction causes compaction of fine-grained units within pumped aquifers – these intra-aquifer thin units are often called interbeds – and compaction of under- and/or overlying aquitards (Figure 3.2). Interbeds compact virtually in concert with the pore pressure decline in the more permeable parts of the pumped aquifer. Compaction of aquitards, by contrast, can develop with considerable delay relative to the head decline in the aquifer as aquitard drainage towards the aquifer is slow and the propagation of pore pressure decline away from the aquifer-aquitard interface occurs over an extended period. The delay – referred to as **hydrodynamic delay** and equivalent to the term consolidation time in the geotechnical community - can be up to a decade or more. The subsidence associated with individual groundwater abstraction wells tends to be largest in the nearfield of the well and decreases away from the well. As part of the subsidence is usually elastic in origin, some uplift can occur when hydraulic head drawdowns recover as pumpage is stopped or significantly reduced.

Progressive burial of soft-strata such as clays and peat by newly deposited sediments causes **natural compaction** of these strata. The younger sediments act as loads, analogous to artificial surface loads used in construction. The loading tends to enhance pore pressures in the soft-strata which respond by drainage and compaction. The coupled drainage and compaction response is called **consolidation**. In particular in areas with very thick low-permeable soft-strata such as in the Holocene deposits of the MD, the consolidation can be very slow (analogous to the concept of hydrodynamic delay in aquitard compaction in response to groundwater abstraction). That is, the rate of compaction and associated subsidence is slave to the rate of pore-water drainage. This implies that consolidation or compaction and, therefore, subsidence, can be ongoing decades or possibly centuries after

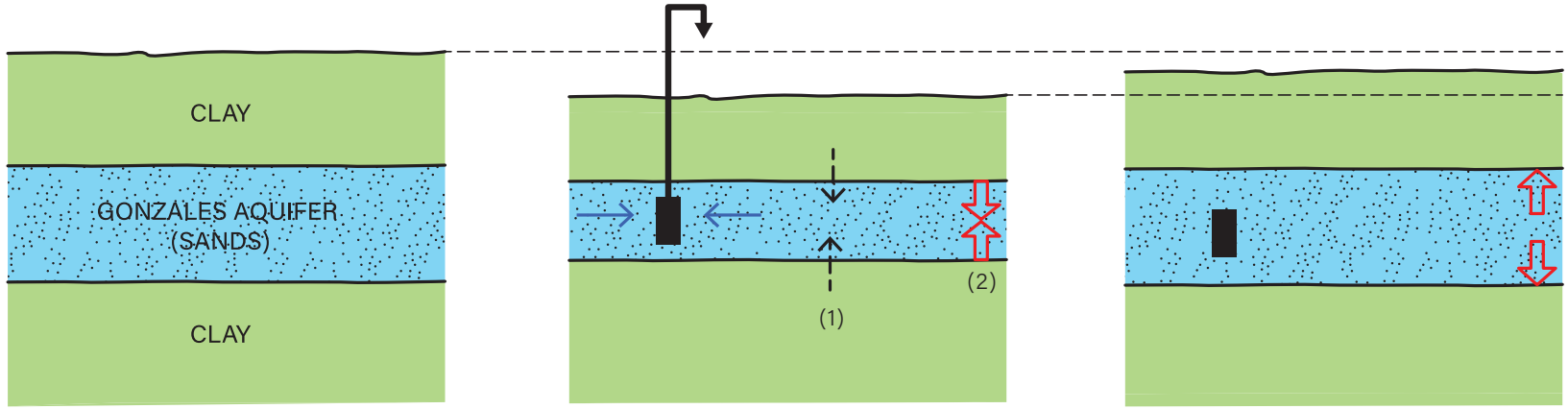

Initial situation

After start pumping, subsidence starts by (1) drainage and compaction of the under- and overlaying aquitards, and (2) compaction of the sand in the aquifer.

After pumping stops, the elastic compaction of sand grains partly recovers and relative uplift develops. The subsidence caused by drainage of aquitards will not recover.

Legend

Compaction/decompaction

Groundwater flow

Figure 3.2 Effect of pumping on the Gonzales aquifer

active sedimentation ceased. The sluggish compaction and subsidence response may be enhanced by **secondary consolidation or creep**, which refers to slow adjustments in the clay or peat fabric that causes compaction at constant effective stress (after the phase of **primary consolidation** and completion of the phase of drainage due to loading).

Anthropogenic addition of loads at the land surface, or on shallow foundations, causes **loading-induced compaction** (Figure 3.3). In engineering practice, the associated subsidence of the land surface or the construction is called settlement. The loading tends to enhance pore pressures in the soft-strata which respond by drainage and compaction (consolidation). Consolidation and associated land subsidence or settlement can occur up to several decades after the load was applied (primary and secondary consolidation).

Drainage-induced compaction is driven by intended or unintended lowering of the groundwater table by drainage of near-surface groundwater by pipes or canals/ditches. Unintended drainage is usually caused by leaky sewage or storm water drain pipes. The water table lowering lowers heads or pore pressures in, and thereby causes compaction of, underlying soft-strata. For water table lowering over extensive areas, strata up to great depth can be involved. Additionally, compaction of the more near-surface layers above the (lowered) water table can be involved. The latter contribution to land surface subsidence can be particularly large during land reclamation and drainage of wetlands where soils are, for the first time, impacted by the negative pore pressures (suction) due to the entry of air into the pores.

Where organic clays or peat are present in the shallow subsurface, intended or unintended lowering of the water table causes subsidence by **drainage-induced oxidation**. Penetration of air into the pore space causes organic solids in the subsurface to be converted to carbon-oxide and emitted to the atmosphere, causing volume loss and land surface subsidence.

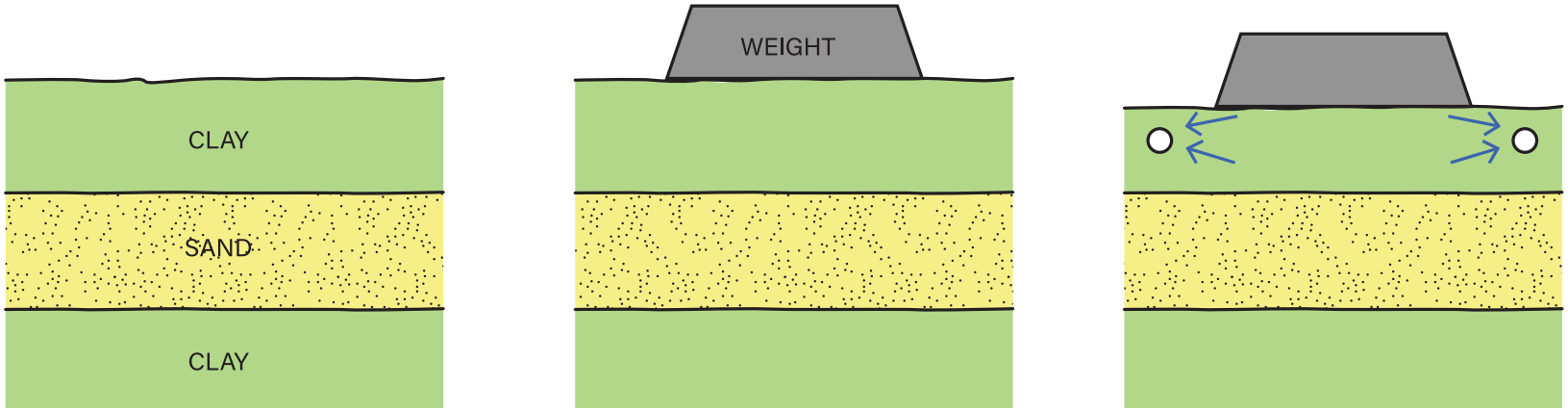

Figure 3.3 Additional compaction due to anthropogenic action.

Wetting and drying of clay-rich soils and/or peat above the groundwater table associated with weather conditions (seasonal or shorter time scales) causes **shrinkage and swelling** of these soils. This results in dynamic land surface movement, alternating between uplift and subsidence. Movement of the order of one centimeter is common but can reach more than one decimeter for very susceptible soil conditions. Shrink-swell behavior has important implications for land subsidence since the dynamic nature of land surface motion can obscure the longer-term trend of land subsidence when temporal spacing of measurements is sparse, as is typically the case with various observational methods such as geodetic leveling or air-borne techniques with a long temporal baseline.

3.2 Literature review

The ultimate challenge is to accurately characterize the changes in elevation associated with subsidence, and to separate out, or deconvolve, the large suite of processes that contribute to the total subsidence on temporal and spatial scales that are relevant to policy and management (Allison et al., 2016). To date, many studies have provided input for this challenge using various types of observational data, theory and modelling. Our assessment of the literature is as follows.

3.2.1 Observational data

Different types of observational subsidence data have been used to assess subsidence in southern Louisiana and GNO. These data vary hugely in temporal resolution, represented period/epoch, spatial resolution and coverage, depths in the subsurface the movement pertains to, and reference frame. The types of data are discussed first. Findings and inferences from the data are discussed in the next section.

Geological data

Chronostratigraphic data, primarily of Holocene strata, have been collected and used to constrain subsidence in the MD. Basal peat data have been used to reconstruct Holocene (last 10 ky) relative sealevel (RSL) rise for different parts of the delta and adjacent areas. Comparison of the various local RSL curves provides valuable constraints on differential subsidence of the underlying Pleistocene surface (e.g., Törnqvist et al, 2006; Yu et al, 2012). Additionally, the present depth of a dated (1,400 years before present), buried late Holocene surface near Paincourtville in the western delta has been used to estimate the subsidence of that surface since its dated age (Törnqvist et al, 2008). Together with other information such as a nearby RSL curve inferred from basal peat, and a strong positive correlation of inferred amount of subsidence of the dated surface with present overburden thickness, the subsidence has been attributed to (natural) compaction of the underlying Holocene strata. It is of fundamental importance that the subsidence estimates derived from these geological data are millennial-scale averages and cannot be considered representative for the past decades, past century, the present, or the near future unless the dominant underlying subsidence mechanism can be considered stable on time scales of a millennium or more. Late Pleistocene (130-120 and 80 ka) long-river profiles along the lower Mississippi river have been invoked to estimate the long-wavelength (hundreds of kms) subsidence and uplift since those times by taking the difference with the present-day long river profile (Wolstencroft et al, 2014). Chronostratigraphic data have also been used to estimate long-term average throw rates across the Tepetate-Baton Rouge fault zone which bounds the MD to the north (Shen et al., 2016). Although the (very low) relative subsidence rate estimated this way can be linked with high confidence to a tectonic origin, similar to the other the estimates from chronostratigraphy, the inferred rates may not be representative for recent times or the near future. A similar approach was used to estimate average through rates across the Michoud Fault near Michoud, albeit for time intervals that span at least one million years (Edrington et al, 2007). Morphological observations have also been interpreted in some studies as indicators for historical or recent fault activity.

Maps/DEMs with (historic) elevation information

In 2006 URS Consultants from Baton Rouge completed a study for FEMA of the vertical ground movement in New Orleans between 1895 and 1999 by using mapped elevations for those years. A Digital Elevation Model (DEM) for 1895 was created from a historic contour map and compared to the 1999/2002 DEM extracted from LiDAR data and benchmark (elevation) data. The map was published in the report of the Independent Levee Investigation Team (ILIT) report in 2006 and is shown in Figure 3.4. It is important to realize that the DEMs that underlie the subsidence map are interpreted data (information), each with its own uncertainty/accuracy. However, since the subsidence map includes rather large subsidence magnitudes, the general patterns are expected to be reliable.

Geodetic leveling data

The NOAA/National Geodetic Survey (NGS) archives contain geodetic leveling data for the MD and surrounding areas that allow study of height changes of individual benchmarks for various periods since at 1955. Although some studies used straightforward differencing of elevations recorded for different times (e.g., Zilkoski and Reese, 1986; Burkett et al, 2003), this approach is considered problematic to infer land subsidence because of the way recorded benchmark heights are established (Dokka, 2011). Proper subsidence studies, therefore, only

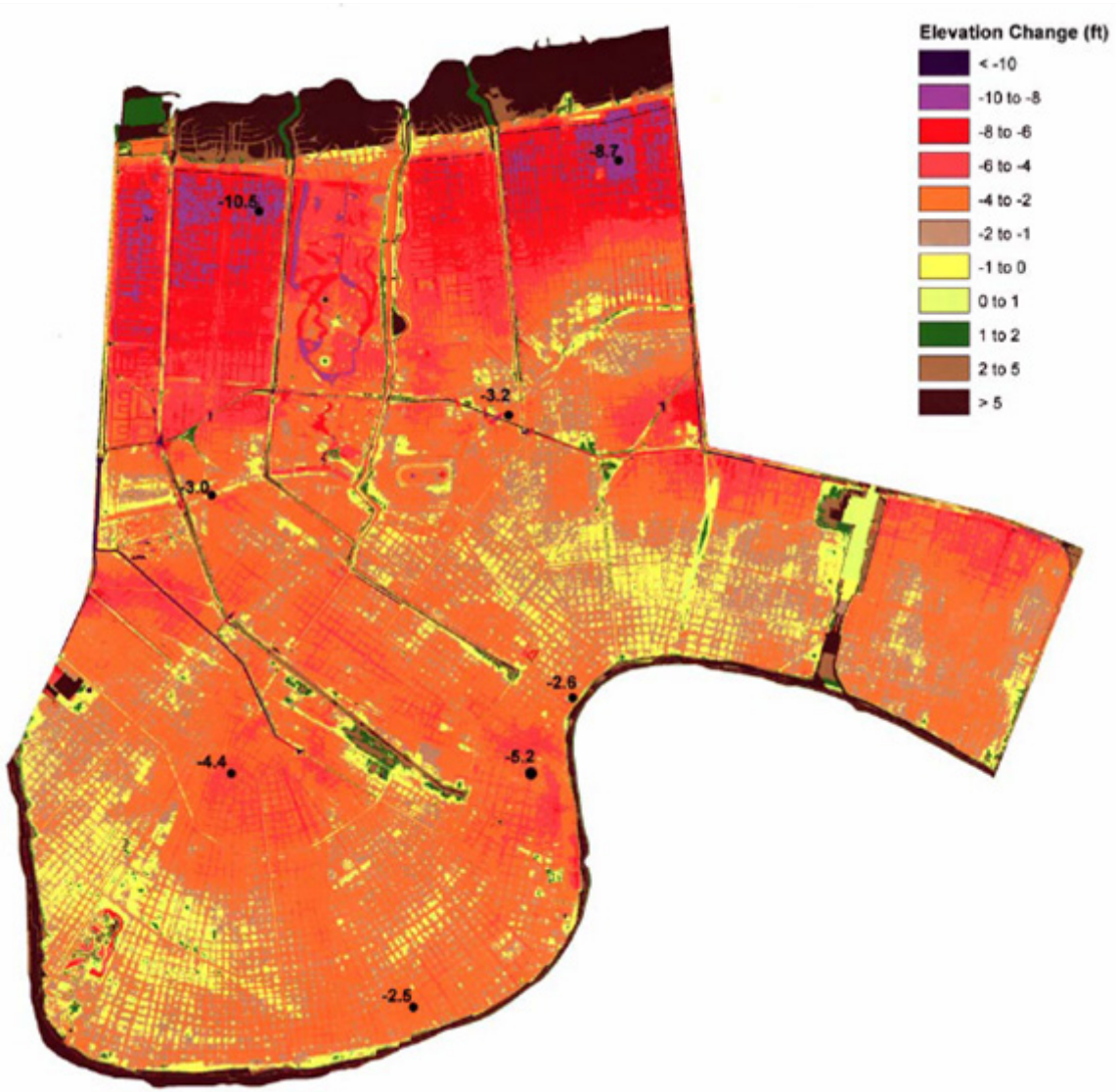

Figure 3.4 Map showing relative elevation change between 1895 and 1999/2002 estimated by differencing an historic elevation map and a 'recent' lidar-based DEM. From: ILIT (2006; chapter 3).

analyse the field height differences between adjacent benchmarks measured in the original surveys and connect the network to a common datum (Shinkle and Dokka, 2004; Dokka, 2006, 2011). Although this yields properly calculated height changes for the monuments or structures to which the benchmarks are attached, use in land subsidence investigation must be done with great caution since the monuments and structures record movement at different depths (shallow and deep foundations), some monuments or structures may be instable and move relative to the ground, and because temporal sampling of the measurements tends to vary (different periods from one benchmark to another).

Shinkle and Dokka (2004) produced subsidence rate estimates for multiple transects of first-order benchmarks across the state of Louisiana and beyond. Dokka (2006) presented subsidence estimates for benchmarks with both shallow and deep (top Pleistocene to > 2000 m) foundations in the Michoud area of Orleans Parish (Figure 3.4). Dokka (2011) reported results for a transect from Biloxi, MS, to New Orleans only using benchmarks affixed to deep rods that penetrate Holocene strata (Figure 3.5).

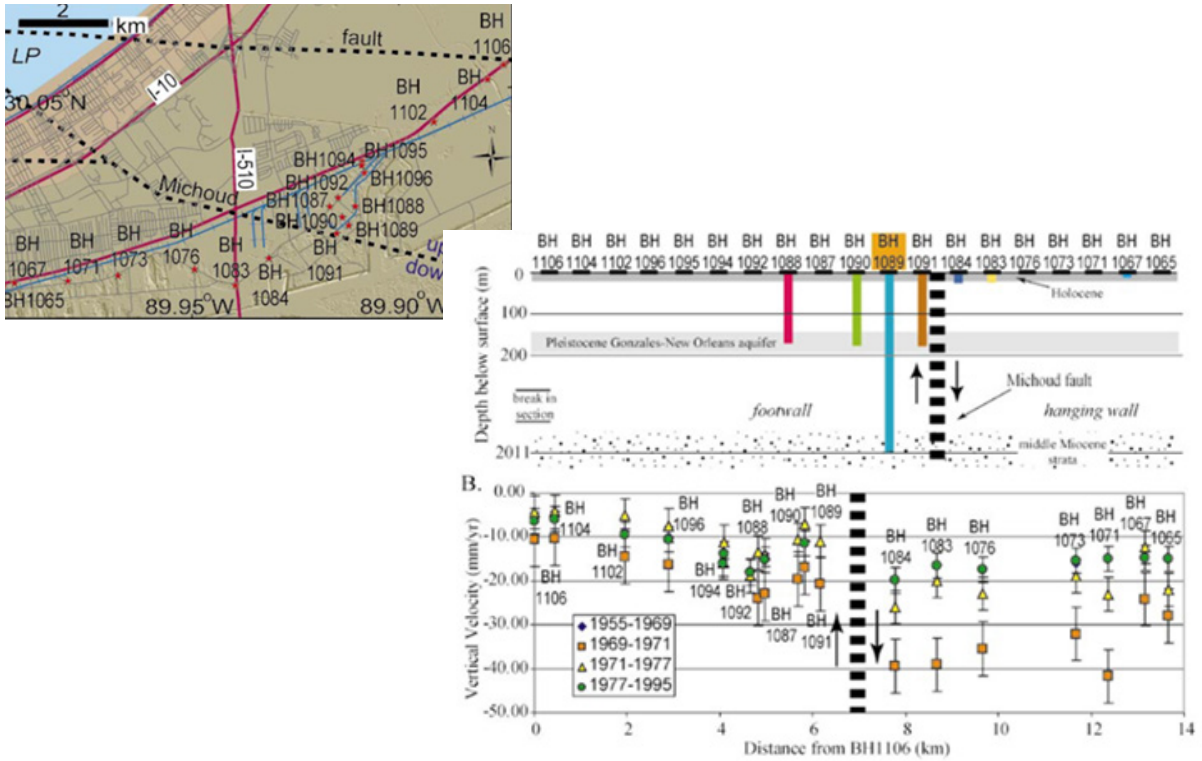

Figure 3.5 Subsidence rates for several epochs (lowest panel) inferred from leveling data for the cross-section shown in the top panel. The middle panel shows the footing depth of structures to which the benchmarks are attached. Three are based in the Gonzales aquifer, one to a depth > 2 km. Note that the middle and lower panel show results from east to west (right to left on the map, or view from the north). From: Dokka (2006)

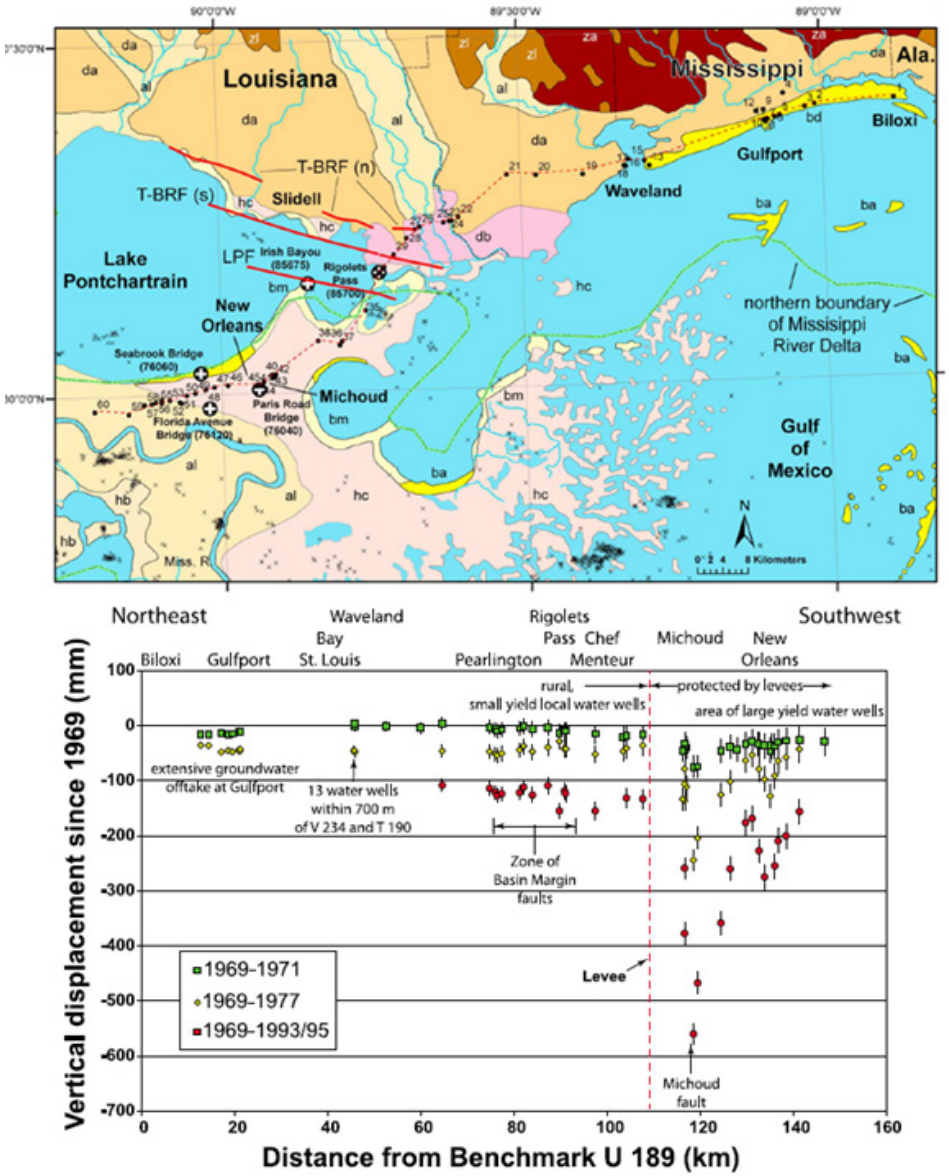

Figure 3.6 Subsidence for three epochs since 1969 inferred from leveling data. Note that the cross-sectional data shown in the lower panel correspond to a view from the north. From: Dokka (2011).

Tide gauge and water-level gauge data

Several tide gauges in the MD and surroundings record local relative sea-level rise (RSLR) relative to the associated structure to which the gauge is attached, which, in turn, is referenced to a nearby benchmark. RSLR records, therefore, include subsidence of (the base of) the associated benchmark (Keogh and Törnqvist, 2019). Of these gauges, the tide gauge of Grand Isle (GRIS) has been used most extensively because it has a relatively long record (1947-present). It may be relevant to note that the base of the GRIS benchmark is situated about 37 m above the top of the Pleistocene. Shinkle and Dokka (2004) and Dokka (2006; 2011) used the GRIS gauge to establish a fixed reference level for their analysis of leveling data (to approximate (NAVD88). Kolker et al (2011) compared the GRIS RSLR record with that of the tide gauge station at Pensacola, FL, to infer a subsidence contribution at the GRIS gauge.

Dokka (2011) also used five U.S. Army Corps of Engineers water level gauges in and near New Orleans East. Differencing of the records relative to the one at Rigolets Pass Bridge was used to remove a (presumed) common water level change component, and subsidence of a benchmark attached to Rigolets Pass Bridge was added to add back subsidence at that bridge. In this way subsidence records were constructed for all five gauge stations.

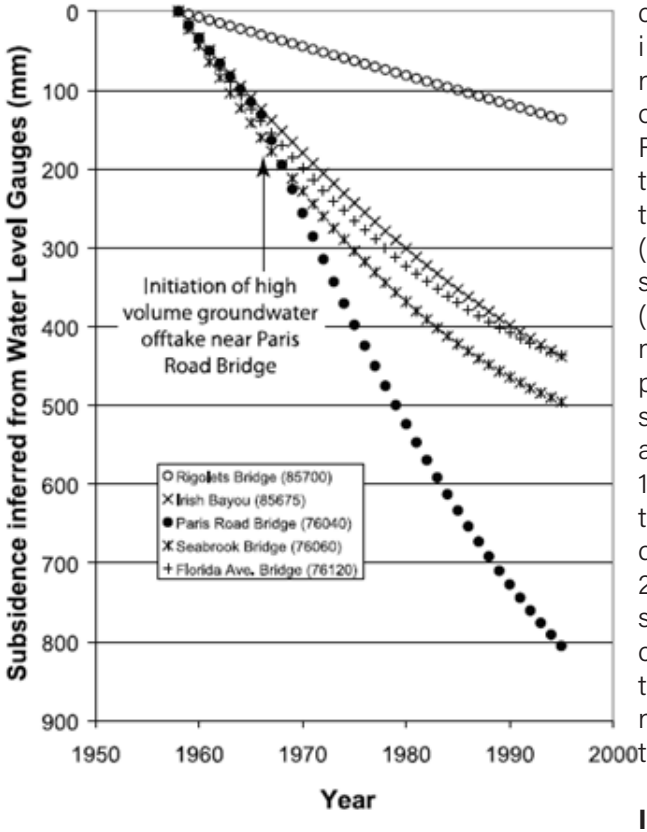

Figure 3.7 Subsidence inferred from USACE water level gauges shown on the map of Figure 4.3 (black-filled circles with white cross). From: Dokka (2011).

GPS data

GPS stations have been installed in Louisiana since the mid 1990's. Dokka et al (2006) analysed the records of both episodic (EGPS) and continuous (CGPS) GPS stations covering a period up to about one decade. The data revealed very minor motion in central and northern Louisiana, but significant subsidence and southward motion of the stations south of the Tepatate-Baton Rouge fault. Karegar et al (2015) expanded the analysis more recently with extended time series (4 – 18 years) and new stations (Figure 4.6). Results largely confirmed the subsidence patterns inferred by Dokka et al (2006), but yielded a lower rate of southward motion. Keogh and Törnqvist (2019) emphasized that the GNSS stations (n=10) in southern Louisiana are anchored between 1 and 36.5 m below land surface and between 10 and 78 m above the top of the Pleistocene. For many stations the foundation depth appears to be unknown (Karegar et al. 2015; supplementary materials). Via the website of the Nevada National Laboratory data can be accessed for other GPS stations than those used in the above studies and that do not appear to be present in the database of the National Geodetic Survey.

InSAR data

Using satellites the movement (elevation change) of the earth surface can be monitored very accurately (mm). Interferometric Synthetic Aperture Radar (InSAR) uses phase differences between consecutive radar images of the same area to infer elevation change (elevation is poorly constrained). A key advantage of InSAR over the methods discussed previously is the large spatial density of subsidence information that is obtained. A drawback is that the position and nature of individual scatterers (points at or near the land surface that return a meaningful signal) is not precisely known. InSAR generally contains mixed information of subsidence from the land surface (e.g., roads) and from buildings and constructions with different foundation depth. InSAR based on satellite images exploit the high frequency of imaging, allowing construction of detailed time series of subsidence. Dixon et al (2006) used 33 scenes acquired by RADARSAT (C-band) to map subsidence for the period 2002-2005 in GNO (Figure 3.5). Jones et al (2016) used two scenes (L-band) obtained with an unmanned aerial vehicle about three years apart to quantify subsidence between June 2009 and July 2012 for roughly the same area.

In section 3.4 new InSAR data for the Envisat (2005-2009) and Sentinel-1 (2016-2019) satellites are presented.

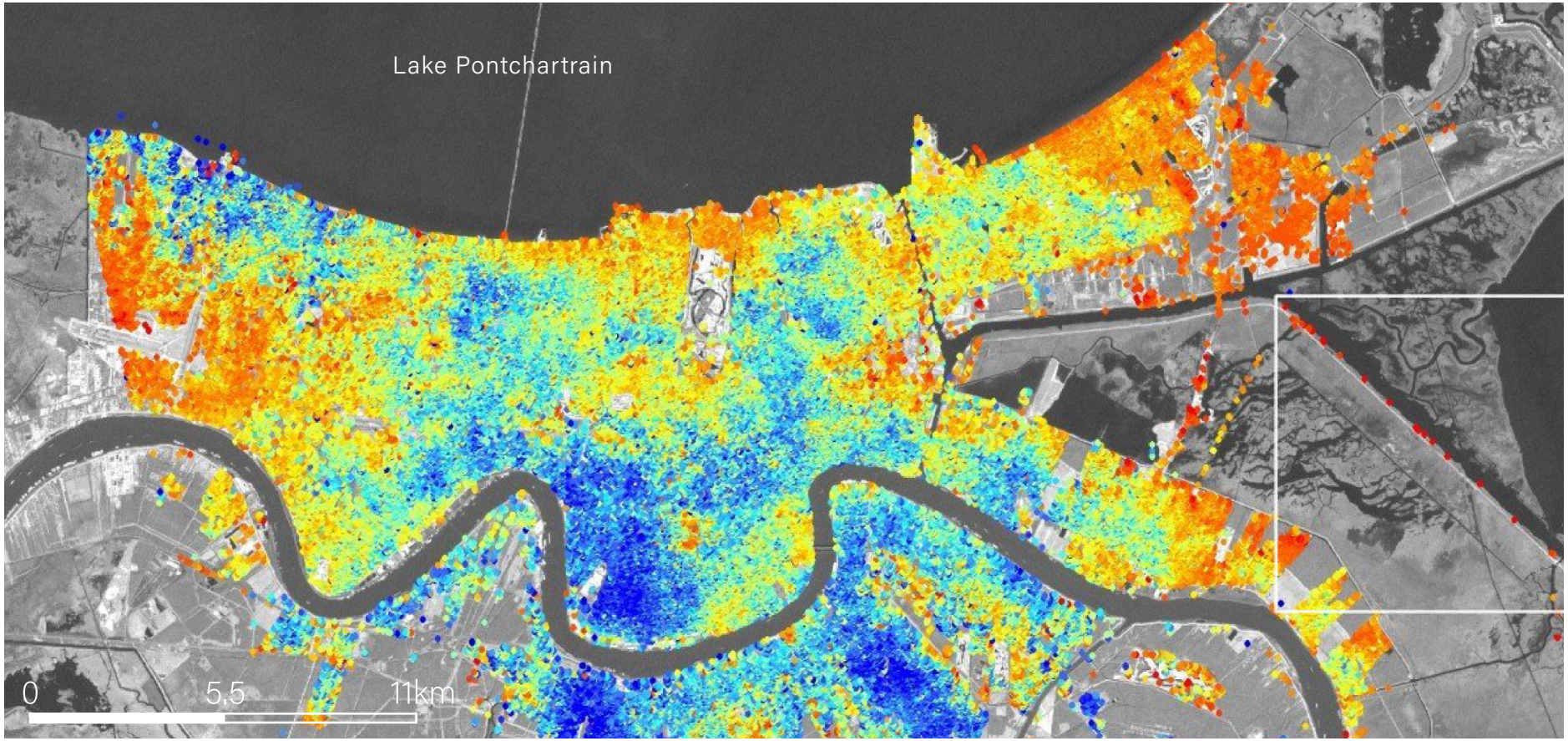

Figure 3.8 Rates of vertical (land) movement derived from InSAR data (2002-2005) in mm/yr. Negative indicates subsidence. From: Dixon et al (2006). Movements are referenced wrt a GPS station (ENG) SE of the city.

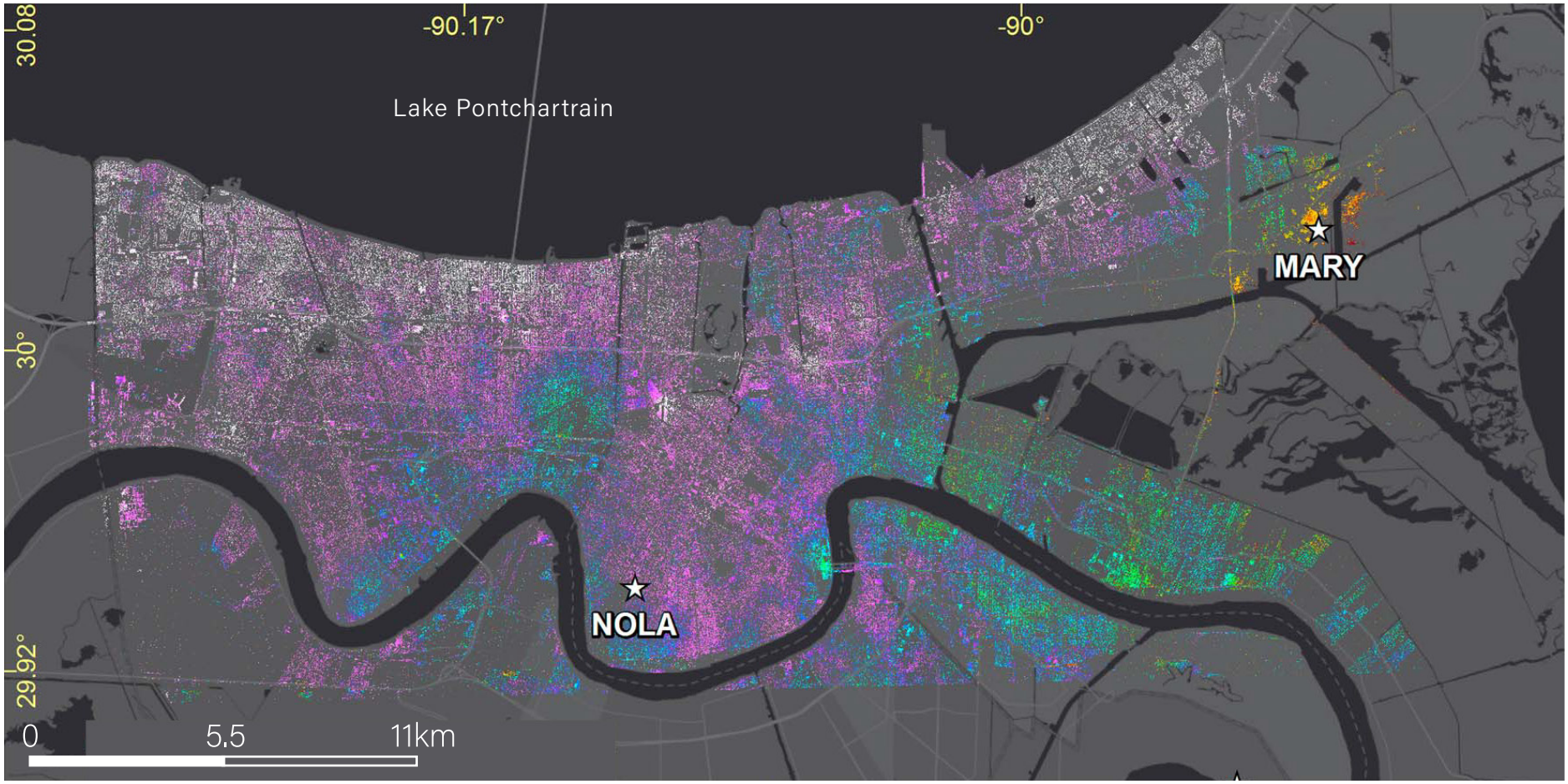

Figure 3.9 Rate of vertical (land) movement inferred from InSAR data (two images 6/2009-7/2012) in mm/yr. Negative indicates subsidence. From: Jones et al (2016).

Extensometry
Borehole extensometers are used to measure the continuous change in vertical distance between the land surface and a reference point in the subsurface (base of a rod hammered till refusal or attached to the soil with an anchor). When multiple reference points are used at different depths in a single borehole, the thickness change can be inferred for intervals between the reference points. We are only aware of single-reference point systems in the MD. In a powerpoint presentation, Mugnier (2014) shows an extensometer at Cocodrie that recorded 15 inches of land surface subsidence between 1986 and 2001 (1 inch/year) relative to the reference point (originally) at 8.3 feet below ground surface. Since 2006, several hundred special type of extensometers - the Coast-wide Reference Monitoring System - were installed in the coastal zone of Louisiana through a partnership of the United States Geological Survey and Louisiana's Coastal Protection and Restoration Authority. These instruments are called 'rod surface-elevation table-marker horizon stations' (RSET's). RSET's measure both the subsidence of the original surface relative to the base of the rod (about 20 m depth) and the vertical accretion of sediment above the original surface (Figure 3.9). Jankowski et al (2017) reported subsidence (and accretion) rates for 274 RSET's in the coastal area of the MD and the Chenier plain to the west.

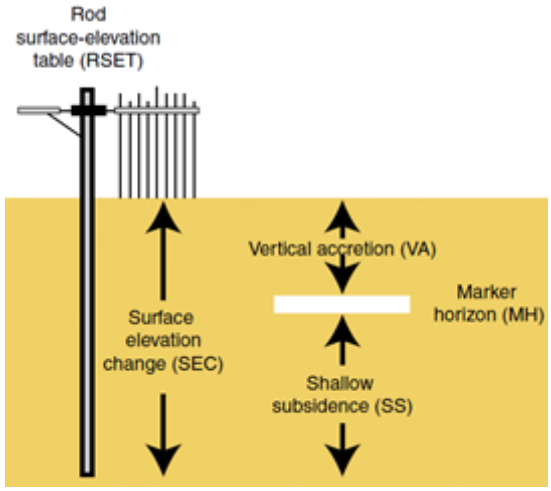

Figure 3.10 Concept of a rod surface-elevation table-marker horizon station (RSET) to measure both 'shallow subsidence (SS) and vertical accretion (VA). From: Jankowski et al (2017).

3.2.2 Inferences regarding (land surface) subsidence and the role of component processes

In this section we give our assessment of subsidence in the MD and GNO based on the consulted subsidence literature. We do this by first discussing what is known about the component processes distinguished in 3.1. Then we discuss what this means for total (land surface) subsidence. Component processes are first discussed on the wider scale of the MD. Then the areas of GNO and, in particular Michoud, are addressed.

Isostasy
Present-day isostatic subsidence is rather well constrained through process modeling and observational data (Figure 3.4). The rates are consistent with geological observational data (Holocene RSL curves in the MD and late Pleistocene long-river profiles extending to northern Louisiana). Subsidence at GNO is about 1.4 mm/yr. Wolstencroft et al (2014) convincingly show that the isostatic signal is dominated by GIA (glacio- and hydroisostatic adjustment) and that SIA (sediment-isostatic adjustment) plays a very minor part.

Interestingly, GPS stations in and to the north of GNO show rates of vertical land movement (Figure 3.5) that are very similar to the expected isostatic values for various recent periods (4 – 18 yr) (Karegar et al 2015). Jones et al (2016) reported a similarly low rate for GPS (CORS) station in Michoud (MARY) with a foundation at more than 2 km depth (rate: -1.3 mm/yr), as well as for a few other GPS stations in GNO. This suggests that apart from isostasy, in recent years, other subsidence components play a minor role below the footing of the structures on which the GPS stations are mounted. These GPS observaions do not allow inferences regarding shallow subsidence contributions from depths above the GPS footing. Isostatically driven subsidence at GNO is 1.4 mm/yr. More to the south GPS stations show considerably higher subsidence rates (Figure 3.5) indicating that additional subsidence components are involved.

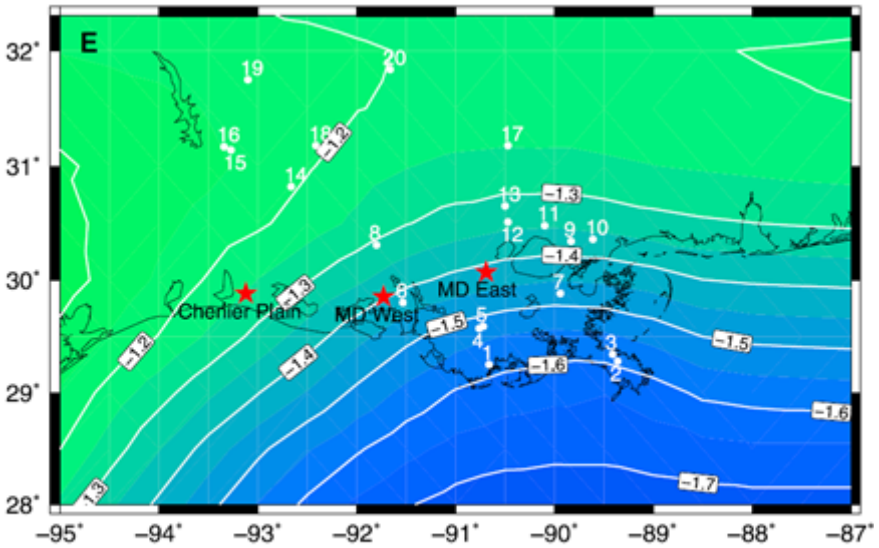

Figure 3.11 Contour map of present-day isostatic land subsidence rates (mm/yr). From: Wolstencroft et al (2014).

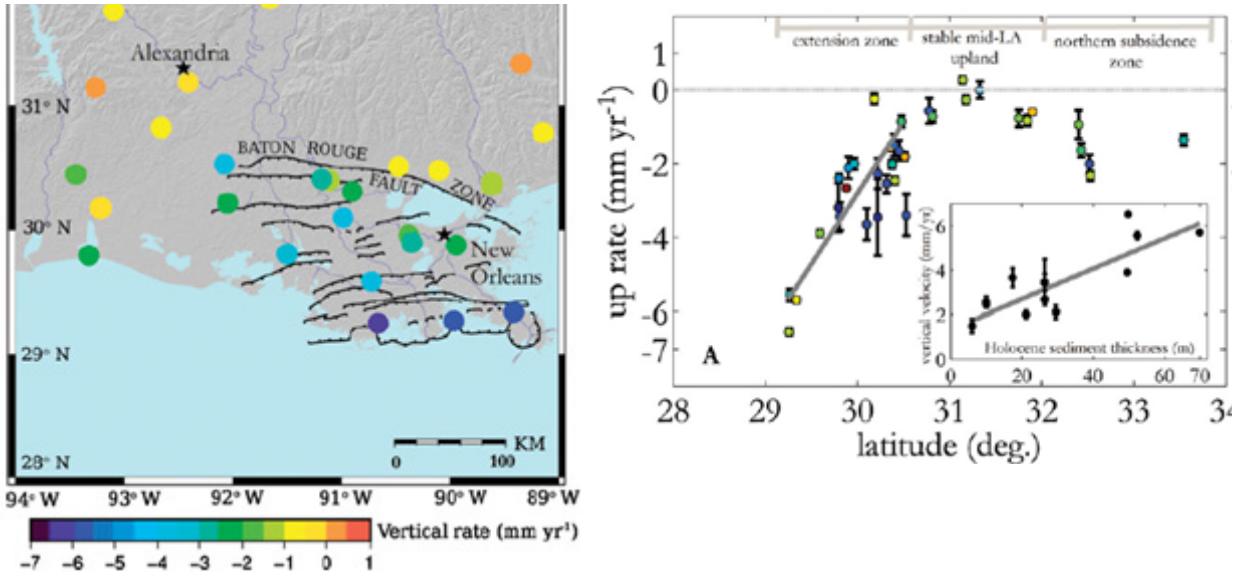

Figure 3.12 Vertical rates inferred for GPS stations in southern Louisiana. Left panel: map view; right panel: latitude-based south-north cross-section. From: Karegar et al (2015).

Superstations Myrthe Grove (in the wetlands east of New Orleans) shows for that location that current overall subsidence is mostly by deformation of Pleistocene and underlying strata (approx. 2.5 mm/yr)x. The authors (Zumbergh et al., 2022) attribute this to the glacial and sedimentary isostatic adjustment (GIA and SIA) and perhaps oil and gas mining contributions.

Tectonics

Compared to isostasy, the role of tectonics in land subsidence is very uncertain. It seems evident from geological data that tectonics has not played a significant part during the Holocene in the MD; average rates over time periods of one to ten thousand years are < 1 mm/yr (Yu et al 2012; Shen et al 2016). However, to explain high late 20th century and early 21st century subsidence rates inferred from geodetic data, tectonic subsidence has been invoked in several publications by Roy Dokka.

In an earlier study of GPS data that was later extended by Karegar et al (2015), Dokka et al (2006) proposed that the southward increasing subsidence rate south of GNO that was inferred from GPS data (right panel Figure 3.5), is the result of southward sliding of much of the MD above a large south-dipping detachment fault (gowth fault) that extends beneath the Gulf of Mexico (Figure 3.6).

Although this is an elegant proposition, in particular since GPS stations in the MD

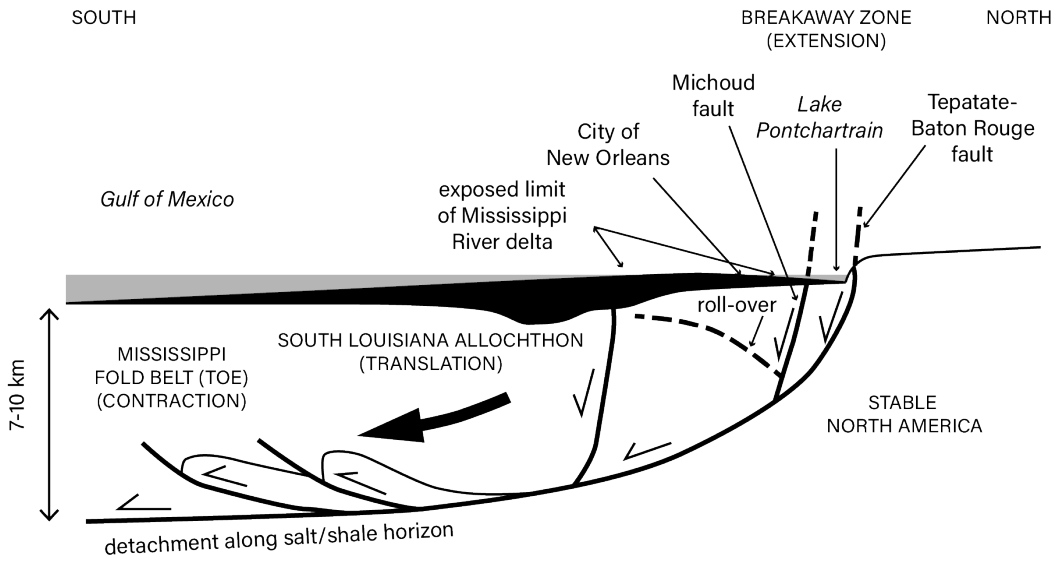

Figure 3.13 Conceptual idea of tectonic mechanism proposed by Dokka et al (2006) to explain high late 20th century subsidence rates in the MD south of the city of New Orleans.

also show a small southward motion relative to parts of Louisiana just to the north, it is by no means established that such a tectonic process is at play. The base of the monuments or structures on which the GPS stations are mounted generally sitting within the Holocene soft-sedimentary strata, often several tens of meters above top of the Pleistocene (Jankowski et al. 2017; Keogh and Törnqvist 2019). Other component processes, including natural compaction of (Holocene) sediments, and possibly (delayed) compaction due to hydrocarbon production below the base of the foundations, may therefore provide equally or even more-viable alternative explanations for the southward increasing subsidence in the MD. Several studies have proposed that if fault movement does indeed play a role in the subsidence, it may involve reactivation due to massive hydrocarbon production (Morton et al 2006; Meckel, 2006). In the absence of ample observational data, it is currently not possible to unequivocally discriminate among the various alternatives.

Dokka (2006, 2011) further proposed that displacement of the Michoud Fault in Michoud, would explain high subsidence rates between 1969 and 1995 in that area (Figure 3.4 and Figure 3.5), probably in response to large-scale industrial groundwater abstraction.

We have not found studies dealing with recent salt tectonics in the MD. Figure 3.6 shows that there are salt domes in the south-western MD, including ones pretty close to GNO.

Natural compaction

The best constraints on the present-day natural compaction contribution land subsidence have been obtained from the 274 RSET measurements in the coastal area of the MD and the Chenier plain (Jankowski et al 2017). The direct measurements of compaction over the rod depths (typically about 23 m) have been made in wetlands over a period up to 9 years and are unlikely to contain a significant anthropogenic component. The compaction rates have a median value of 6 mm/yr. However, it should be noted that spatial variance is very high (Figure 3.14). It is unclear if this variance reflects variance of natural compaction, or a spurious effect of the potentially limited precision of the measurement over the relatively short period of measurement. If it is a natural variance, land subsidence inferred from benchmarks and GPS stations with a relatively shallow foundation would also include this variance.

The natural compaction rates of Figure 3.5 underestimate the total natural compaction rate of the Holocene (and potentially deeper) strata because of the limited depth of the RSET-rods (top ~ 20 m). Moreover, it is pres-

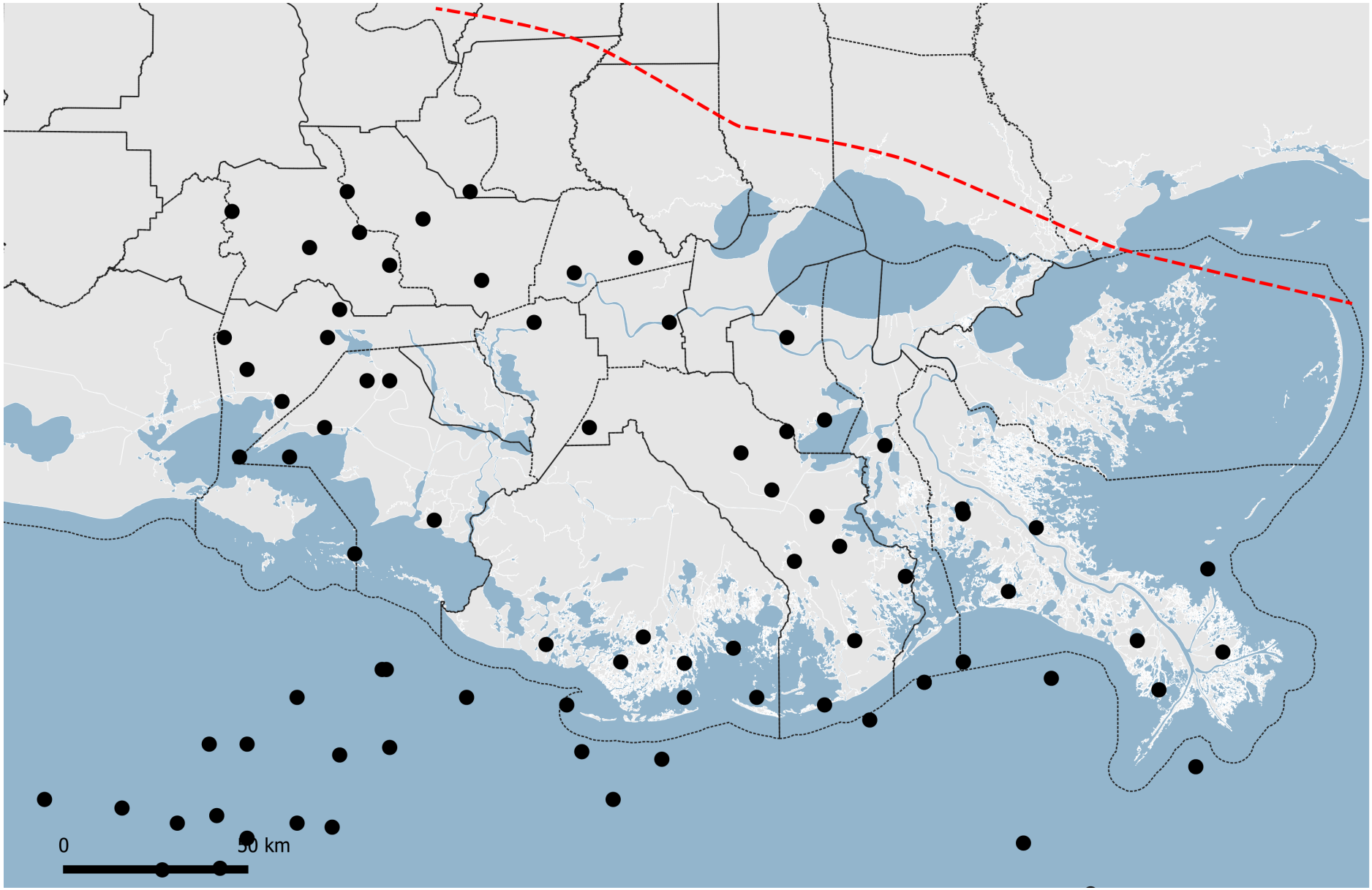

Figure 3.14 Black dots indicate the location of (known) salt domes that penetrate the base of the middle Miocene (~ 800 m depth). Modified from: Beckman and Williamson (1990).

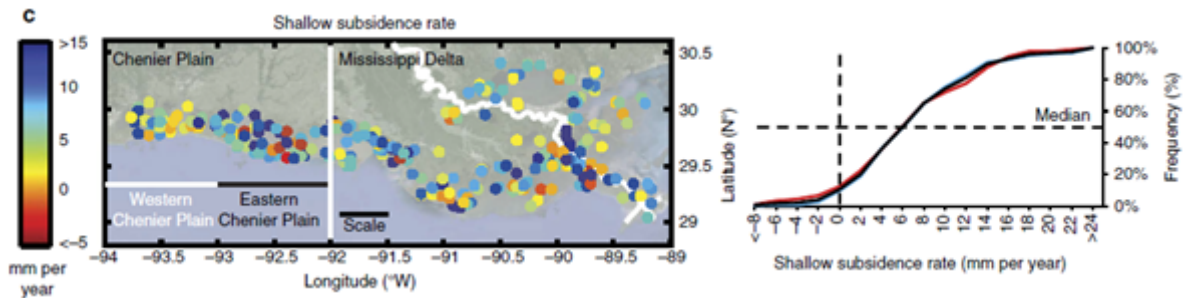

Figure 3.15 Natural compaction rates inferred with RSET measurements from the Chenier Plain to the west to the bird-foot delta in the east. The right panel shows the cumulative frequency distribution of the rates with a median value of 6 mm/yr. From: Jankowski et al 2017.

ently unknown how natural compaction rates would change to more northern parts of the MD and in GNO. Meckel et al (2006) found considerably lower estimates of present-day natural compaction rates from modeling (5 mm/yr requiring exceptionally favorable conditions and including compactable strata to great depth). The observation that for the RSET measurements over a limited depth 5 mm/yr is very typical indicates that the model underestimates potential natural compaction rates, possibly by neglecting creep processes. Although a comparable natural compaction rate of 5 mm/yr has also been inferred from geological data (Törnqvist et al, 2008), this is a local estimate and represents an average over a timescale of more than one millennium, and, therefore, should not be considered an estimate for the present-day.

Hydrocarbon production

South of Lake Pontchartrain, numerous oil- and gas fields occur in the MD (Figure 3.16 anf Figure 3.17). Production of oil and/or gas has, therefore, undoubtedly contributed to land subsidence, in particular since the late 1950's.

Kolker et al (2011) differenced the tide gauge record of Grand Isle (GRIS) against that of Pensacola, FL, to separate a land subsidence time series for that location. The result revealed a temporally varying subsidence pattern with rather low rates in the periods 1947-1958 and 1992-2006, but a much higher rates in the intermediate period (1959-1992) with a peak rate in the period 1959-1974 (left panel Figure 3.8). Temporal correlation of the subsidence rate with oil production (and land loss; not shown) in south Louisiana led the investigators to conclude that the subsidence in the period of high subsidence rates is closely linked to hydrocarbon production (right panel Figure 3.8).

Voyiadjis and Zhou (2018) proposed that local scale relatively greater subsidence rates inferred by Shinkle and Dokka (2004) for a transect along highway 1 from Raceland to Grand Isle in their leveling study, are caused by enhanced subsidence by to hydrocarbon production (Figure 3.8). During the first period (1965-1982) fluid production peaked with significant pore pressure drawdown, and pore pressures slightly recovered during the second period (1982-1993). The leveling data indicate that subsidence rates were higher during the second period.

Voyiadjis and Zhou (2018) explain the delayed, accelerated subsidence after reservoir depletion by a combined effect of slow drainage (and pressure diffusion) in shales over- and underlying the reservoirs and an elasto-viscoplastic model for the rock-mechanical behavior of the shales. Although this might be a possible explanation, a role for tectonic deformation following the ideas put forward by Dokka (2006) cannot be ruled out. Furthermore, fault movement may also be induced (reactivated) by stress changes associated with reduced reservoir pressure (Figure 3.10) (Morton et al 2006; Chan and Zoback 2007). Natural compaction, however, is not likely to account for the higher subsidence rate in the more recent period following reservoir depletion.

It may be worth noting that where Voyiadjis and Zhou (2018) propose a large subsidence delay to be a prime characteristic of

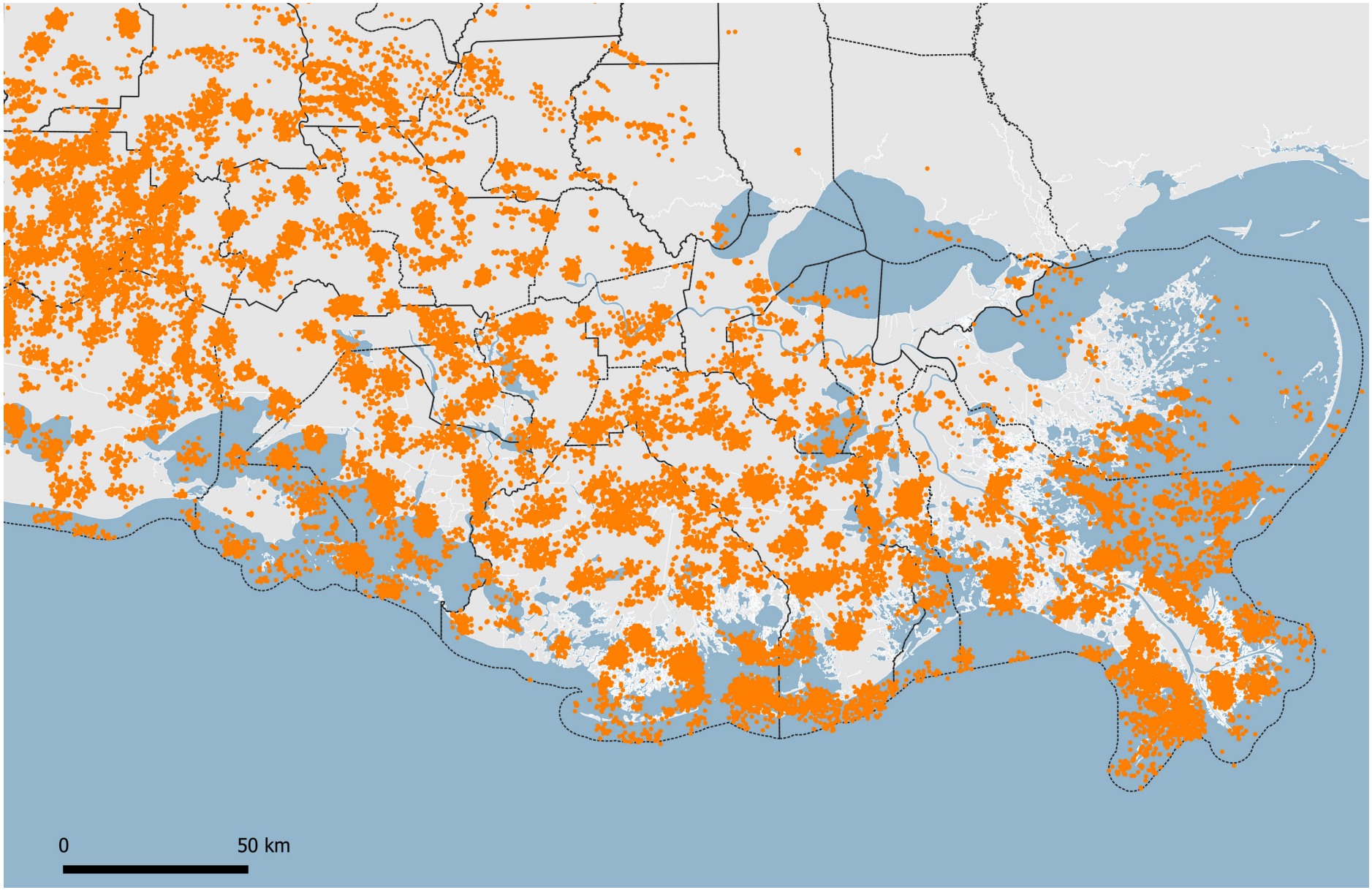

Figure 3.16 Oil/gas fields in southern Louisiana. Data from: https://data.doi.gov/dataset/louisiana-gas-and-oil-fields-with-cumulative-production-from-1977-20143f413

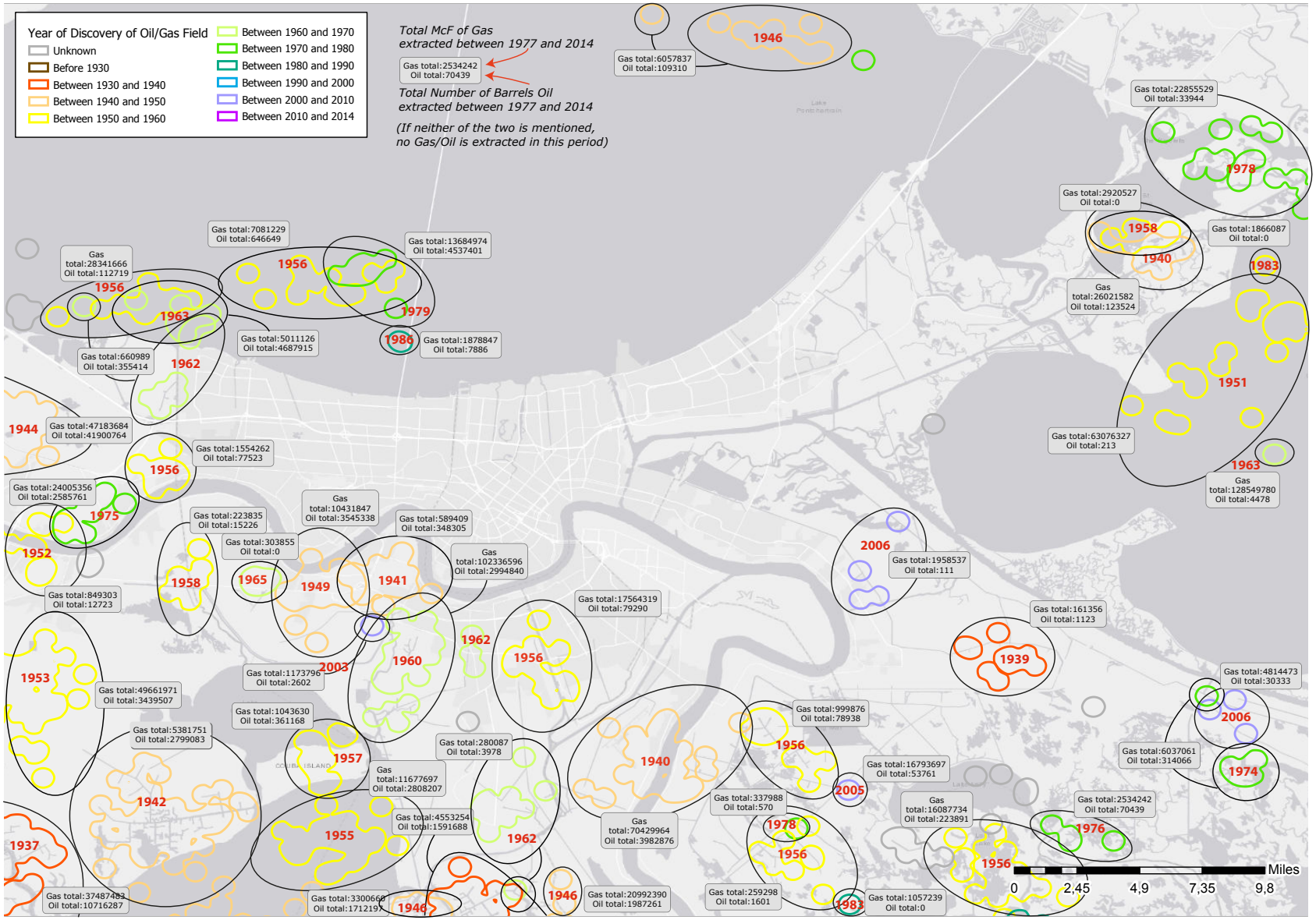

Figure 3.17 Oil/gas fields in southern Louisiana

the subsidence behavior associated with hydrocarbon production in reservoirs in southern Louisiana, Kolker et al (2011) use a direct correlation without invoking any delay. Together this indicates that understanding of the impact of hydrocarbon production is still limited and inconclusive.

The map of Figure 3.13 does not show hydrocarbon reservoirs close to the locus of the largest subsidence in the late 20th century in the Michoud area. It seems less likely, therefore, that hydrocarbon production plays a role in the subsidence in and around Michoud.

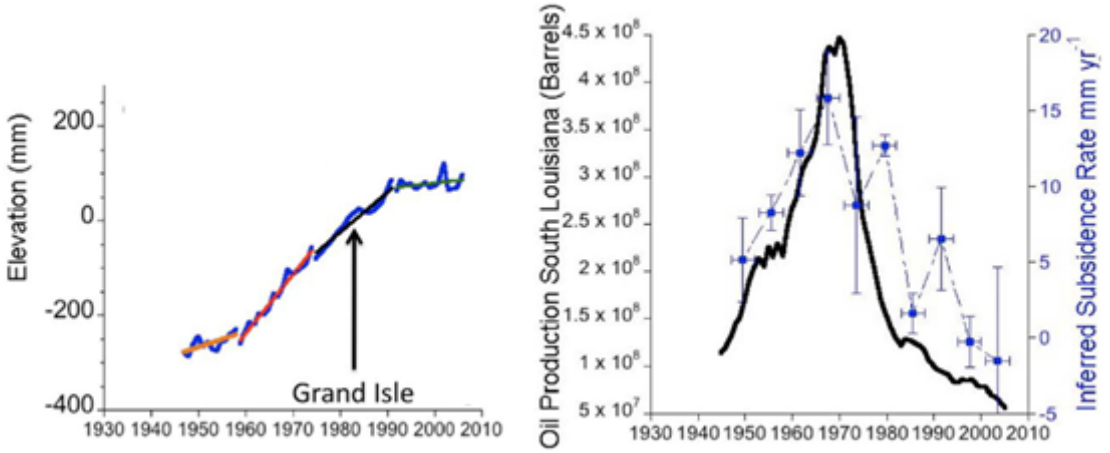

Figure 3.18 Left: inferred subsidence (shown as relative sea-level rise) for the tide gauge location at Grand Isle (GRIS). Right: comparison of subsidence rate and (annual?) oil production in south Louisiana. Modified from: Kolker et al (2011).

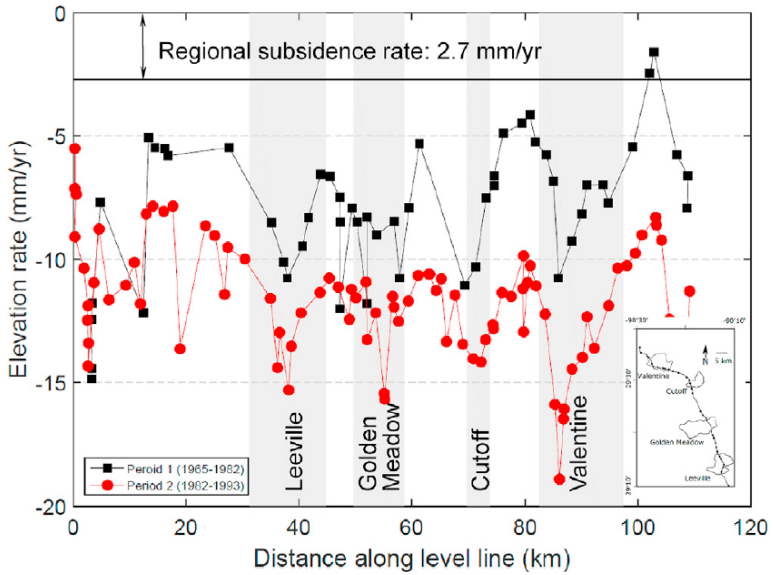

Figure 3.19 Subsidence rate along a transect following highway 1 (see Figure 4.7) originally inferred in the leveling study of Shinkle and Dokka (2004) for two periods (1965-1982 and 1982-1993). Subsidence are higher over reservoirs Leeville, Golden Meadow, Cutoff and Valentine. This is interpreted to be caused by hydrocarbon production.

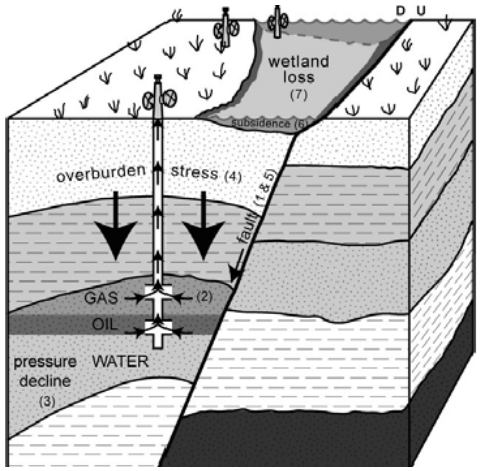

Figure 3.20 Schematic, conceptually illustrating fault reactivation by reservoir production. From: Morton et al (2006); original caption text: "Sequence of production-related subsurface events that may induce land subsidence and reactivate faults. Prolonged or rapid production of oil, gas and formation water (2) causes formation pressures to decline (3). This increases the effective vertical stress of the overburden (4), which causes compaction of the reservoir rocks and may cause formerly active faults (1) to be reactivated (5). Either compaction of the reservoir and surrounding strata or slip along fault planes can cause land-surface subsidence (6). Where compaction or fault-related subsidence occurs in wetland areas, the wetlands typically are submerged and converted to open water (7).

Groundwater abstraction

Quantitative studies of subsidence due to groundwater abstraction only exist for central Louisiana (Baton Rouge) (Nunn, 2003). Large drawdowns of hydraulic head up to ~80 m developed primarily in the 50's and 60's in aquifer units to great depth (~ 650 m). Limited leveling data and modeling indicates that subsidence rates likely reached peak values of about 15 mm/yr (averaged over periods of about 5 yr), and that total subsidence incurred until about 2000 was of the order of 0.6 m. Dokka (2011) suggested that high late-20th century subsidence rates of that magnitude and higher in the Michoud area in GNO are also mostly caused by groundwater abstraction by industry in that area.

Loading-induced compaction

Quantitative information on settlement associated with surficial loading is very sparse. In various reports and articles, loading-induced compaction is acknowledged to be an important process. Furthermore, settlement by surficial loading clearly is an important part of engineering practice as is evident from the use of pile foundations and staged construction of levees to allow for settlements and consolidation (ILIT, 2006). Surcharges or increased weight associated with renovation of roads are expected to enhance subsidence rates, but often also involve an initial increase in land surface elevation during the construction. Paragraph 3.7.5 of the latter document also suggests that the weight of buildings in the Central Business District ("structural surcharging") has increased settlement in that area with 5 inches in 100 years relative to the surrounding area. This would imply compaction of rather deep geological strata since the tallest structures are founded on deep piles.

Jones et al (2016) show from their InSAR study that in two neighborhoods on the west bank of the Mississippi River in Jefferson parish, greater subsidence is observed in the period 2009-2012 where houses were built around 2009 than where houses were built earlier, suggesting a relatively short-lived period (~ 5 years) in which distinct settlement by surficial loading contributes to subsidence. However, the data do not allow one to discern whether the settlement concerns the buildings themselves or also pertain to the adjacent land surface in the neighborhoods. Results suggest that subsidence rates can be enhanced by about 20-30 mm/yr averaged over a period of 3 years.

Drainage-induced compaction and drainage-induced oxidation

Quantitative information regarding drainage-induced compaction of Holocene strata is lacking. No direct measurements appear to have been conducted. ILIT (2006; chapter 3) state that simple drainage of the surficial peaty soils can induce consolidation of up to 75% of their original thickness. Direct information on oxidation rates also does not

appear to be available. However, the importance of the combined impact has been recognized for quite some time (Snowden et al., 1980). ILIT (2006; chapter 3), for instance, present a 'historic subsidence model' for the town of Kenner that was drafted by Kolb and Saucier (1982) which appears to provide estimates of the combined subsidence by drainage-induced compaction and oxidation (Figure 3.10). The model not only suggests subsidence rates were high (> 50 mm/yr) during or immediately after a drainage event, but also shows a prolonged tail of subsidence over many decades after the event with rates of the order of 10 mm/yr. It is unknown to us to what extent such rates and trends are constrained by actual land surface elevation-change data.

ILIT (2006) also report that the ground beneath the homes built in lower New Orleans after the mid-1950's has settled/subsided 10 to 40 inches over ~50 years, relative to the homes themselves, which are founded on pilings that are typically driven about 30 feet deep (Figure 3.11). This subsidence was attributed to oxidation. However, separate contributions from compaction and oxidation cannot be objectively made. The net subsidence rate would amount to 5 - 40 mm/yr.

Mugnier (2014) report 15 inches of subsidence over 15 years (1986-2001) from a single-point extensometer at Cocodrie (Figure 3.12), which amounts to 25 mm/yr. The subsidence would have been incurred over a

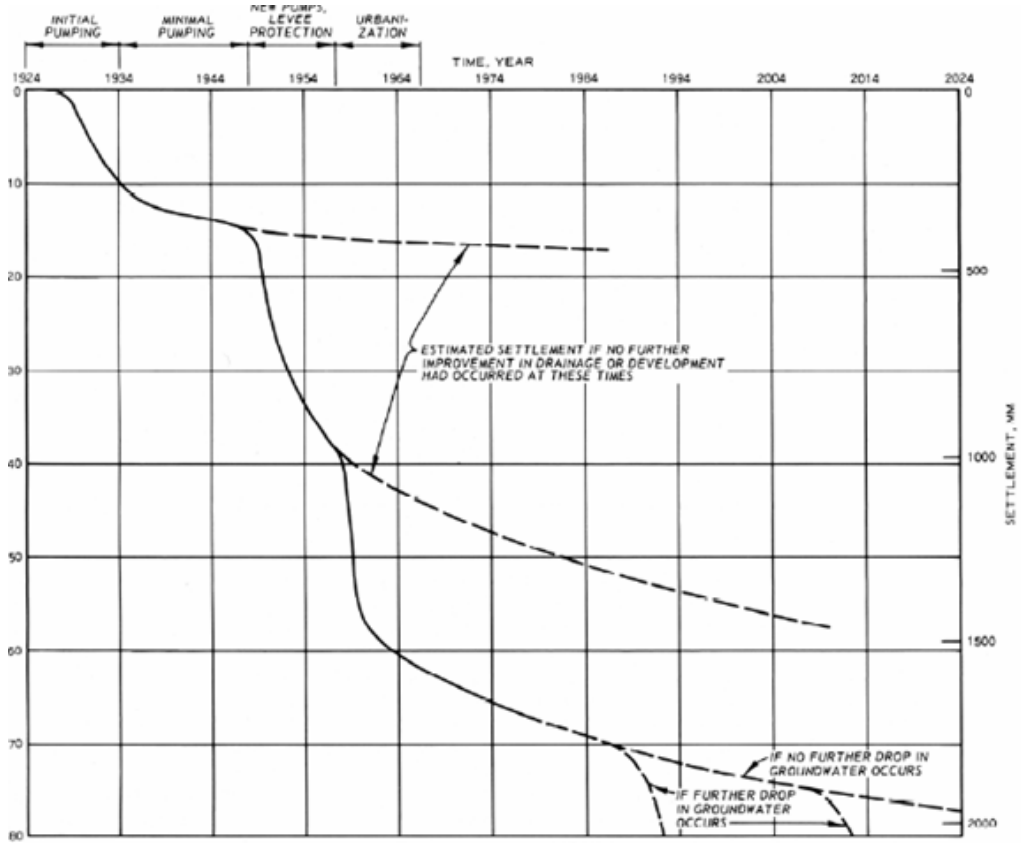

Figure 3.21 Estimate/reconstruction of subsidence of the town of Kenner presumed to be caused by drainage-induced compaction and drainage-induced oxidation. Original by Kolb and Saucier (1982); figure taken from ILIT (2006).

Figure 3.22 Ground settlement/subsidence relative to a house in lower New Orleans. From: ILIT (2006)

Figure 3.23 Shallow 'single-point' extensometer at Cocodrie. Subsurface and historical conditions not known. From: 2014 01 17 - Subsidence in LA-Elevations-A Moving Target LSU.pdf; by Mugnier (2014).

depth of 2.5 m (8.3 feet) only.

3.3 Results of groundwater abstraction-induced subsidence modeling

This section presents the results of the modeling assessment of subsidence due to groundwater extraction from New Orleans aquifer systems (see Melman, 2019). Figure 3.22 shows how the results of groundwater models compare to head data from observation wells in two aquifers. Figure 3.23 presents subsidence results. The results reveal a large discrepancy between observed and predicted subsidence which points out insufficiency of groundwater abstraction to explain most of the subsidence. Subsidence is predicted in the period 1960-1970 when drawdowns increase to reach their maximum values, but predicted subsidence rates are substantially lower than observed. After 1970, the model generally predicts land surface uplift associated with rising hydraulic heads (Figure 3.22). This uplift is caused by elastic behavior of the sands and clays that constitute the aquifers and aquitards.

Based on an internal review of the above results, which were obtained in the MSc-thesis work of Melman (2019), the range of geotechnical parameter values adopted in the work may have been chosen too conservatively. Additional test runs with lower values for the overconsolidation ratio (OCR; a measure of the overconsolidation state) than the minimum one adopted in the study

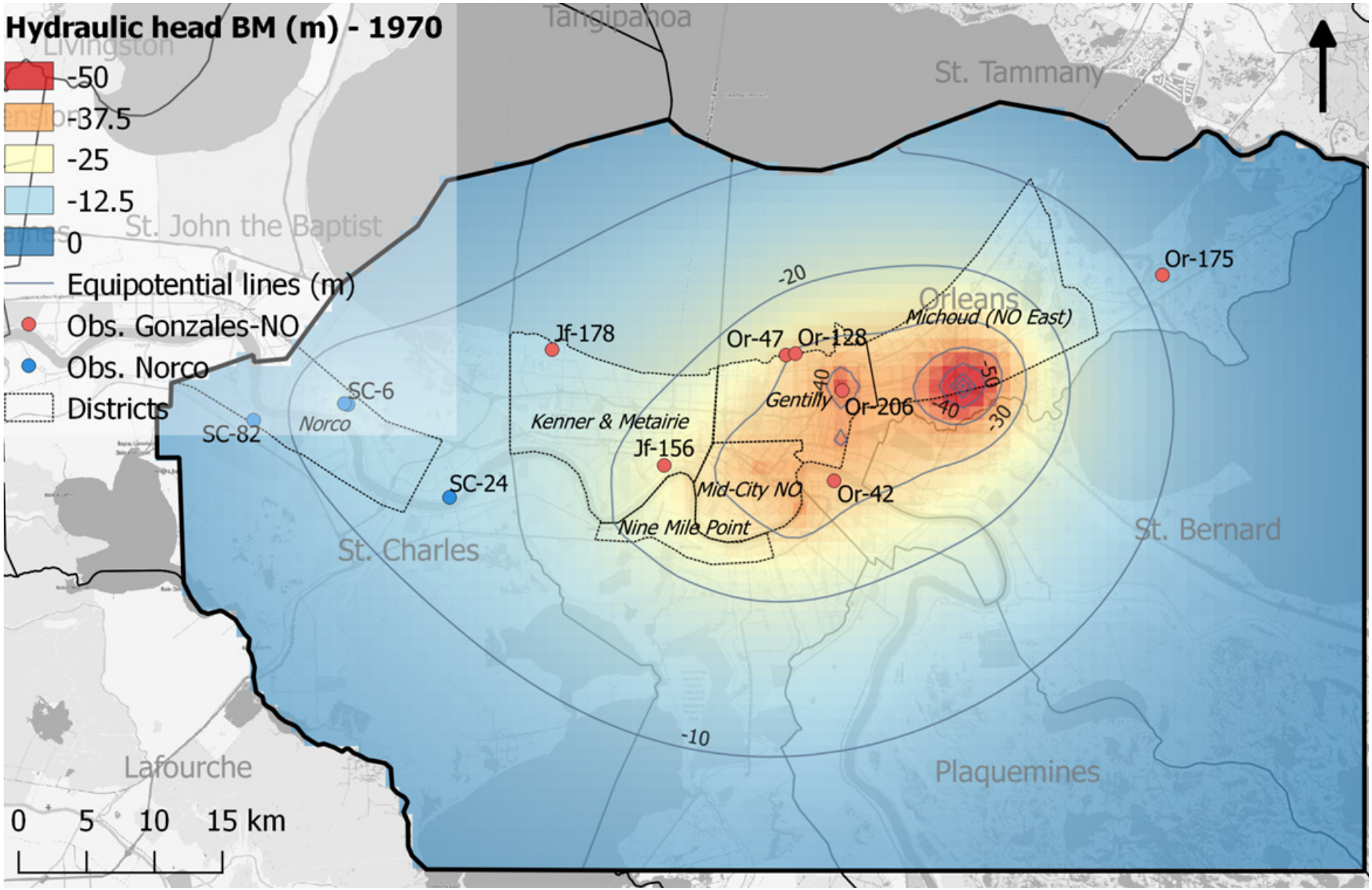

Figure 3.24 Map-view of the modeled hydraulic head in the Gonzales-NO aquifer (best-fit model) in 1970. Contours are in m.

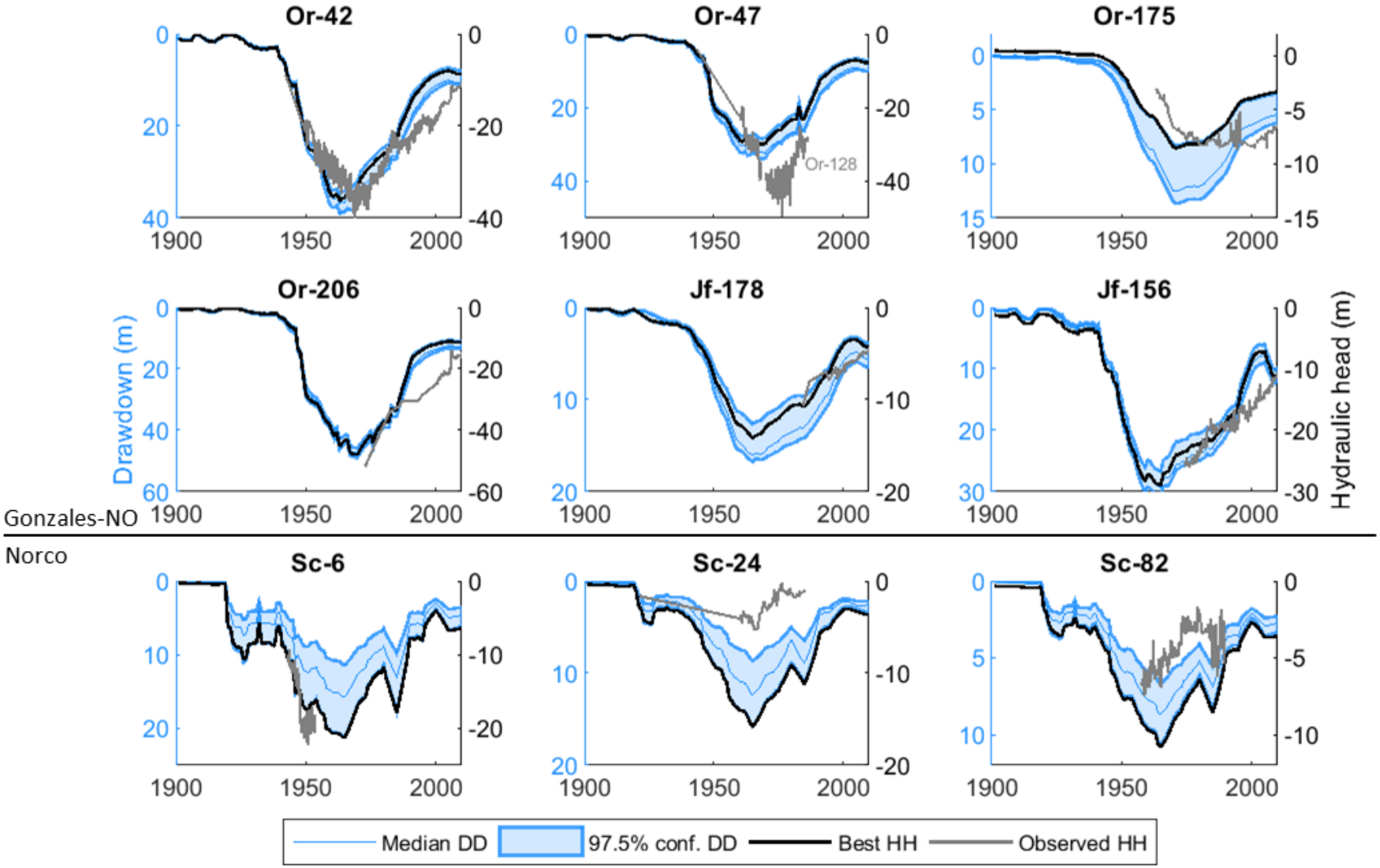

Figure 3.25 Comparison of modeled drawdown (left axis) and modeled hydraulic head (right axis) and observed drawdown/head for the wells shown in the top panel. For modeled drawdown estimated confidence limits are shown.

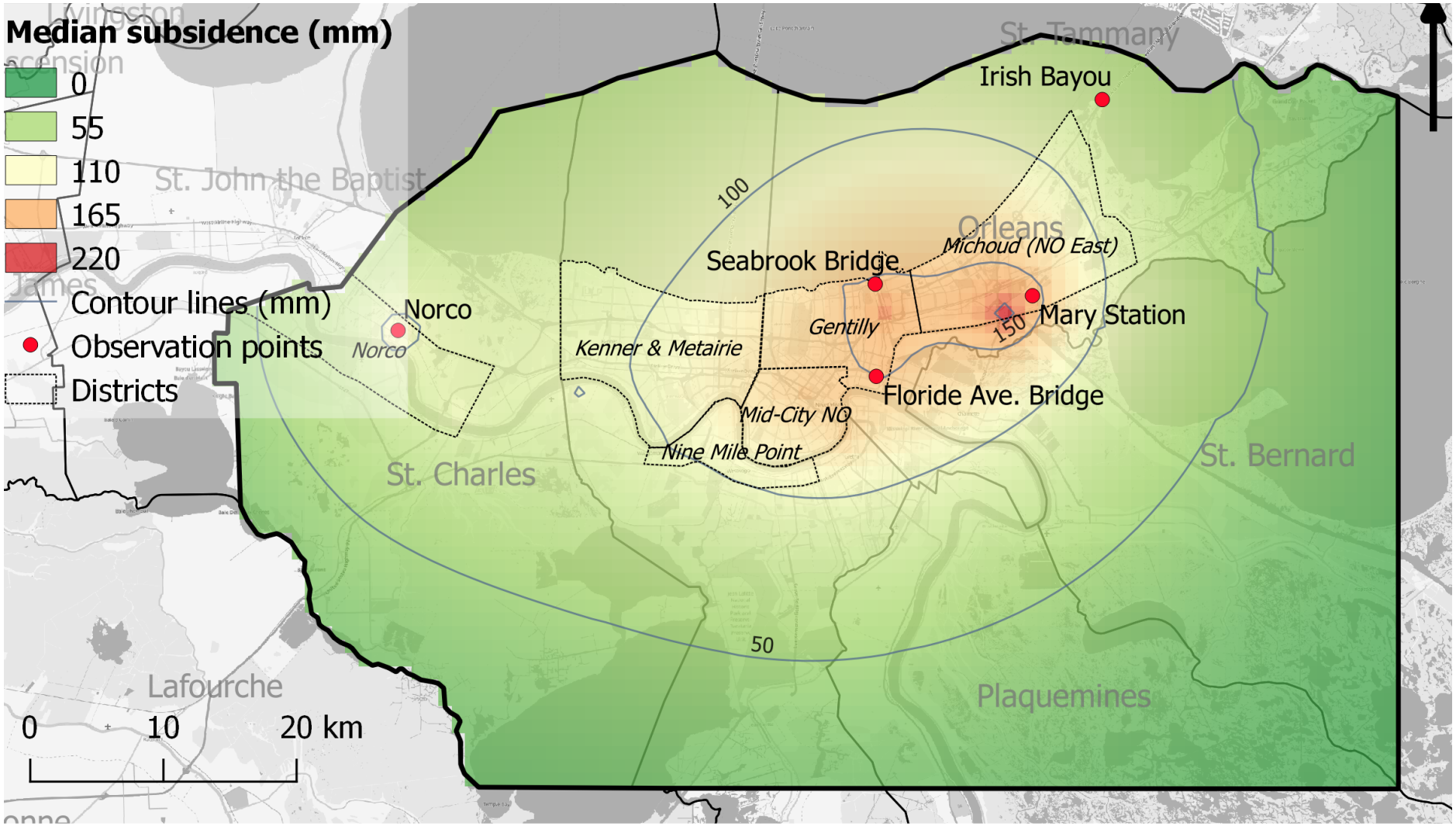

Figure 3.26 Mapview of modeled land surface subsidence starting at 1900 in mm for 1970 (best-fit model of hydraulic data)

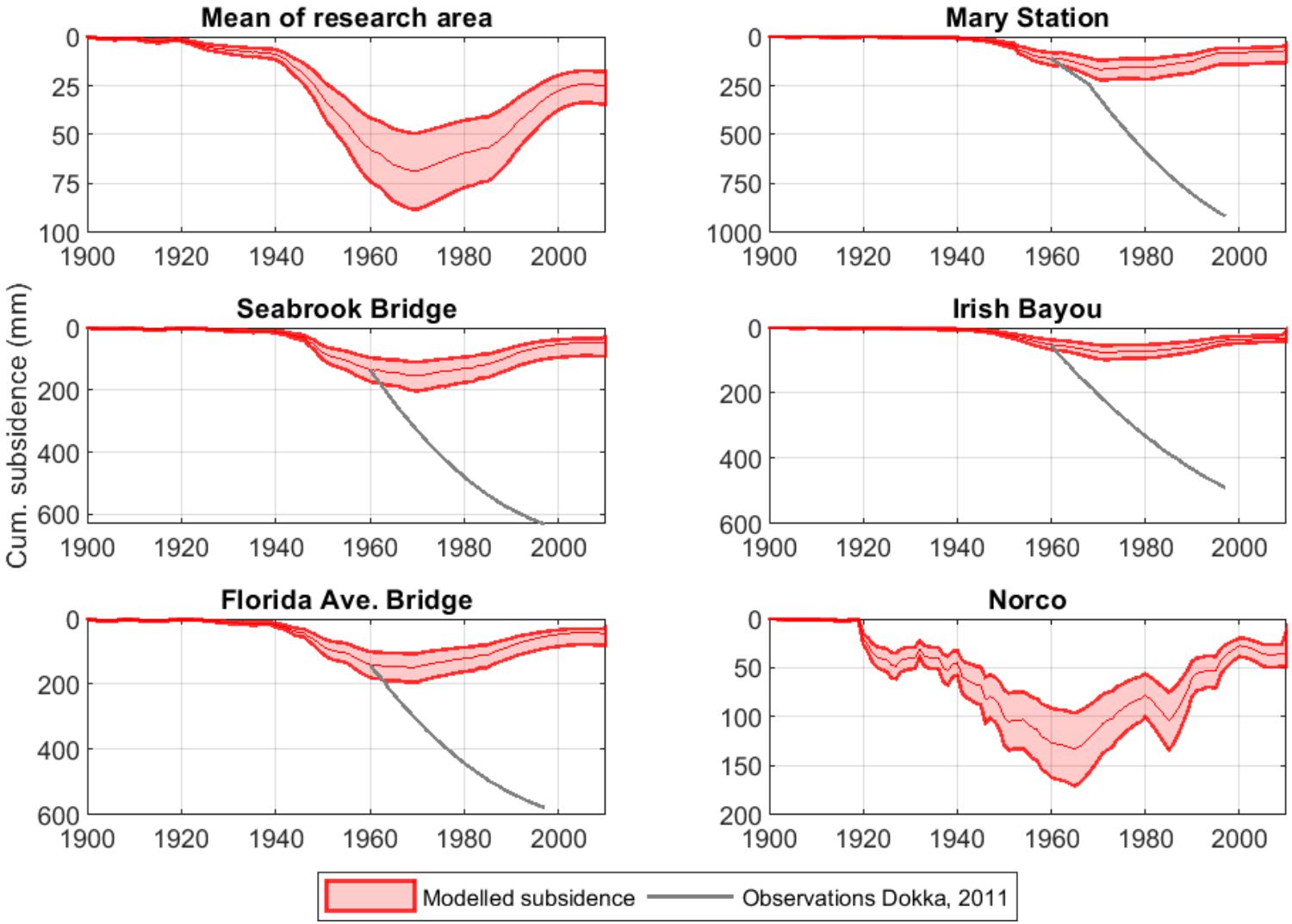

Figure 3.27 Comparison of modeled subsidence history and 'observed' subsidence at four locations shown in the top panel. Note that the vertical scale differs among panels. The 'observed' subsidence represents the reconstructed subsidence at several water gauge stations (Dokka 2011). The subsidence observations included for Mary Station are observed at Paris Road Bridge, which is located about 4.5 km west of Mary Station. According to the model, which addresses the effects of groundwater use, Norco shows a rebound. The observational reconstructions by Dokka show otherwise. If correct, these observations indicate that other drivers than groundwater use have been at play.

(OCR=1.3), can increase the (maximum) subsidence by more than a factor of two, where most of the additional subsidence is irreversible. However, after 1970 subsidence rates still decrease quickly and change to uplift at rates that are comparable to those shown in Figure 3.23. The large discrepancy with respect to 'observed' subsidence, therefore, remains. There are two possible explanations for this finding:

1. Other mechanisms than compaction induced by groundwater abstraction from the New Orleans aquifer system cause most of the observed historic subsidence in the period 1960-1995.
2. There are large drawdowns by groundwater abstraction in other (shallower/deeper) aquifers in the area that have gone undetected.

The first explanation seems to be the most plausible one.

3.4 Results of the InSAR study (Envisat and Sentinel)

Figure 4.23 and Figure 4.24 display the linear rate of vertical land movement for the Envisat (2004-2009) and Sentinel (2016-2019) satellite, respectively.

Checks on the 'validity' of the Envisat rates.

The Envisat data (Figure 4.23; 2004-2009) overlap with and succeed the period of the Radarsat data (Figure 4.6; 2002-2005) that were used by Dixon et al. (2006). Figure 4.25 compares time series of both data sets for points in the vicinity of the ENG1 GPS station which shows a rather stable elevation in the period and which was used as a reference point by Dixon et al. In the period of overlap, both the Radarsat results of Dixon et al. and the Envisat results of this study show negligible vertical movement and, therefore, are compatible, which provides some confidence that both maps use a comparable reference. In large parts of the maps, rate patterns are fairly coherent, in particular south of the Mississippi River and in Chalmette. The Michoud area and the road connecting Michoud and Chalmette also show relatively high subsidence in both data sets. However, rates appear to be smaller in the Envisat results.

Check on the 'validity' of the Sentinel-1 rates.

Figure 4.26 compares the vertical motion of the Sentinel-1 data set with that of the CORS GPS station MARY in Michoud. Both monitoring methods provide very similar results (uplift). This provides some confidence that the reference used in the processing of the Sentinel data is consistent with or very similar to that of the CORS network.

Example: uplift in Delft
The Netherlands (Hoes, 2021)

In the center of Delft exists a 100-year old industrial groundwater extraction (approx. 10-15 M m3/yr). The company started phasing out this extraction because of tax fees (> 1 million $/year). In light of anticipated risks the government demanded a step-by-step reduction of 1 M m3/yr in combination with monitoring (InSAR + groundwater wells). The reduction started in 2016 and since 2018/2019 there has been uplift. In 2020 the uplift velocity was 1 mm/yr.

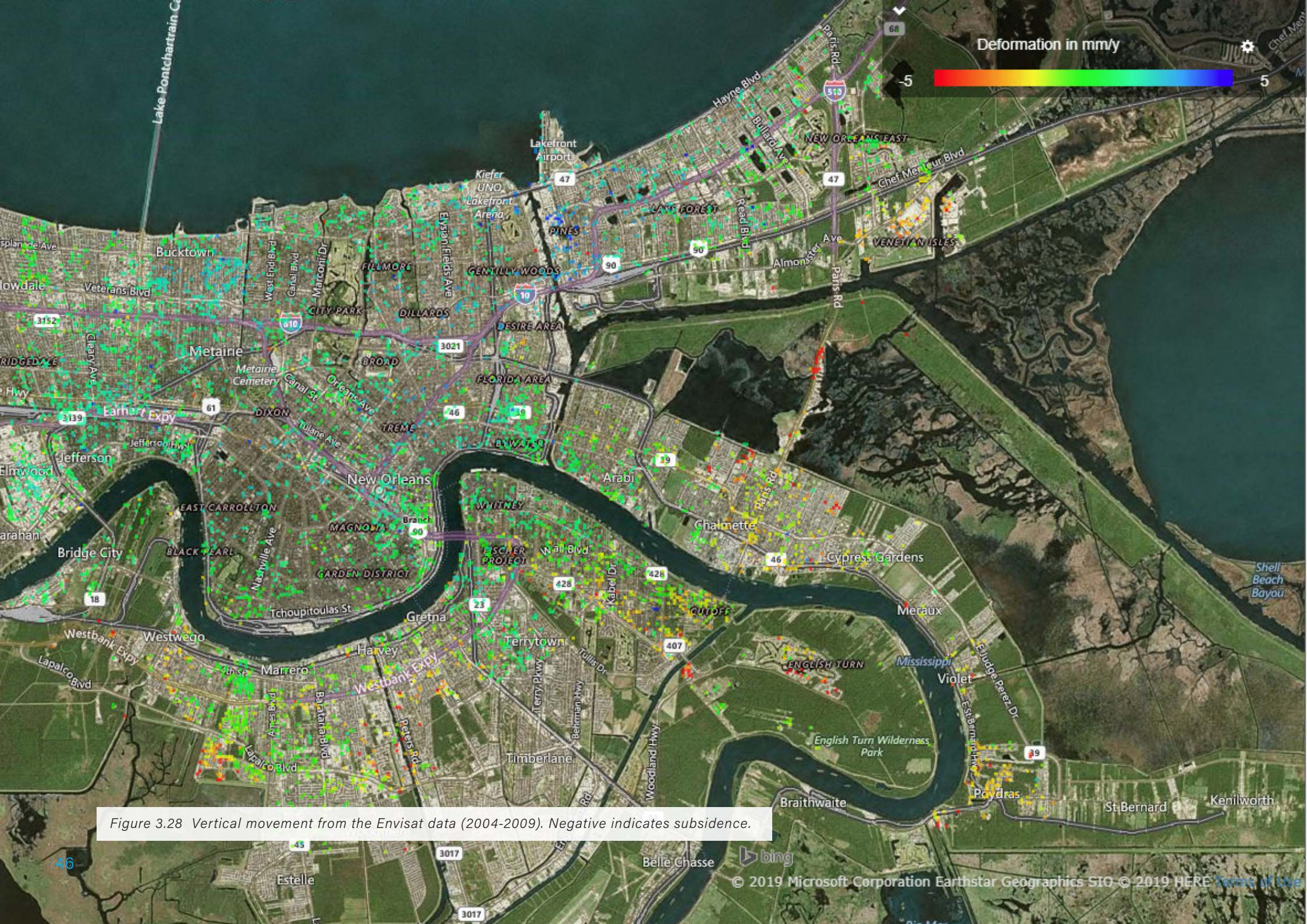

Figure 3.28 Vertical movement from the Envisat data (2004-2009). Negative indicates subsidence.

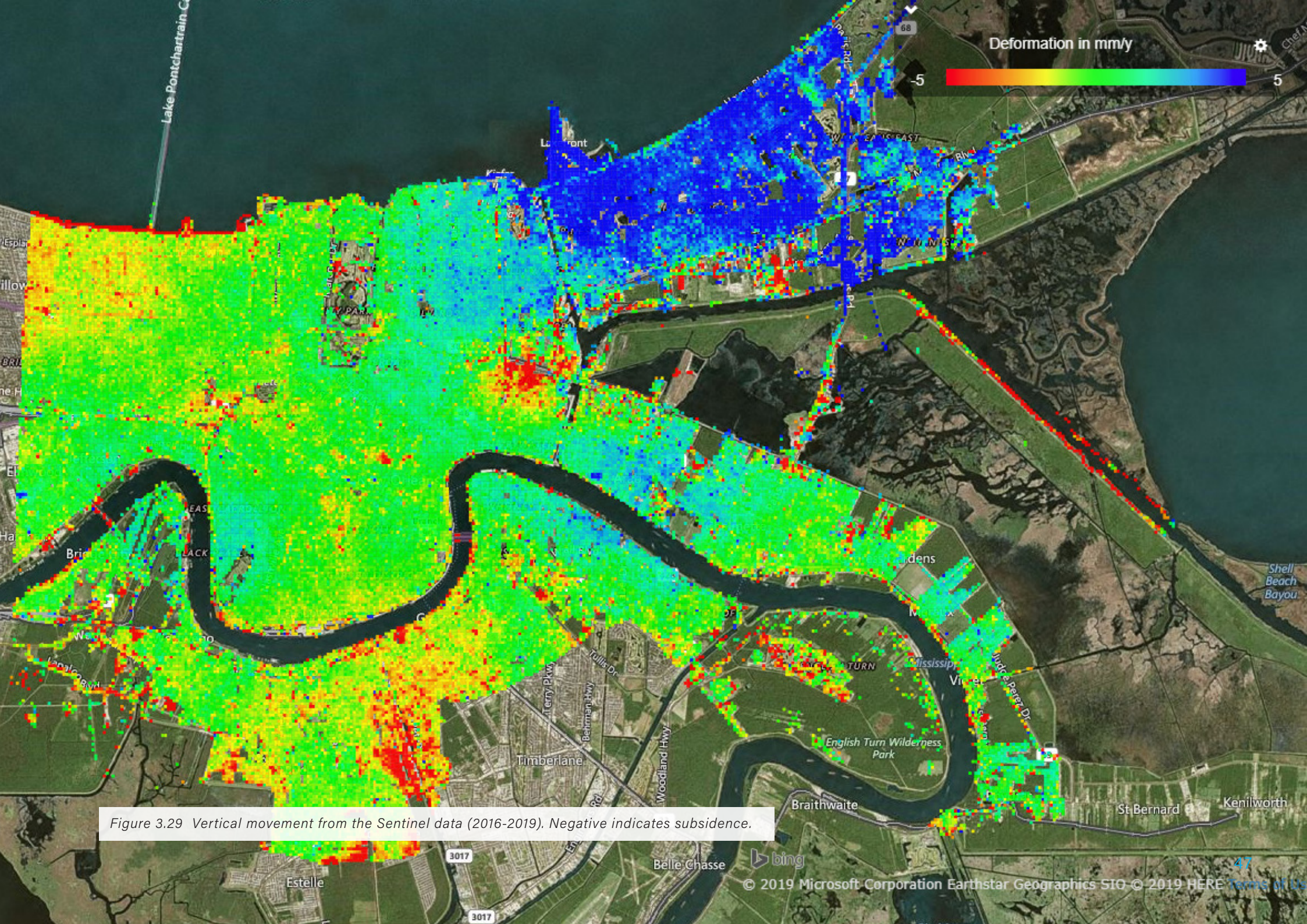

Figure 3.29 Vertical movement from the Sentinel data (2016-2019). Negative indicates subsidence.

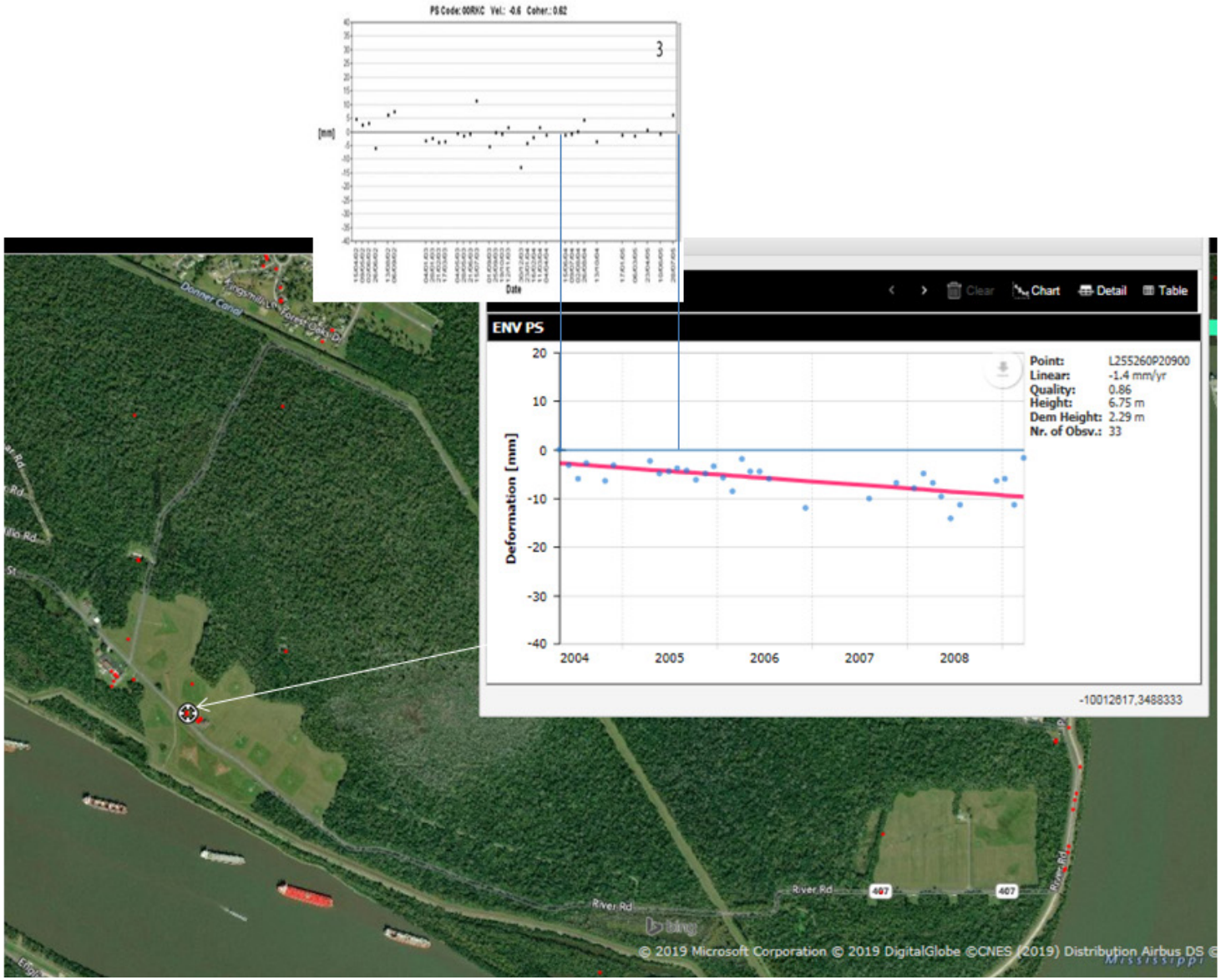

Figure 3.30 Check on the 'validity' of the Envisat results. Upper time series: from the data of Dixon et al. (2006) near the GPS station ENG1 at English Bend. Lower time series: result of the Envisat processing showing negligible vertical motion in the period of overlap of both data sets (May 2004 – July 2005).

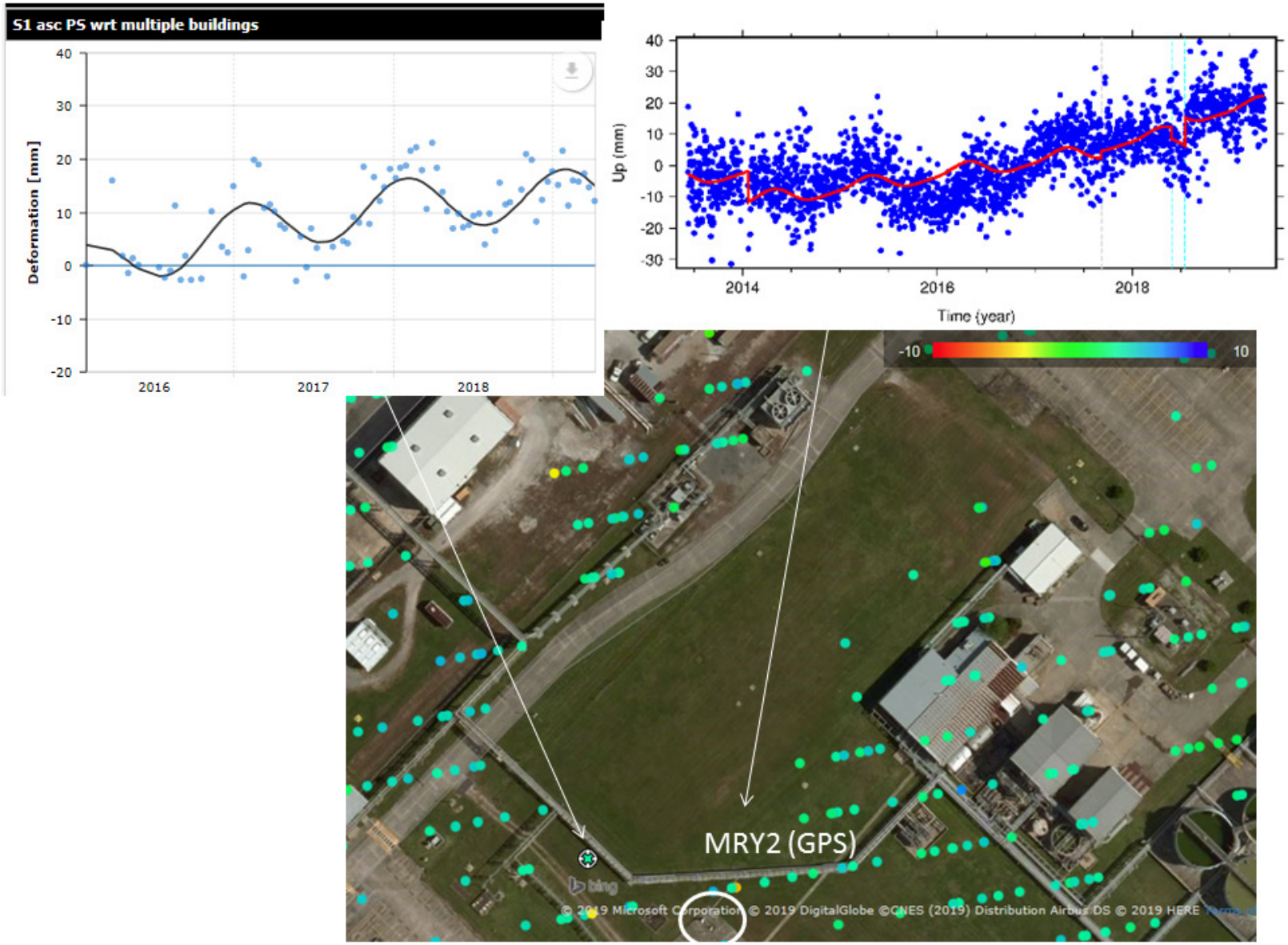

Figure 3.31 Check on the 'validity' of the Sentinel-1 results. Comparison of vertical motion of the Sentinel-1 InSAR data (upper left) against that of CORS GPS station MARY in Michoud (upper right). Locations of the points/locations are shows in the map. For location of MARY, see Figure 4.28.

3.4.1 No indications of significant subsidence of urban districts bordering Lake Pontchartrain

Dixon et al. (2006) reported relatively high subsidence rates (-6 to -10 mm/yr) in the districts bordering Lake Pontchartrain, with the highest rates in New Orleans NE north of Michoud (Figure 4.6; 2002-2005), more or less in line with the findings of Dokka (2011) from leveling data and water level gauges (Figure 4.4). In both the Envisat (Figure 4.23; 2004-2009) and the Sentinel (Figure 4.24; 2016-2019) data, subsidence is mostly absent or insignificant in those parts of GNO. The greatest subsidence ratest occurred in the past causing elevations several feet below sea level. Only in Metairie some spatially extensive subsidence of 4-5 mm/yr is apparent in the Sentinel data.

Locally, high subsidence rates are recorded in the parks, some roads (land surface). Also, the levee along Lake Pontchartrain in Metairie shows large subsidence rates of 20-40 mm/yr in the Sentinel data, probably representing settlement caused by levee improvement works. The absence of significant spatially-distributed subsidence along Lake Pontchartrain in the new data sets since about 2004 suggests that the relatively large subsidence rates inferred by Dixon et al. (2006) were temporary and fairly short-lived. This is consistent with the maps produced by Jones et al. (2016) (Figure 4.7) for the period 2009-2012, although their inferred rates are also likely associated with large uncertainty (inherent to the use of a very small number of SAR images).

3.4.2 Temporally strongly varying vertical movement and recent uplift in Michoud and New Orleans NE by industrial groundwater use

Largest subsidence over the period 1955-1995 (~ 0.8 m) was inferred for the area just northeast of Paris Road Bridge in southern Michoud at the location of the Entergy Michoud plant (Dokka, 2011) (Figure 4.5) indicating long-lived, relatively deep seated (sub-Holocene) subsidence. Dixon et al. (2006) found a rate of about 12-13 mm/y in that area for 2002-2005. Jones et al. (2016) also inferred large subsidence rates. The ENV data, by contrast, reveal much lower rates of 2-5 mm/yr for 2004-2009 (Figure 3.28). However, the time series of the ENV

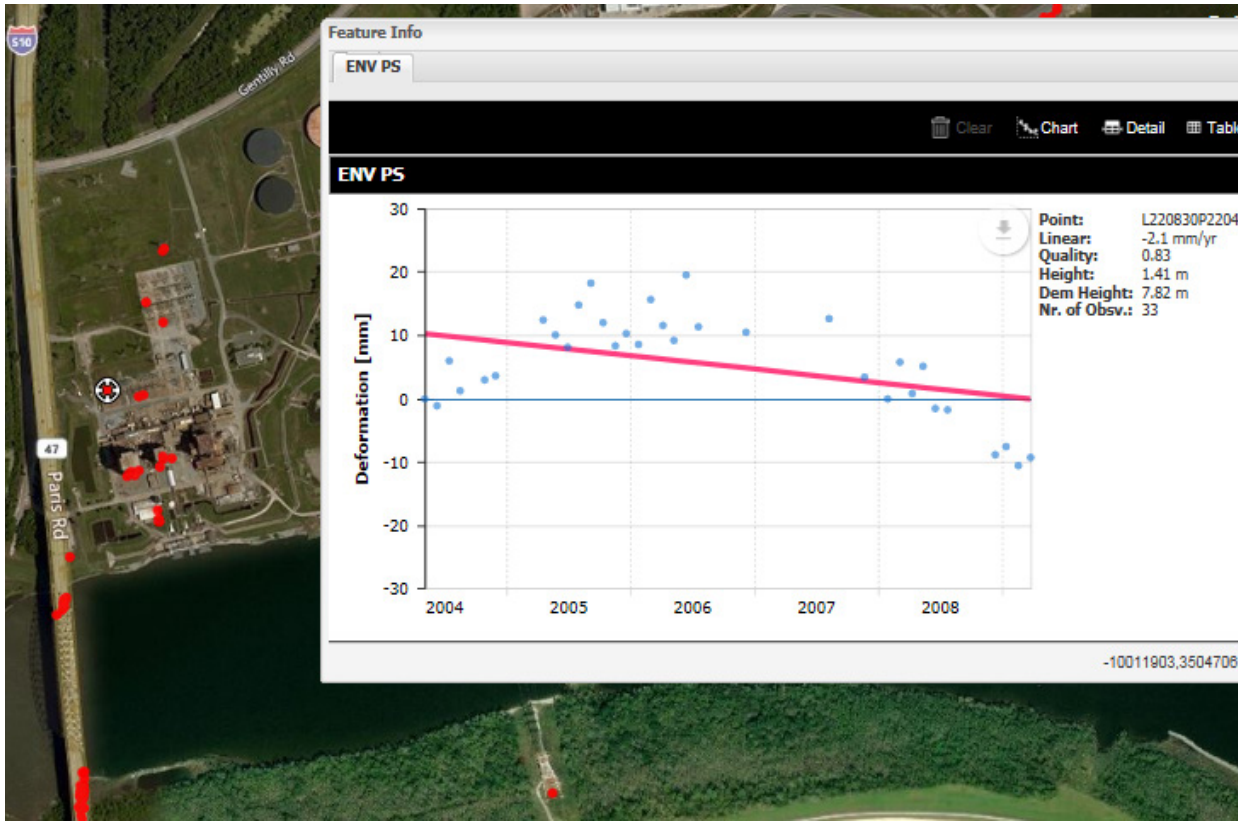

Figure 3.32 Example time series of vertical movement on the Entergy premises next to Paris Road Bridge showing markedly variable movement. The average rate is low, but the average rate over shorter time periods can be both much higher and lower, including uplift.

data also that movement varied strongly and systematically in that period, with uplift occurring from 2004 to 2005/2006 followed by a rather high subsidence rate to 2009 (Figure 3.30). This variability implies that rates measured over short periods (such as the three years of Dixon et al. (2006)) do not necessarily yield rates that are representative for more extensive periods of time. The cause of the variability probably resides in the variance of the industrial groundwater pumping in near Paris Road Bridge.

The Sentinel data even shows uplift in New Orleans NW in 2016-2019 with the locus of uplift at the Entergy Michoud plant (~ 10 mm/yr) and uplift decreasing away from this locus in all directions (Figure 3.34). That the uplift is not merely surficial is evident from the uplift of the series of power line structures which extend to the south into the marsh area, and which have a rather deep foundation. The CORS GPS station MARY, which shows uplift that is consistent with the Sentinel results, is indicated on the map. The MARY GPS is Mounted on a deep waste well extending to 2011 m depth. This suggests uplift is very deep-seated. However, the uplift patterns also correlate with a phase of rather rapid head rise in the Gonzales-NO aquifer at about 200 m depth (bottom panel of Figure 4.29), which alternatively suggest that elastic expansion of the aquifer and over- and underlying confining units are responsible for the uplift. Also, the non-linear character of the uplift and head-rise are compatible with highest rates in 2017, decreasing to lower rates in 2019. At observation well Or-203 the head rise is about 30 ft (10 m) in 2017. The head recovery at the locus of major groundwater abstraction near Paris Road Bridge must be several times larger. Back-of the envelope calculations with realistic elastic properties indicates that this can readily yield uplift of about 10-20 mm (per year) as indicated by the InSAR data. It seems probable; therefore, that significant reduction, or cessation, of industrial groundwater abstraction is responsible for the regional uplift. The fact that the continuous GPS station MARY also shows uplift does not seem to be compatible with this interpretation and is rather enigmatic.

It may be worthwhile to investigate to what extent the casing of deep well on which the GPS is mounted, is damaged/broken/corroded at a level in or above the depth of the Gonzales-NO aquifer. The uplift we described was also observed during another independent InSAR study by Tulane University (Fiaschi et al., 2020). This research team also associated this uplift with the reduction of groundwater extraction at the Michoud power plant. They determined an uplift velocity of 3.5 mm/yr starting in 2016. Their analysis was published in March 2020.

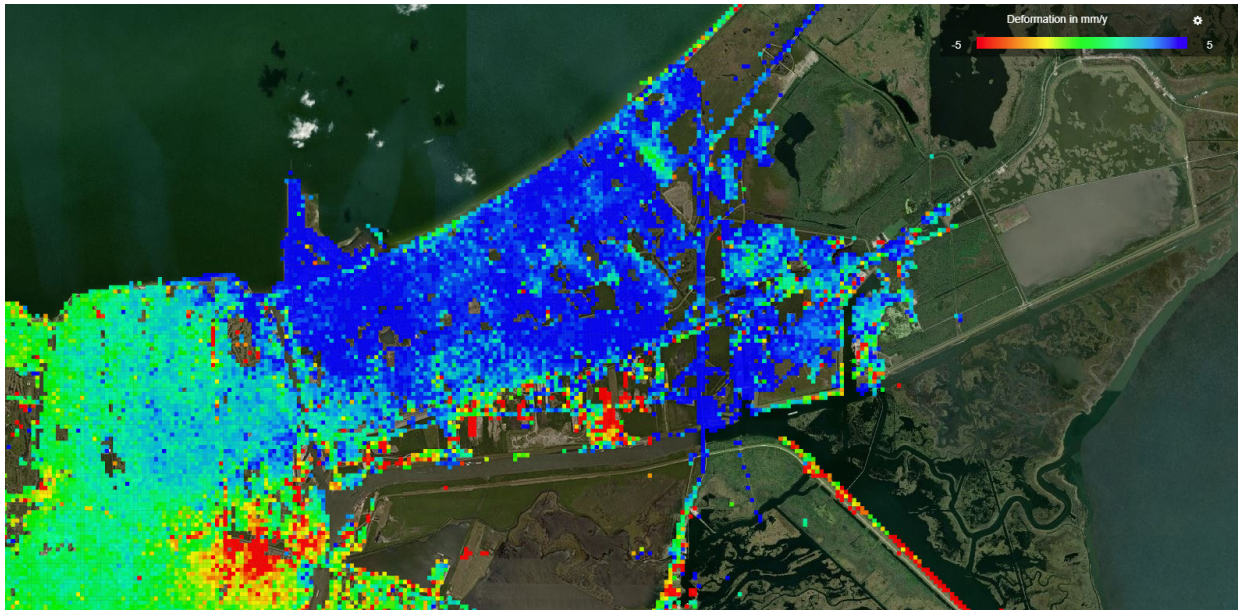

Figure 3.33 Uplift in New Orleans NE in the Sentinel data shown in map view.

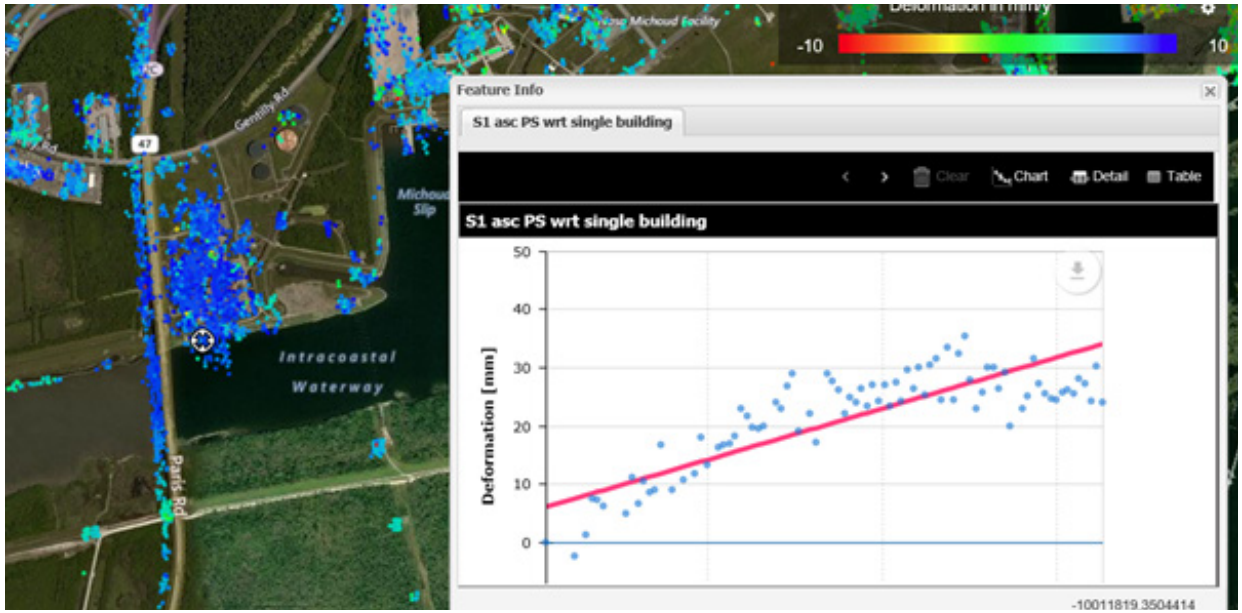

Figure 3.34 Time series of the uplift near the Paris Road Bridge (location indicated with a white circle). Also note the power line structures south of the waterway.

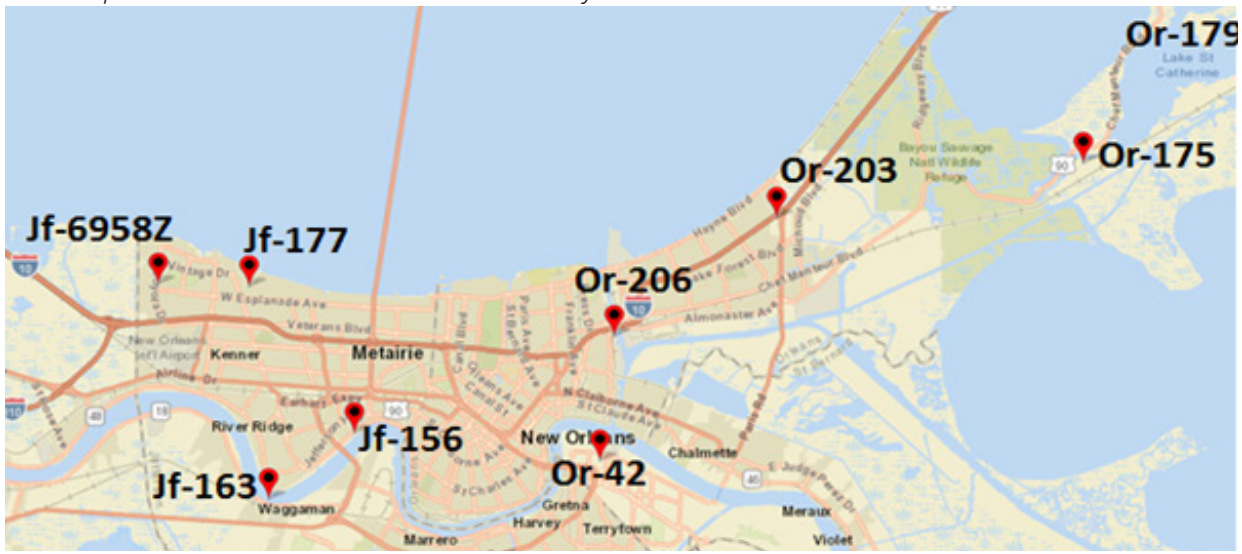

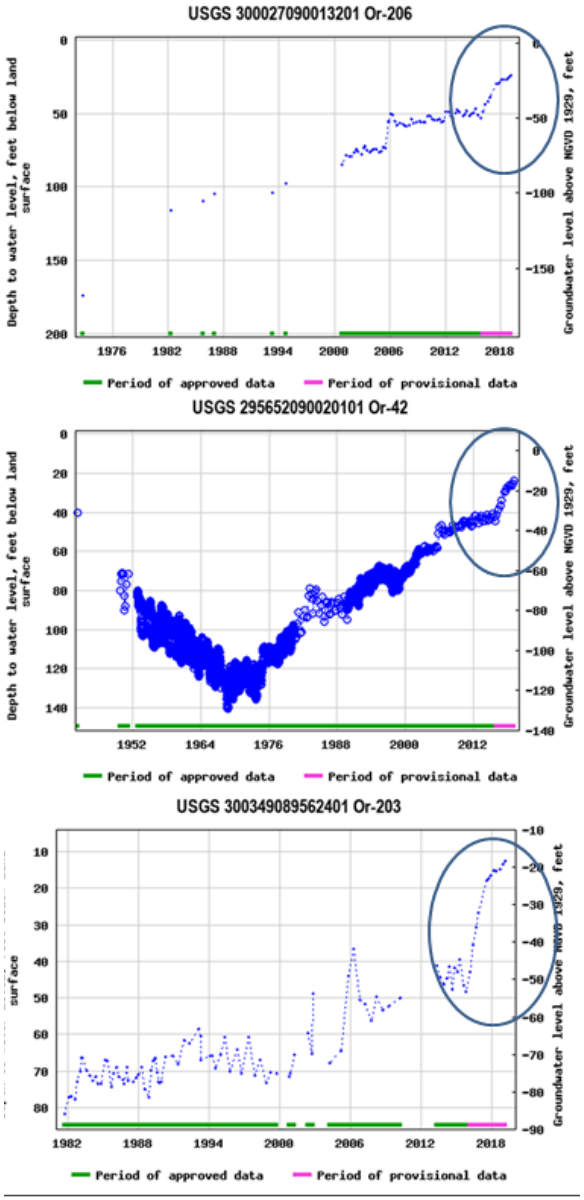

Figure 3.35 Figure 4.29 Increased rate of head rise in observation wells in the Gonzalez-NO aquifer in the period 2016-2019. The rise is caused by reduced groundwater pumping.

3.4.3 Evidence for superimposed shallower compaction contributions

Interestingly, within the zone of uplift, localized (or extended) patterns of subsidence are present (Figure 3.34); to the west of the Paris Road Bridge, and along the levee of the Mississippi River-Gulf Outlet Canal to the southeast. It seems likely that the regional uplift also impacts those locations, but that local subsidence by other component processes that are active at the same time, are more important and thereby overwhelm and obscure the uplift. To the west, the subsidence locations correspond to landfill or waste dumps/storage locations along Almonaster Avenue. This type of subsidence is because of added mass and can be still active when the dump is no longer used. Along the Outlet Canal, settlement/deformation associated with the load of the levee must be the cause of subsidence.

Further too the west, a pronounced zone of subsidence with rates up to 10 mm/year and higher is present along the borders of the Florida Avenue Canal (Figure 3.34). This subsidence is attributed to widening of the canal, works that extend from 2015 to present. Pumping activities and lowering of phreatic level extending laterally into property surrounding the canal, and associated compaction, are expected to be the cause of the subsidence.

3.4.4 Shrink-swell

Figure 3.35 depicts the estimated/fitted amplitude of the seasonal variation of the vertical movement. The amplitude varies from about 1 mm, for instance along the border of Lake Pontchartrain, to more than 1 cm in various zones more to the south. The low values often seem to reflect noisy signals which do not allow detection of a clear sinusoidal variation. The amplitude of the actual variation may then be significantly underestimated. The yearly low elevations occur in January-March and the highs in July-August. It is not clear if the seasonality is dominated by shrink-swell that is governed by seasonal soil moisture variation or if deeper soil volume changes are involved. Areas with buildings often show amplitudes that are like that of the land surface (roads etc.). This may indicate that at least part of the signal is associated with deeper pore pressure changes (hydraulic head). In the surroundings of the Entergy plant in Michoud this is plausible given the greater reliance on groundwater as a source of cooling water in the summer. However, the same seasonality is seen throughout the area covered by the InSAR data.

Differential shrink-swell beneath the foundation of buildings is a common cause of structural damage. The seasonal vertical movement also has implications for methods to measure land subsidence since sparse 'sampling' in time (e.g. Jones et al 2016) may give a biased signal that can under- or overestimate the subsidence trend over timescales of several years and longer.

3.4.5 Uplift considerations

Our InSAR study presented uplift in the northeastern part of New Orleans. This area is also vulnerable to shallow subsidence due to drainage. In the case shallow subsidence rates are lower than the uplift velocity, the net InSar velocity is still upwards.

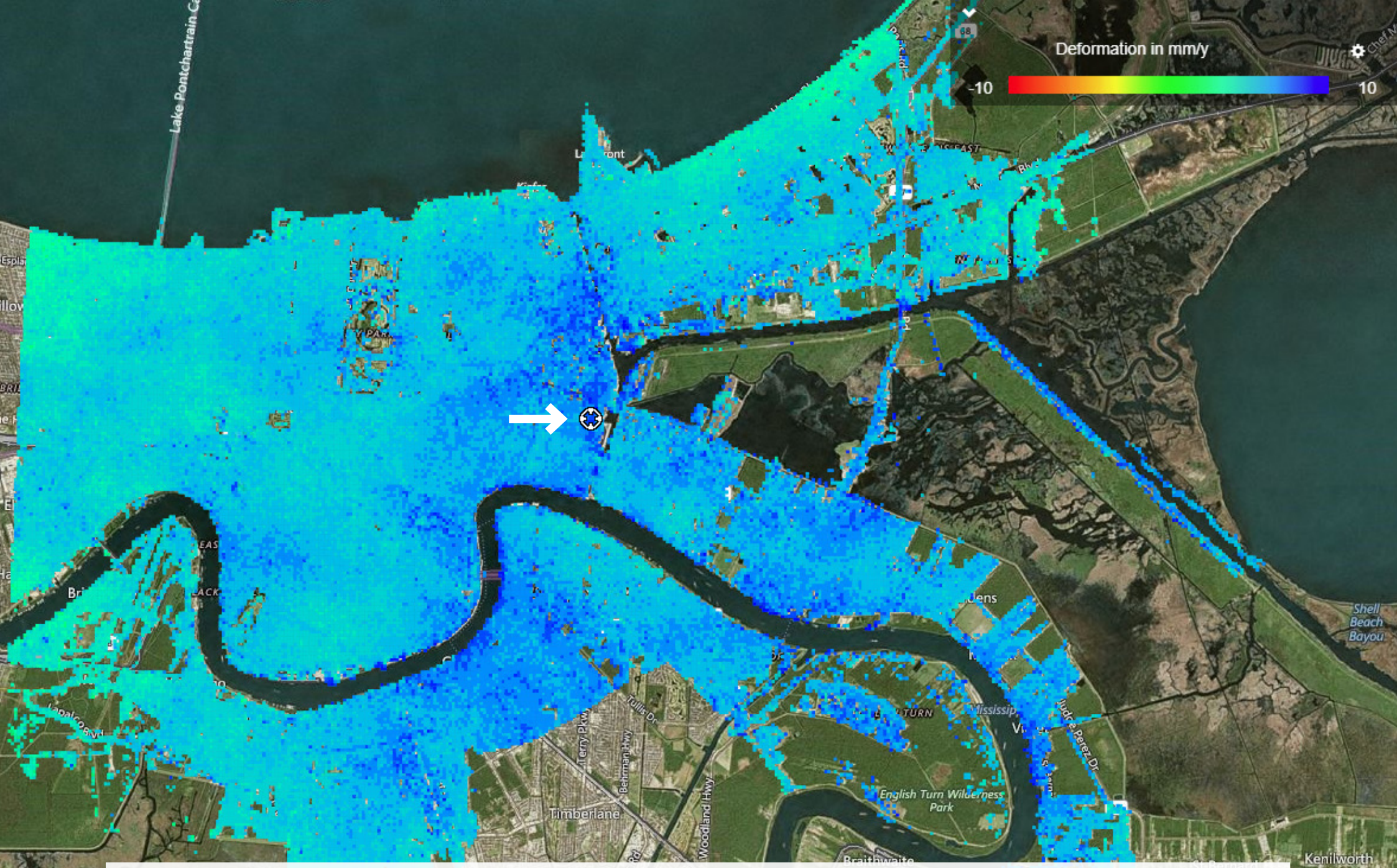

Figure 3.35 Amplitude of seasonal variation of the vertical movement (Sentinel-1). The variance is twice the amplitude. The legend must be interpreted in mm rather than the mm/y shown. Only positive values occur (green to blue). An example time series is shown for the location indicated with the white circle.

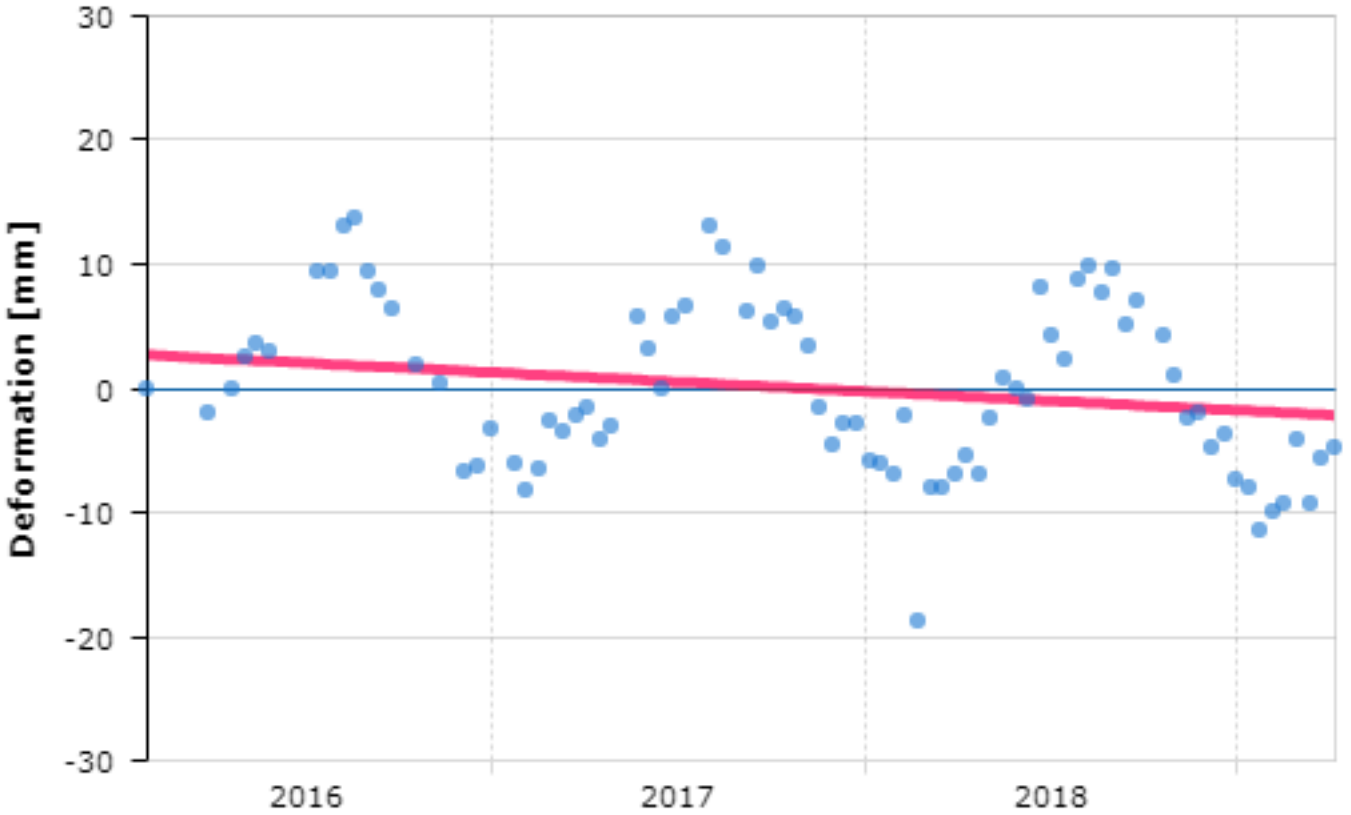

Figure 3.36. Example time series of the amplitude of seasonal variation of the vertical movement (Sentinel-1) for the location indicated with the white circle in Figure 3.35. This variation follows the seasonal rainfall fluctuation.

4. FINDINGS

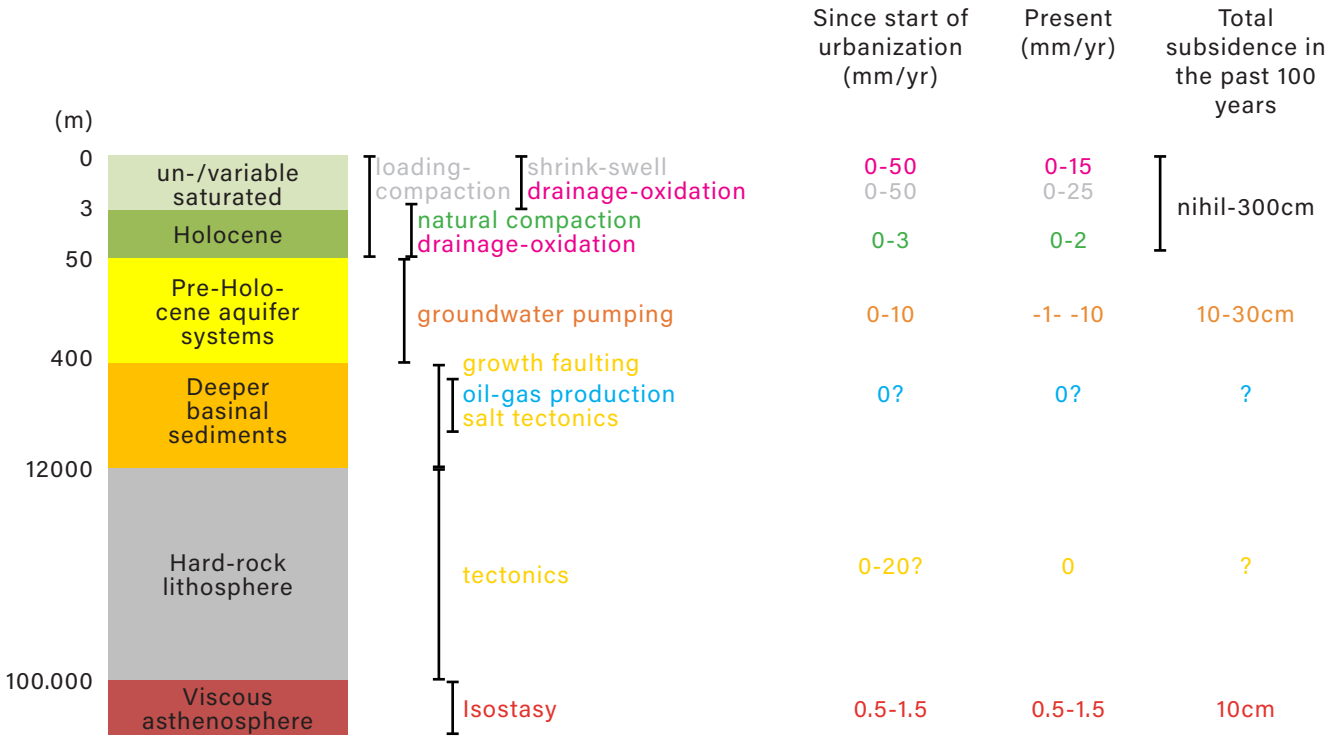

Figure 4.1 Summary of estimated subsidence in New Orleans (study area), both in historic times (since start urbanization) and at present. Negative values indicate uplift. Ranges are shown to indicate uncertainty and/ or expected variance in space and in time.

Focus of this synthesis is on the subsidence in study area in New Orleans. Regional results for the MD are used to support the interpretation.

'Measured' subsidence rates for the study area do not show a clear coherency among the various measurements methods. Also, the three InSAR results (Dixon et al 2006; Jones et al 2016; this study) show marked differences. Although there is always the possibility that biases/inaccuracies play a role in this, we believe it to be more likely that apparent differences primarily reflect subsidence that is both temporally and spatially variable (in mapview ánd with depth). The land surface movement is a complex, integrated signal from various contributions, each with its own characteristics and spatially and temporally varying drivers. This implies that temporal and spatial variability is an essential characteristic of the subsidence situation.

Our assessment in terms of component processes is visually summarized in Figure 4.1 and elucidated below.

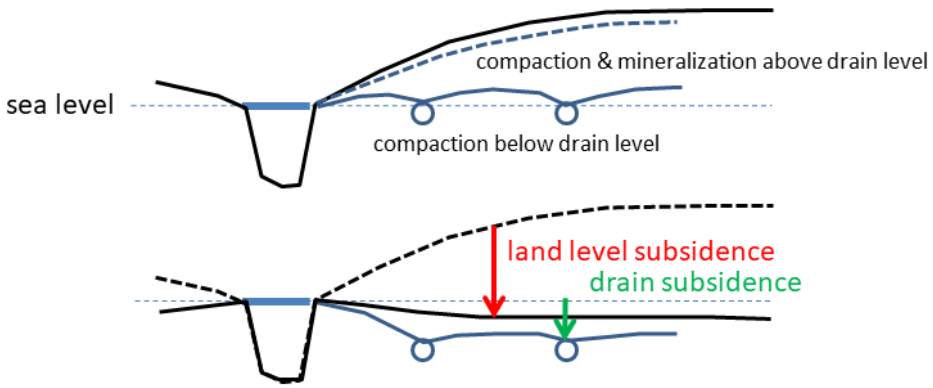

Figure 4.2 Schematic illustration of land surface subsidence caused by drainage-induced compaction and oxidation (mineralization). Progressive lowering of drainage levels enhances and prolongs the subsidence.

Dominant and/or well-established processes:

a) **Isostasy** provides a stable and spatially uniform (for the study area) subsidence contribution with a magnitude of about 1.5 mm/yr or less. This is borne out by various CORS GPS stations in and around the study area which show ~ 1 mm/yr subsidence rates.

b) **Drainage-induced oxidation and compaction** subsidence rates were very high (up to ~ 50 mm/yr) at times in the past following major drainage enhancements. This is expected to be the predominant cause of the large subsidence up to about 3 m in the neighborhoods bordering Lake Pontchartrain since land use started. Drainage levels of canals/drains in the subsiding areas had to be progressively lowered to compensate for the subsidence, and subsidence of leaky storm drains contributed to water table lowering, compaction and oxidation (Figure 4.32).

At present these rates are much subdued, but nevertheless a prominent and potentially dominant subsidence component in parts of the study area that are underlain by compaction- and oxidation-sensitive strata (Sensitivity maps, Report Shallow Subsidence Vulnerability in New Orleans). Subsidence can be accelerated by renewed enhanced drainage. The rather high recent subsidence rates of 10-15 mm/yr around Florida Av. Canal from Sentinel InSAR data are considered a key expression of the sensitivity to drainage-induced subsidence in the study area. Temporally and spatially variable water table conditions likely contribute to the variance in the measured subsidence rates inferred from InSAR.

c) In places with relatively recent (~ 5 years) renovation works involving surficial load changes (roadworks etc.), loading-induced subsidence can be prominent, yielding subsidence rates ranging between 5 – 25 mm/yr. Examples may be the landfill/waste storage sites along Almonaster Avenue and some of the levees.

d) Industrial groundwater use, notably in the Michoud area (Entergy; Nasa) currently seems to cause uplift in New Orleans NE due to reduction of abstraction amounts and associated increasing hydraulic head in the Gonzales aquifer. The uplift rate is > 10 mm/yr near the locus of uplift around Paris Rd Bridge and decreases to ~ 5 mm/yr north of the Chef Menteur Boulevard. Separate rates associated with head change are difficult to evaluate (requires extensometers), however, because the InSAR rates provide the net movement that is expected to include other components. The uplift will not be stable but is likely to decrease and cease as head increases will slow down and stop. And if groundwater abstraction would be stepped up again, renewed subsidence is expected to start. In the 1960's an early 1970's, when groundwater abstraction grew in the

Michoud area and head strongly declined, this must have caused subsidence through compaction of the impacted aquifer system (including confining layers). However, the large subsidence around Michoud from the 1970's to 1995 that was inferred by Dokka and the rather high rates of subsidence revealed by Dixon et al for 2002-2005 and by Jones et el for 2009-2012, cannot be explained by groundwater abstraction and the history of head development in the Gonzales aquifer. Renewed subsidence by abstraction from the Gonzales-NO aquifer is expected to be reversible (recovers when abstraction stops) because of the very low historic heads in the 1960's and early 1970's. The map presenting the actual uplift zone (Figure 3.27) is more or less hiding damaging shallow (at the surface) subsidence processes. It represents the resultant of uplift by expansion of the deep aquifer and expected shallow subsidence processes (Figure 4.3). This conclusion corresponds with this interpretation of Karagar et al. (2020) that GPS-station MARY's uplift is the result of deep groundwater change starting in 2016.

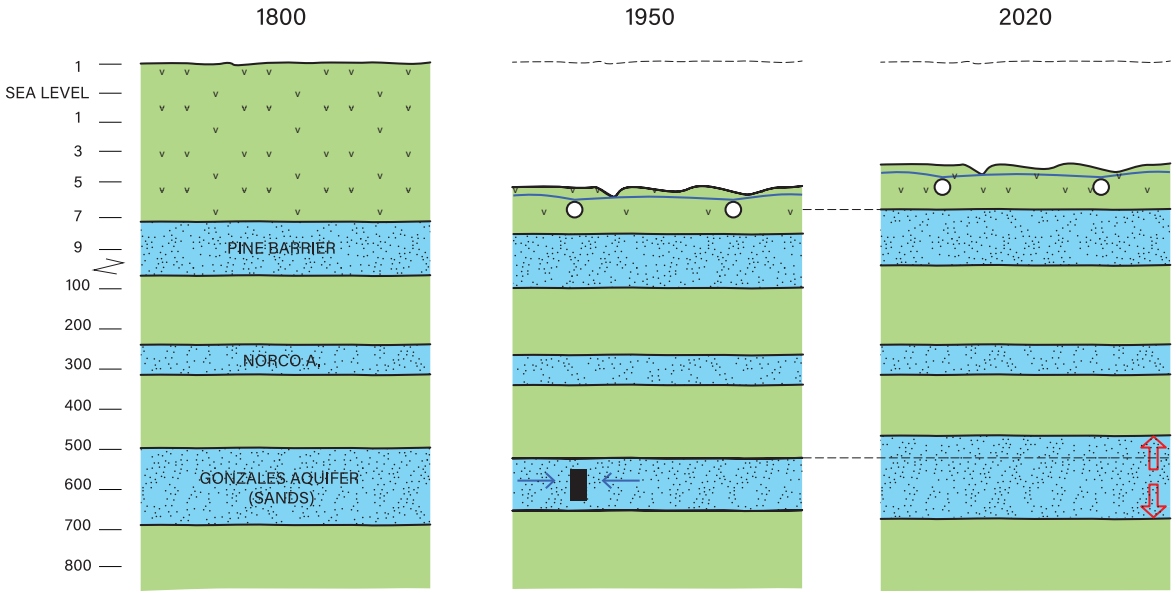

Figure 4.3 Effect of pumping on the Gonzales aquifer, temporally expansion of deeper layers, but continuous shallow differential compaction by drainage etc.

Not by deep groundwater recharge as they refer too, but by reduced pumping.

Our modeling (including the head recovery since about 1975) and the new InSAR results do not support the ideas propagated in various previous studies that groundwater withdrawal is the prime cause of the observed high subsidence rates in Michoud and surroundings in various periods since 1980 (Dokka, 2011; Dixon et al., 2006; Jones, 2016; LPHI&AAE 2016). During and prior to the period analyzed by Dixon et al, for instance, extraction at the Michoud plant had been stable for a long time, and heads in USGS observation wells generally recorded head recovery (Figure 4.29). The same applies to the period analyzed by Jones et al. Given the large uncertainty in the subsidence estimate by Jones et al for New Orleans NE, the reliability of the high rate at Michoud may be questioned. If the assessments of Dixon et al and Jones et al are indeed correct, other component processes appear to be involved. Discrimination between subsidence of buildings and structures with pile/pole foundation and subsidence of the land surface is needed to check whether shallow compaction might have prevailed during those periods. If buildings and structures subsided at the same rate as the land surface, then a deeper cause is implied.

We agree with CKA (2016) that it is unlikely that groundwater withdrawal at the Michoud plant has been a (significant) cause of dam-

age to buildings, roads and flood protection infrastructures, and that renewed (relatively limited) future groundwater use would pose risks to cause such damage. Differential vertical movement on the scale of individual buildings, for instance, most probably is very small. Differential movement is of a rather long-wavelength nature. Although not relevant for direct damage, the induced land subsidence does impact the height of flood defense structures. Large magnitude subsidence such as inferred by Dokka near Paris Road Bridge (~0.8 m; not clear at all that this is caused by groundwater withdrawal) could also cause damage to infrastructure by raised phreatic groundwater levels that can impact the stability of foundations.

The suggestion by CKA that groundwater withdrawal at the Entergy plant in Michoud, or its successor (NOPS), that hydraulic head decline and associated subsidence would be limited to several hundred feet of the water well is incorrect and untenable. Hydraulic principles, our modelling (Figure 4.22) and the observed cone of depression of hydraulic head (Figure 3.4) show that the impact of the deep abstraction extends 5-10 miles (8-16 km) from the well or well cluster. High rates of extraction at about 600 ft depth do not create a 'steep cone of depression' as indicated in their Figure 2. The suggested scale of the graphic is incorrect/deceiving. Moreover, the graphic also is unclear in that it does not clarify that the phreatic level (water table) is hardly lowered by the withdrawal; the cone of depression represents hydraulic head of the confined aquifer, which is a measure of the groundwater pressure in the aquifer rather than a representation of the water table.

e) The Envisat and Sentinel InSAR data highlight there is marked seasonality of land movement in the study area with observed seasonal variation up to 3 cm. Much of this seasonality is probably caused by shrink-swell of near-surface clay and peat layers. However, since buildings also show seasonal movement, it is partly also of a deeper origin, probably the elastic response of the aquifer system to seasonal variation in industrial groundwater pumping. The seasonal land movement is not relevant for longer-term land subsidence. However, it has important implications for subsidence monitoring, favoring methods that include frequent measurements (such as in satellite-based InSAR) over sparse measurements in occasional leveling or automated-airborne-vehicle SAR imaging. Furthermore, shrink-swell likely is a major cause of damage to property.

Processes that play a minor or unclear role:

- Meaningful figures for **natural compaction** in the study area cannot be provided based on the available information. In most areas natural compaction has been overwhelmed and overprinted by anthropogenic influences. Separate distinction of a natural component is not useful in those areas. Natural compaction could potentially play a role in the marshy area around the MGRO canal west of Lake Borgne. Subsidence rates would not be expected to exceed a few mm/yr.

- The large subsidence between 0.4 mand 0.8 m in NE New Orleans between the late 1950's and 1995 inferred by Dokka for structures founded in the Pleistocene (Figure 4.4), remain without a clear explanation, but do suggest that one or more other components do play a role in that area. **Induced tectonics/faulting** as suggested by Dokka remains a candidate, where required changes in stress conditions may have been related to groundwater pumpage, but perhaps also to hydrocarbon production in reservoirs surrounding New Orleans. Furthermore, it cannot be ruled out that changing stress conditions would interact with and mobilize salt layers at depth.
- The good news is that overall, present subsidence rates in GNO are lower than several studies have indicated over the last decades. Locally, high rates of ten to several tens of mm/yr occur. These high rates are largely of anthropogenic origin. This implies that high rates can be influenced positively, or prevented, through integrated urban management.

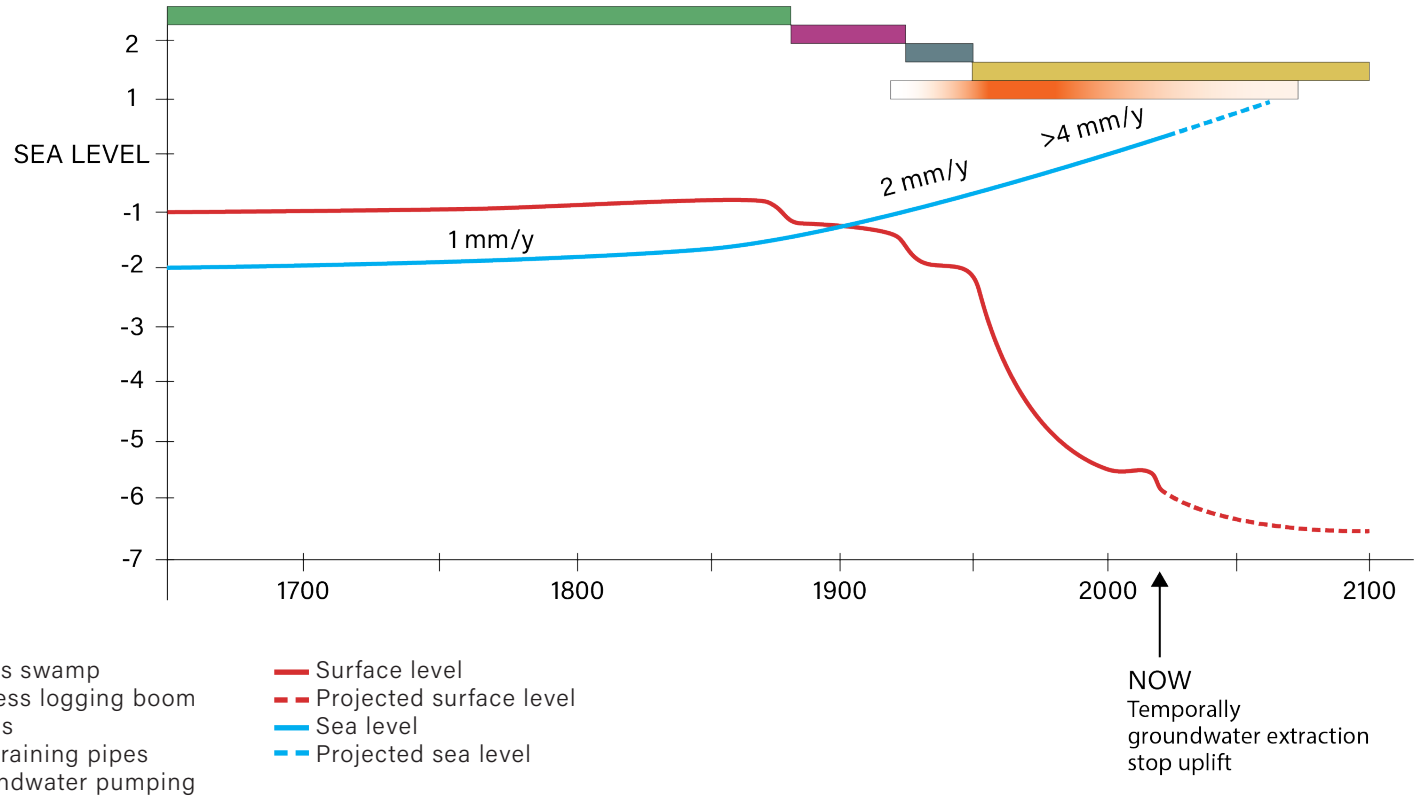

Figure 4.4. New Orleans subsidence process in time. Until the end of the 19th century, the northern part of New Orleans was covered with fresh water cypress swamps. These swamps raised gradually in equilibrium with sea level rise. After the start of the industrial cypress logging boom and the creation of the cypress wood transport canals, serious subsidence started (dewatering). A next subsidence phase started after the construction of the (urban) drainage canals at the begining of the 20th century. But real acceleration in subsidence started during urbanization of this area. The main factor was groundwater drainage by underground storm drainage and sewerage pipes. Groundwater pumping starting at the beginning of 20th century with the highest extraction ratesbetween 1950-1980, also added to subsidence, but to a much smaller amount. The stop of the Michoud extraction created a temporarily uplift.

5. RECOMMENDATIONS

The following recommendations regarding subsidence are made:

- Expand and continue the use of satellite-based InSAR. Insight in the characteristics of land movement can be significantly enhanced, and future development of land movement can be monitored in considerable detail, in particular when combined with other high-quality geodetic infrastructure (developed at LSU/C4G). In the present work Sentinel-1 images were used. Other satellite platforms offer higher resolution, and capabilities of InSAR in general are still improving (Figure 5.1). Differential subsidence of buildings (with pile foundations) and adjacent land surface allow distinction of shallow and 'deep' (below pile foundation) subsidence contributions. Moreover, true shrink-swell behaviour can be distinguished from deeper seasonally varying subsidence components. InSAR also offers insight in the gradients of land subsidence that modify surface water runoff conditions. Long-term monitoring can be an important base for urban water management.
- Continue (if possible, expand) groundwater monitoring in the Norco and Gonzales-NO aquifers in conjunction with land movement to check if subsidence may kick in again after head rise abates, ceases or reverts again to lowering.
- Validate/compare the results of Jones et al. (2016) against Terrasar-X – based subsidence for the same period.
- Consider using the ERS satellite to study subsidence in the period 1992-2001.
- Develop a shallow (phreatic) groundwater monitoring network to allow study of the effectiveness of urban water management with respect to land subsidence.
- Consider installing extensometers in strategic locations in the city an adjacent marshland to clarify contributions from various depths and types of geological materials in the Holocene strata. This may include dedicated monitoring at relevant renovation projects
- Check the integrity of the casing of the deep waste water well on which GPS of station MARY is mounted. That is, what is its effective foundation? This knowledge is essential to prevent bias in subsidence interpretation.
- Provide GPS data of station Moon (next to Mary)

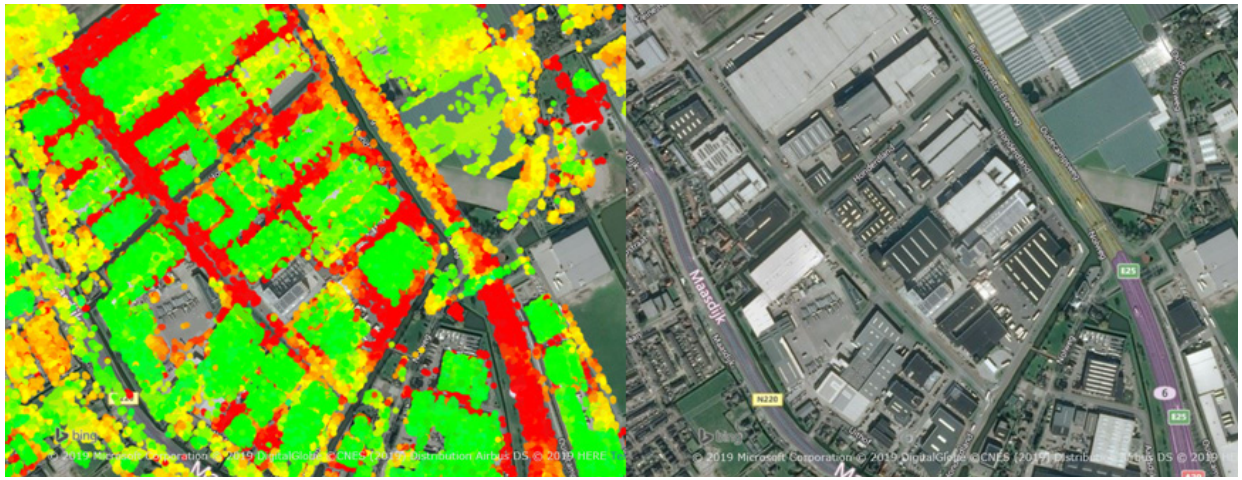

Figure 5.1. Example of high-resolution vertical land movement based on TerraSar-X images for an urban area in The Netherlands. The high spatial resolution allows monitoring of the differential movement of buildings and land surface (roads).

REFERENCES

Beckman, J.D., & Williamson, A.K. (1990). Salt-dome locations in the Gulf coastal plain, south-central United States. U.S. Geological Survey Water-Resources Investigations Report 90-4060.

Burkett, V. R., D. B. Zilkoski, and D. A. Hart (2003). Sea level rise and subsidence: Implications for flooding in New Orleans, Louisiana, U. S. Geol. Surv. Open File Rep., 03–308, 63

Chan, A.W., & Zoback, M.D. (2007). The role of hydrocarbon production on land subsidence and fault reactivation in the Louisiana coastal zone. J. Coast. Res. 23, 771-786.

CKA (CK Associates) (2016). Technical report – evaluation of groundwater withdrawal and air quality; New Orleans Power Station Energy New Orleans, Inc. 3601 Parid Road New Orleans, Louisiana 70129

Dixon, T.H., Amelung, F., Ferretti, A., Novali, F., Rocca, F., Dokka, R., Sella, G., Kim, S.-W., Wdowinski, S., & Whitman, D. (2006). Space geodesy: Subsidence and flooding in new orleans. Nature, 441(7093), 587.

Dokka, R. K. (2006). Modern-day tectonic subsidence in coastal louisiana. Geology, 34(4), 281–284.

Dokka, R. K., Sella, G. F. & Dixon, T. H. (2006). Tectonic control of subsidence and southward displacement of southeast Louisiana with respect to stable North America, Geophys. Res. Lett., 33, L23308, https://doi.org/10.1029/2006GL027250

Dokka, R. K. (2011). The role of deep processes in late 20th century subsidence of new orleans and coastal areas of southern louisiana and mississippi. Journal of Geophysical Research: Solid Earth, 116(B6).

Edrington, C.H., Blum, M.D., Nunn, J.A., & Hanor, J.S. (2007). Long-term subsidence and compaction rates: a new model for the Michoud area, South Louisiana. Gulf Coast Association of Geological Societies Transactions, v. 58, p. 261-272.

Fiaschi, S., Mead A., Cathleen, J. (2020). Using InSAR to measure subsidence in the Mississippi River Delta. Presentation at Louisiana Coastal Neotectonics workshop 3 (June 2020).

Hoes, O. (2021). Groundwater extraction Delft-North (in Dutch). Monitoring 2021, municipality report.

ILIT (Independent Levee Investigation Team), (2006). Chapter three: Geology of the New Orleans Region. In: Investigation of the Performance of the New Orleans Flood Protection Systems in Hurricane Katrina on August 29, 2005. http://projects.ce.berkeley.edu/neworleans/

Jankowski, K. L., Törnqvist, T. E. & Fernandes, A. M. (2017). Vulnerability of Louisiana's coastal wetlands to present-day rates of relative sea-level rise, Nat. Commun., 8, 14792, https://doi.org/10.1038/ncomms14792

Jones, C. E., An, K., Blom, R. G., Kent, J. D., Ivins, E. R., & Bekaert, D. (2016). Anthropogenic and geologic influences on subsidence in the vicinity of New Orleans, louisiana. Journal of Geophysical Research: Solid Earth, 121(5), 3867–3887.

Karegar, M. A., Dixon, T. H. & Malservisi, R. (2015). A threedimensional surface velocity field for the Mississippi Delta: Implications for coastal restoration and flood potential, Geology, 43, 519–522, https://doi.org/10.1130/G36598.1

Karegar, M. A., Kristine M. L. Kusche, J. & Dixon, T. H. (2020). Novel quantification of shallow sediment compaction by GPS Intfererometric reflectometry and implication for flood susceptibility. Geo Research Letters 47.

Keogh, M.E., & Törnqvist, T. E. (2019). Measuring rates of present-day relative sea-level rise in low-elevation coastal zones: a critical evaluation. Ocean Sci., 15, 61–73, 2019 https://doi.org/10.5194/os-15-61-2019

Kolker, A. S., Allison, M. A. & Hameed, S. (2011). An evaluation of subsidence rates and sea-level variability in the northern Gulf of Mexico, Geophys. Res. Lett., 38, L21404, https://doi.org/10.1029/2011GL049458

LIPS&AAE (Louisiana Public Health Institute & Alliance for affordable energy) (2016). Groundwater for power plants: a big risk to New Orleans East.

Nunn, J.A. (2003). Land surface subsidence caused by groundwater withdrawal in southeastern Louisiana. GCAGS/GCSSEPM Transactions, 53, 630-638.

Meckel, T. A., U. S. ten Brink & S. J. Williams (2006). Current subsidence rates due to compaction of Holocene sediments in southern Louisiana, Geophys. Res. Lett., 33, L11403, doi:10.1029/2006GL026300

Melman (2019). The sensitivity of land subsidence model predictions to parametric and structural uncertainties; a case study to groundwater extraction-induced subsidence in New Orleans. MSc-thesis, Utrecht University, 88 pp.

Morton, R.A., Bernier, J.C., & Barras, J.A. (2006). Evidence of regional subsidence and associated interior wetland loss induced by hydrocarbon production, Gulf Coast region, USA. Environmental Geology, 50, 261–274
Mugnier, C. (2014). Subsidence in Louisiana, elevations – a moving target. Powerpoint presentation

Zumbergh, M. A. (2022). Novel integration of gedetic and geologic methods for high-resolution monitoring of subsidence in the Mississippi Delta. Journal of Geophysical Research: Earth Surfaces, 127(9).

Prakken, L. B. (2009). Groundwater resources in the New Orleans area, 2008. 80. Louisiana Department of Transportation and Development.

Rollo, J. (1966). Groundwater resources of the greater new orleans area, louisiana: La. dept. Public Works and Lousisian Geological Survey. Bull.

Shen, Z., Dawers, N.H., Törnqvist, T. E., Gasparini, N.M., Hijma, M.P., & Mauz, B. (2016). Mechanisms of late Quaternary fault throw-rate variability along the north central Gulf of Mexico coast: implications for coastal subsidence. Basin Research, 1–14, doi: 10.1111/bre.12184

Shinkle, K. D., and R. K. Dokka (2004), Rates of vertical displacement at benchmarks in the Lower Mississippi Valley and the northern Gulf Coast, NOAA Tech. Rep. 50.

Snowden, J. O., Ward, W. C. & Studlick, J. R. J. (1980). Geology of Greater New Orleans: Its Relationship to Land Subsidence and Flooding, pp. 25, New Orleans Geol. Soc., New Orleans, La.

Törnqvist, T. E., Bick, S.J., van der Borg, K., & de Jong, A.F.M. (2006). How stable is the Mississippi Delta? Geology, 34, 697-700. doi: 10.1130/G22624.1

Törnqvist, T. E., Wallace, D. J., Storms, J. E. A., Wallinga, J., Van Dam, R. L., Blaauw, M., Derksen, M. S., Klerks, C. J. W., Meijneken, C., and Snijders, E. M. A. (2008). Mississippi Delta subsidence primarily caused by compaction of Holocene strata: Nat. Geosci., 1, 173–176, https://doi.org/10.1038/ngeo129

Voyiadjis, G.Z., & Zhou, Y. (2018). Time-dependent modeling of subsidence due to drainage in bounding shales: Application to a depleted gas field in Louisiana. Journal of Petroleum Science and Engineering, 166, 175-187. doi: 10.1016/j.petrol.2018.03.032

Wolstencroft, M., Shen, Z., Törnqvist, T.E., Milne, G.A., &Kulp, M. (2014). Understandingsubsidencein the mississippi delta region due to sediment, ice, and ocean loading: Insights from geophysical modeling. Journal of Geophysical Research. Solid Earth, 119(4), 3838–3856.

Yu, S-Y. Y., Törnqvist, T. E., & Hu, P., (2012). Quantifying Holocene lithospheric subsidence rates underneath the Mississippi Delta. Earth and Planetary Science Letters, 331-332, 21-30. doi: 10.1016/j.epsl.2012.02.021

Yuill, B., Lavoie, D., & Reed, D. J. (2009). Understanding subsidence processes in coastal louisiana. Journal of Coastal Research, (pp. 23–36).

Zilkoski, D. B., and S. M. Reese (1986). Subsidence in the vicinity of New Orleans as indicated by analysis of geodetic leveling data, NOAA Tech. Rep. NOS 120 NGS 38.

RELEVANT LITERATURE FOR SUBSIDENCE IN URBAN AREAS IN NEW ORLEANS

Year	Title	Authors
1980	Geology of Greater New Orleans: Its relationship to Land Subsidence and Flooding, pp. 25, New Orleans Geol. Soc., New Orleans, La.	Snowden, J. O., Ward, W. C. & Studlick, J. R. J.
1986	Subsidence in the vicinity of New Orleans as indicated by analysis of geodetic leveling data, NOAA Tech. Rep. NOS 120 NGS 38	Zilkoski, D. B., and S. M. Reese
2003	Sea level rise and subsidence: Implications for flooding in New Orleans, Louisiana, U. S. Geol. Surv. Open File Rep., 03–308, 63	Burkett, V. R., D. B. Zilkoski, and D. A. Hart
2003	Land surface subsidence caused by groundwater withdrawal in southeastern Louisiana. GCAGS/ GCSSEPM Transactions, 53, 630-638.	Nunn, J.A
2006	Space geodesy: Subsidence and flooding in New Orleans. Nature, 441(7093), 587	Dixon, T.H., Amelung, F., Ferretti, A., Novali, F., Rocca, F., Dokka, R., Sella, G., Kim, S.-W., Wdowinski, S., & Whitman, D
2006	Chapter 3; Geology of the new orleans region. Report by independent levee investigation team.	Rogers, j. David et al.
2008	Development of the New Orleans Flood Protection System prior to Hurricane Katrina. Journal of Geotechnical and Geo environmental Engineering 134 (5). doi: 10.1061/(ASCE)1090-0241(2008)134:5(602)	Rogers, J.D.
2009	Water & Soil in the Mississippi delta. Chapter in Dutch Dialogues: New Orleans Netherlands. Common Challenges in Urbanized Deltas, ISBN: 9789085067764 (published by SUN)	Roelof Stuurman Edit: Han Meyer, Dale Morris, David Waggonner.
2011	The role of deep processes in late 20th century subsidence of New Orleans and coastal areas of southern Louisiana and Mississippi. Journal of Geophysical Research: Solid Earth, 116(B6).	Dokka, R. K.
2016	Subsidence and flooding in New Orleans. Nature 441	Dixon, T.H., Amelung, F., Ferretti, A., Movali, F., Rocca, F., Dokka, R., Sella, G., Kim, S.-W., Wdowinski, S., Whitman, D.
2016	Anthropogenic and geologic influences on subsidence in the vicinity of New Orleans, Louisiana. Journal of Geophysical Research: Solid Earth, 121(5), 3867–3887.	Jones, C. E., An, K., Blom, R. G., Kent, J. D., Ivins, E. R., & Bekaert, D
2019	The sensitivity of land subsidence model predictions to parametric and structural uncertainties; a case study to groundwater extraction-induced subsidence in New Orleans. MSc-thesis, Utrecht University, 88 pp.	Melman, R.
2020	Using InSAR to measure subsidence in the Mississippi River Delta. Presentation at Louisiana Coastal Neotectonics workshop 3	Fiaschi, S., Mead A., Cathleen, J.
2020	Shallow subsidence vulnerability in New Orleans (final version July 2020)	Asselen, s. van, B. Arellano Jaimerena, R. Stuurman